THE UNIVERSITY OF CHICAGO

MECHANISM OF DENGUE VIRUS INDUCTION OF LIPOPHAGY

A DISSERTATION SUBMITTED TO

THE FACULTY OF THE DIVISION OF THE BIOLOGICAL SCIENCES

AND THE PRITZKER SCHOOL OF MEDICINE

IN CANDIDACY FOR THE DEGREE OF

DOCTOR OF PHILOSOPHY

COMMITTEE ON MICROBIOLOGY

BY

TRISTAN XAVIER JORDAN

CHICAGO, ILLINOIS

DECEMBER 2016

Table of Contents

List of Figures

Glossary of Terms

AMPK – 5'-amp activated kinase (AMPK) is a central sensor and regulator of the cellular energetic state. In autophagy, AMPK serves as a pro-autophagy factor that directly phosphorylates and regulates several core complexes of the autophagy cascade.

Autophagy – the process by which cytosolic contents are sequestered in *de novo* formed double-membraned vesicles and delivered to the lysosome for degradation.

Lipid droplets – Storage organelles for neutral lipids (e.g., cholesterol esters and triglycerides). LDs are composed of largely neutral lipid cores surrounded by a phospholipid monolayer, and have little protein content. The proteins the LDs do have are associated with the phospholipid monolayer.

Lipophagy – the speciic and selective targeting of lipid droplets for depletion by autophagy.

mTORC1 – mammalian target of rapamycin complex 1 is a regulator of cellular homeostasis, and acts as a sensor for cellular amino acids through its associatiation with amino acid transporters. Activation of mTORC1 leads to the suppression of autophagy.

NBR1 – neighbor of *BRCA1* is a selective autophagy adaptor important for the degradation of peroxisomes, focal adhesions, and lipid droplets.

TAK1 – transforming growth factor β (TGFβ)-activated kinase 1 is a mitogen activated kinase kinase kinase whose activity is important for many aspects of inflammation, innate immunity, and cell fate. TAK1, along with liver kinase B1 (LKB1) and Calcium/calmodoulin-dependent protein kinase kinase β (CaMKKβ), is a regulator of AMPK activation through phosphorylation of Thr172 in the AMPK activation loop.

TGFβ – transforming growth factor β is a pleiotropic cytokine involved in wound healing and immunosuppression (among other activities).

TGFβR1 (TβR1/ALK5) – the type I TGFβ receptor is responsible for the SMAD and non-SMAD signaling associated with TGFβ activity.

TGFβR2 (TβR2) – the type II TGFβ receptor is responsible for binding TGFβ, and subsequently phosphorylating and activating the type I receptor.

Acknowledgements

This thesis would not have been accomplished without the help of many people. Glenn Randall, for allowing me the opportunity to work in his laboratory, spend insane amounts of his money on pet projects and pipe dreams, and occasionally my main project, in order to allow me to develop into a decent scientist. Yasmine Baktash for being my comrade-in-arms durng the last several years, and for being a positive light during the times when I secretly considered giving up and leaving science. Your Keystone Meeting kicked off a lot of things for yourself, but the one I'm most thankful for is the excitement for science it instilled in you. When you came back bright-eyed and filled with passion about pursuing science I was seriously considering leaving the PhD program and figuring out what else this life could be. However, your persistent excitement reminded me why I love doing science, and eventually helped me out of my malaise.

This project leans heavily on microscopy, and I couldn't have been able to produce this work without our amazing core facility and the staff their. Specifically, Christine with whom I interacted the most and whose ImageJ macros classes really allowed me to develop the tools I needed to expedite the analysis of all these images. You are truly a saint.

In addition to the academic support, there are many friends and family members to thank for their moral support during these long seven years. Avery Adams, Emmanuel Sterling, Michael Sullivan, Daniel Lasley, and my brother James Jordan were essential to my sanity during these times, and were always available when I needed to rant about another experiment not working. And equally important, they would remind me that life

is lived outside of one's lab, and not to get so caught up in my academics that I let the the years pass me by.

Finally, I must thank my parents Fred and Linda Jordan without whom none of this would even be conceivable. Thanks mom and dad. I love you and hope you're proud.

Summary of Findings

Previous research in our lab described that dengue virus induces a lipid droplet (LD) specific autophagy program (lipophagy) that benefits viral replication by increasing b-oxidation of free fatty acids, presumably for increased ATP and energetic intermediates. However, it was unclear how dengue virus triggered this process. In this thesis, I show i) that lipophagy depends on a TGFβ-TAK1-AMPK-mTORC1-dependent signaling cascade; ii) LDs are targeted for degradation in an ubiquitin- and NBR1-dependent fashion; and iii) that NS1-3 is sufficient for lipophagy induction. Below is a summary of the findings in this thesis.

Chapter 1

1. Dengue virus replication activates AMPK, and increases its activity in infected cells
2. DENV replication requires AMPK and its kinase activity
3. Inhibition of AMPK blocks DENV-induced lipophagy
4. DENV infection inhibits mTORC1 signaling
5. Constitutively activating mTORC1 signaling inhibits DENV replication and lipophagy

Chapter 2

1. DENV lipophagy requires TGFβ, TGFβR signaling, and TAK1 activity
2. Inhibition of TGFβR, but not TAK1, inhibits viral replication
3. TAK1 has antiviral effects on dengue separate from autophagy and known MAPK signaling
4. TGFβ is insufficient to induce lipophagy in the absence of DENV infection

5. TAK1 and TGFβ are not general modulators of autophagy

Chapter 3

1. DENV infection increases K63-linked ubiquitin chain accumulation at LDs
2. Inhibition of TGFβ-dependent signaling pathway does not block K63-ubiquitin accumulation at LD
3. NBR1, but not p62 or OPTN, localize to LDs in DENV infected cells
4. Depletion of NBR1 inhibits DENV-lipophagy
5. Expression of NS1-3, but not individual NS proteins, is sufficient to induce lipophagy

Chapter I. Introduction

Dengue Virus

Dengue virus (DENV) is comprised of four distinct serotypes (DENV1-4). DENV infection can result in dengue fever and, in severe cases, can cause dengue hemorrhagic fever (DHF) and dengue shock syndrome (DSS). It is spread by the mosquito vectors *Aedes aegypti* and *Aedes albopictus*. Approximately 400 million people are infected with DENV annually, and nearly half of the world's population lives in DENV-endemic areas, including tropical and sub-tropical climates, with recent reports of DENV infections in parts of the southern United States (1, 16, 218, 219, 237). The resurgence of DENV within the past decades has been attributed to a combination of human, viral, vector, and ecological factors (142). As the infections have resurged, DENV has gained prominence as a re-emerging viral infection with a significant global health impact. There are no therapeutics for DENV infection. Recently, a tetravalent DENV vaccine has been approved in some endemic countries, which provides protection against ~2/3 of DENV infections (73).

In cell culture, DENV exhibits a wide tropism of susceptible cell types. Many human cell lines, including fibroblasts, epithelial, endothelial, and hepatocytes are capable of supporting viral replication via direct infection with the virus. However, while supportive of infection these cells are not the primary targets of DENV infection *in vivo*. Rather the primary sites of DENV infection are cells of the myeloid lineage, including monocytes, macrophages, and dendritic cells (18, 216). Counter-intuitively, these cell types cells are poorly infected *in vitro*, unless by an antibody-dependent enhancement of infection (ADE) mechanism (22, 24, 75, 76). Non-

neutralizing or sub-neutralizing concentrations of neutralizing antibodies bind the virion and facilitate its uptake into FcγR-expressing cells (21, 24, 162). *In vivo,* this occurs upon secondary infection with a heterotypic virus allowing the virus to replicate to high titer in a greater number of cells than via direct infection. It is believed that ADE can underlie the progression of the infection to the more severe DHF and DSS pathologies (40, 71).

DENV is a small (~10.7kb) positive-stranded RNA virus that replicates in the cytoplasm of infected host cells. Infection begins via receptor-mediated endocytosis and fusion out of an acidified endosomal compartment to release the viral genome into the cytosol (4, 63, 64, 103, 137, 193, 194, 272). Following entry, the cap-dependent translation of the viral genome produces one polyprotein, which is cotranslationally cleaved into ten viral proteins. This results in three viral proteins that form the virion structure (C, prM, and E) and seven non-structural (NS) proteins (NS1, 2A, 2B, 3, 4A, 4b, and 5) that are sufficient for viral replication. RNA replication occurs in the viral-induced modifications of the endoplasmic reticulum (ER) that shield viral antigens from cytosolic nucleases and innate immune sensors. Virions are assembled in proximity to the ER, wherein they attain their envelope by budding into the ER lumen. Virions are released via the cellular secretory pathway and become infectious following the proteolysis of prM by the cellular protease furin in the Golgi (155, 257).

As with all viruses, successful DENV infection requires many host processes, and actively manipulates others to its own benefit. While unable to identify a viral receptor, genome-wide screens have shown DENV depends heavily on several

components of the ER translocon - the oligosaccharyltransferase (OST) complex, the signal peptidase pathway, and the ER membrane complex (EMC). Signal peptidase (SPSC1) mediates the cleavage of the C-prM, prm-E, E-NS1, and 4a-2k junctions in the viral polyprotein, but the role of the OST and EMC complexes remains obscure. The virus also invests heavily in antagonizing the innate and adaptive immune systems at various levels. Secreted viral glycoprotein NS1 can antagonize the complement cascade thereby inhibiting opsonization of infected cells. NS3, the viral protease and helicase, inhibits innate immune signaling in protease-independent (RIG-I trafficking to mitochondria) and -dependent (cleavage of STING, and others) manners, both of which lead to decreased activation of T-cells by infected dendritic cells. NS4B, a small hydrophobic protein, mediates the disruption of mitochondrial-associated membranes (MAMs), which are signaling hubs for MAVS-dependent immune surveillance. NS5, the viral RNA-dependent RNA polymerase and methyltransferase, forms a complex with the E3 Ligase UBR4 and STAT2, which leads to the degradation of STAT2 rendering cells unable to respond to exogenous interferon.

Viruses and Autophagy

Autophagy

Autophagy is a highly conserved catabolic process that delivers cytosolic components to lysosomal compartments for degradation and recycling (152, 180). It is central to maintaining cellular homeostasis, responding to various stresses, fighting infections, and essential for proper development of many organisms (23, 74, 138).

Regulation of the autophagy pathway is complex (for a detailed discussion, see (3, 138, 285)). We will briefly discuss three central hubs of autophagy: the AMPK-mTOR-ULK1/2 axis, the Vps34-Beclin1 complex, and the Atg12 and Atg8 (LC3 in mammals) ubiquitin-like conjugation systems. Importantly, these hubs have been implicated in the modulation of autophagy by broad spectra of viruses [reviewed in (47, 112, 128)], and thus may represent points of interface between viruses and autophagy induction.

The activation of autophagy by various stimuli can converge on 5'AMP-activated kinase (AMPK) and mammalian target of rapamycin complex 1 (mTORC1) (138). AMPK and mTORC1 integrate sensing external stresses with the cellular metabolic state by positively and negatively regulating autophagy, respectively (6, 99). They accomplish this, in part, by regulating the activity of uncoordinated 51-like kinases 1 and 2 (ULK1/2) (50, 51, 93, 130). Under basal conditions, mTORC1 binds and inactivates ULK1/2 via multiple phosphorylations (93, 130). Upon stimulation of autophagy signaling, AMPK directly phosphorylates both mTOR and ULK1/2 leading to their dissociation and the activation of ULK1/2 (51, 130, 149). This leads to subsequent phosphorylation of downstream ULK1/2 substrates and the initiation of autophagy. Two recently described substrates of ULK1 and AMPK activity are Vps34 and Beclin1 (228), both of which are also regulated by direct phosphorylation by AMPK (129).

The core Vps34-Beclin1 complex is comprised of Beclin1-Vps34-p150, and is modulated by interaction with a variety of proteins (285). Vps34 and p150 form the class III phosphatidylinositol-3-kinase (PI3K) that generates phosphatidylinostiol-3-

phosphate (PI3P). PI3P enrichment helps to establish the formation site of autophagosomes (the omegasome) as well as expansion of autophagosome through recruitment of various autophagy proteins (9, 195, 223). Interaction with Beclin1 stimulates Vps34-p150 PI3K activity, and this activity is further modulated by an ever-growing list of Beclin1 interacting partners (285). Beclin1 binding partners can also influence the maturation of the autophagosome and its fusion with the lysosome (159, 172, 260, 303). Recently, researchers have uncovered a homolog of Beclin1 (Beclin2) with similar functions in autophagy regulation, and additional roles in endocytic trafficking (87).

Two evolutionarily conserved ubiquitin-like cascades control the expansion of the autophagosomal membrane: the Atg12 cascade which conjugates Atg12 to Atg5, and the LC3 cascade that conjugates LC3 to phosphatidylethanolamine (PE; LC3-PE or LC3-II) (60). Conjugation of Atg12 to Atg5 requires the E1-like activity of Atg7 and E2-like activity of Atg10, but does not require the activity of an E3-like enzyme (181, 249, 266). The Atg12-Atg5 conjugate is recruited to the nascent phagophore by Atg16 (56). LC3 is processed by Atg4 and charged for PE conjugation by Atg7 (E1) and Atg3 (E2) (97, 131). Atg12-Atg5 then serves as the E3-like enzyme for LC3-PE conjugation at the phagophore (78). LC3-II inserts into the growing membrane, remains associated throughout the lifetime of the organelle, and is thus used as a specific marker for autophagosomes. LC3 has been suggested to play a role in driving the membrane expansion of the growing phagophore and the fusion event that seals the autophagosome (281, 283, 294).

While once understood as a bulk degradation of cytosolic components, research has borne out an extensive role for the specific targeting of cargo by the autophagosome ("selective autophagy") (132, 282). Selective autophagy is essential for the clearance of organelles, invading pathogens, and aggregated proteins (132, 282). Targeting is achieved in ubiquitin-dependent and independent mechanisms; however, each relies on the interaction of adaptor proteins with the cargo (discussed below). These adaptor proteins contain LC3-interacting regions (LIRs) that allow the adaptor to directly recruit growing autophagosomes to the cargo (17). Several forms of selective autophagy have been described where organelle-resident proteins themselves contain LIRs that recruit autophagosomes (80, 163, 197, 234). After selective engulfment of the cargo, the autophagosomes continue along to fuse with the lysosome and degrade the components inside.

It is worth discussing the highlights of ubiquitin-dependent and independent pathways of selective autophagy. In ubiquitin-dependent forms of selective autophagy, an E3 ligase decorates the surface of the cargo with ubiquitin chains, predominantly of K27-, K48-, and K63-linkages (126). These ligases can either be recruited to the organelle by sensing some stress (mitophagy/xenophagy), or they can be organelle resident (pexophagy). The deposition of ubiquitin-chains recruits autophagy adaptors to the cargo via interaction with their ubiquitin binding domains. There are at least five ubiquitin-dependent adaptors - p62, NBR1, OPTN, TAX1BP1, and NDP52 - all contain ubiquitin-binding domains and LIRs (109). Specificity for their cargo is determined by (i) different affinities for ubiquitin chain linkages, (ii) different affinities for LC3/GABARAP isoforms, (iii) accessory domains,

or (iv) post-translation modification. For instance, removing the amphipathic J domain from NBR1 inhibits its ability to successfully target peroxisomes for degradation, and transplanting that domain into p62 confers the ability to coordinate pexophagy onto p62 (43). Also, in PINK1-PARKIN mitophagy, PINK1 phosphorylates ubiquitin at Ser65, and a subsequent phosphorylation of OPTN on its ubiquitin-binding domain increases the affinity of OPTN for these phosphorylated chains (136, 145, 222).

In ubiquitin-independent selective autophagy an organelle resident protein exposes a LIR after post-translational modification (126). Hypoxia-dependent phosphorylation and de-phosphorylation of mitochondrial FUNDC1 is important for hypoxia-induced mitophagy (139, 163, 289). Under basal conditions, Src kinase phosphorylates Tyr18 of FUNDC1, which is also the beginning of the LIR in FUNDC1 (163). Tyr18 phosphorylation leads to an electrostatic clash in the LIR docking site on LC3 weakening FUNDC1:LC3 interaction (139). Under hypoxic conditions, Tyr18 is dephosphorylated, and Ser17 is phosphorylated by ULK1 upon its recruitment to the mitochondria (163, 289). Transplant of the N-terminal 50 aa of FUNDC1, which contains the LIR, onto the transmembrane domain of mitochondrial outer membrane protein BCLxl is sufficient to drive hypoxia-induced mitophagy in a FUNDC1 deficient background (139). Organelle resident LC3 adaptors have also been identified for ER-phagy, nucleo-phagy, and other selective autophagy forms (126).

Autophagy is an important component and regulator of the host response against viral infections. As a branch of the immune system, autophagy has both

surveillance and effector functions important for the detection and clearance of viral pathogens. Autophagy can deliver viral components to endosomal compartments to stimulate innate immune signaling and to provide processed antigens for MHC presentation. Furthermore, the intrinsic capacity of the autophagosome to capture and degrade intracellular pathogens (xenophagy) adds to the antiviral capacity of the autophagosome. Consequently, viruses have developed a variety of ways to suppress and subvert the autophagy machinery for their own benefit.

There are numerous events in the viral life cycle that can trigger and benefit from autophagy. Research has demonstrated that engagement with the viral receptor (42, 52, 113, 192, 246), detection of viral pathogen-associated molecular patterns (PAMPS) by host pattern recognition receptors (PRRs) (41, 147), and the actions of individual viral proteins can be sufficient to induce autophagy during infection. Replication drives the generation of double-stranded RNA (dsRNA) intermediates that can be sensed by protein kinase R (PKR) (62, 269). Through the downstream phosphorylation of elongation-initiation factor 2-alpha (EIF2A) PKR can induce autophagy in response to viral infection (263, 264). Robust production of viral proteins is known to induce ER stress during many viral infections (134, 176, 259, 298), which is another potential trigger of autophagy during viral replication (203, 297). As a family, flaviviruses have different interactions with autophagy ranging from antiviral, proviral, and neutral.

Zika Virus

Zika is a recently re-emerged flavivirus that was originally thought to induce mild dengue-like symptoms. However, in this most recent outbreak has been

implicated in causing microcephaly in developing fetuses, and Guillan-barre syndrome, and other neurological defects. The main route of transmission is via Aedes aegeyptii mosquitoes, although there is evidence of sexual transmission. The high incidence of microcephaly and other neurologic disorders in areas affected by the on-going Zika outbreak has increased interest in understanding Zika biology as there are no effective vaccines or therapeutics yet available.

Recent work has demonstrated that Zika virus induces autophagy during infection, and that autophagy is proviral (77, 160). The benefit of autophagy for Zika remains unclear, but recent evidence has pointed to the viral proteins and signaling pathway that may be involved in autophagy induction. Infection of human skin fibroblasts or fetal neural stem cells with Zika induces autophagy. Supra-induction of autophagy using mTORC1 inhibitors rapamycin or TORIN1 increases Zika replication, while inhibition of autophagy via 3-methyladenine (3-MA) limits viral replication (77, 160). Transfection of NS4A or NS4B alone, and in combination, induces autophagy induction in HeLa cells. This induction coincides with the inhibition of Akt and mTORC1 as measured by phosphorylation of Thr308/Ser473 and Ser2448, respectively (160). Inhibition of signaling through the Akt/mTORC1 axis is important for autophagy under several conditions, but whether the inactivation of this pathway is responsible for Zika Virus induction of autophagy remains to be tested.

Japanese Encephalitis Virus

JEV is an encephalitic flavivirus spread by several mosquitoes of the *Culex* spp. It is a zoonotic pathogen whose lifecycle involves pigs as a major

reservoir/amplifying host, water birds as carriers, and mosquitoes as vectors (25). Humans are a dead-end host as their viremic levels are too low to infect feeding mosquitoes. While ~1% of JEV cases present illness, the mortality rate is high – annually 50,000 cases present clinical manifestations and of these 15,000 patients die (271). This makes JEV one of the most important endemic encephalitic viruses in the world, especially in Eastern and Southeastern Asia.

JEV infection induces autophagy in the brains of infected mice, however the in vivo relevance of this is not understood. Several studies suggest that autophagy suppresses JEV in neuronal tissues (244, 278), which is in line with a greater understanding of autophagy being the main mechanism of viral control in neuronal tissues as opposed to interferon (296). Although, one study that analyzes autophagy in neuroblastoma cells suggests autophagy is proviral for JEV in this case, a common theme is that neuronal autophagy protects the cells from cytopathic effects of viral replication – a net benefit for the host (244, 278). Other cell lines tested do not help to clarify whether autophagy is pro- or antiviral, as infection of mouse embryonic fibroblasts (anti), baby hamster kidney cells (anti/pro), procine kidney cells (anti), human embryonic carcinoma cells (pro), and A549 cells (pro) have given different results (106, 154, 244, 278). Different JEV strains have been shown to have different potencies in inducing autophagy, and so it is likely that there is a complex interplay between viral strain and cell type involved.

In addition to the involvement of autophagy, it has been suggested that JEV might utilize LC3-I+ EDEM+ ER-membranes for viral replication, much like mouse hepatitis coronavirus and equinine arteritis virus (183, 221, 244). Indeed, infection

of neuroblastoma cells and MEFS showed co-localization of endogenous LC3, but not GFP-LC3 with markers of the replicase (NS1 and dsRNA), and these areas also stained positive for EDEM1. RNAi-mediated knockdown of LC3a also reduced viral replication in MEF cells. This is distinct from autophagy, as atg5-/- MEFs replicated more virus (244).

Two studies have explored the proviral role of autophagy in JEV infection *in vitro* (106, 154). Both studies showed that across several JEV strains autophagy is induced during infection and inhibiting the process negatively effects viral replication, albeit to different extents. Li et al. (2012) found that incubating infected cells with rapamycin increased viral replication, and that during the early stages of infection, JEV can be found localized to EEA1+ LC3+ structures, presumably amphisomes. However, the relevance of this for the JEV lifecycle remains unclear. Jin et al. (2013) showed autophagy is induced in JEV infected brains of mice. Inhibiting autophagy during JEV infection of neuroblastoma cells led to increased cleavage of caspases-3 and -9 and subsequent cell death. Thus, autophagy may be performing a cytoprotective function in JEV infection. Furthermore, inhibition of autophagy led to enhanced IRF3 and MAVS activation as well as IFN-b promoter activity and production during infection, suggesting that this autophagy program also blunts the innate immune response to JEV infection (106). This is similar to reports that autophagy can limit the innate immune response to various viral infections infection (114, 122, 251, 262). The authors note that the inhibition of interferon is not the only requirement of autophagy for JEV infection, since inhibiting autophagy limited JEV replication in a RIG-I depleted background (106). Thus autophagy appears to be

playing two distinct proviral roles in JEV infection, the stimulation of replication and inhibition of innate immune signaling.

West Nile Virus

WNV is a neurotropic flavivirus spread predominantly by *Culex* spp. of mosquitoes. WNV is maintained in an enzootic cycle between mosquitoes and birds, but can also infect horses, humans, and several other mammals, which serve as dead end hosts. WNV is endemic in parts of Africa, Europe, the Middle East, and Asia, and emerged in the US in 1999. Since 1999, there have been more than 30,000 cases and 1200 resulting deaths from WNV making it the leading cause of mosquito-borne and epidemic encephalitis in the US (2, 215). While there are several vaccines for horses, there are currently no vaccines or treatments approved for WNV in humans.

While the disease symptoms of severe WNV infection often involve neuropathy, it is believed that the initial round of viral replication occurs in infected keratinocytes and Langerhans cells that migrate to regional lymph nodes after being infected (110, 161). After the initial replication, the virus is able to spread systemically where a second round of infection takes places in epithelial cells and macrophages of the kidney and spleen, respectively (10, 15, 233). Combinations of the viremia reached, viral adaptations, and various host factors can allow WNV to cross the blood brain barrier and then lead to encephalitis (12, 13, 61, 232, 273, 274, 276, 277).

Whether WNV induces autophagy is controversial, however, what is clear is that if/when autophagy is induced during infection it is antiviral for WNV. This difference is likely strain and/or cell type specific, however for the majority of

strains tested in most experimental settings there is no net benefit for WNV growth in ATG5 -/- cells. On the whole this suggests autophagy is unimportant for WNV replication. Wortmannin and 3-MA do seem to have an effect on WNV replication, but this is most likely a result of other non-autophagy PI3K-dependent events in the WNV lifecycle (14). Thus, WNV appears to be distinct from other flaviviruses examined in that its replication is not dependent on autophagy.

The suprainduction of autophagy in murine neurons can limit WNV infection. Shoji-Kawata *et al.* developed a specific inducer of autophagy that acts by inhibiting a negative regulator of autophagy, GAPR-1. It consists of a peptide from Beclin-1 that is fused to the HIV tat protein to promote cellular uptake. HeLa cells that were infected with WNV (TX02) then treated with the tat-Beclin-1 peptide showed a 1-2 log reduction in viral titers. When tested against a panel of viruses *in vivo,* it was shown that induction of autophagy via this peptide led to a similar reduction in viral titers in the brains of mice that were inoculated intra-cerebrally with WNV (Egypt 101). In the tat-Beclin-1 peptide treated mice, fewer neurons were infected with WNV, as measured by staining of brain slices, and fewer neurons were apoptotic (250). ~20% of the mice displayed a prolonged survival.

Dengue Virus

The initial study exploring the role of autophagy in DENV infection was performed in Huh7 cells (a hepatoma-derived cell line) and showed that DENV both induces autophagy and that autophagy is beneficial for viral replication (151). Confocal and electron microscopic analysis revealed an increase in GFP-LC3 puncta and LC3+ double-membrane vesicles, respectively, in DENV infected cells. Levels of

LC3-II also increased during infection. The addition of 3-methyladenine (3-MA) inhibited formation of GFP-LC3 puncta and LC3-II conversion during DENV infection. The autophagosomes co-localized with the late endosomal/lysosomal marker LAMP-1, indicating that autophagosomes had fused with lysosomes and were thus maturing. Inhibiting autophagy with 3-MA or infection of murine embryonic fibroblasts (MEFs) deficient in the essential autophagy gene ATG5 (atg5-/-) resulted in a decreased viral replication, while inducing autophagy with rapamycin increased the number of infected cells and viral replication. This suggests that autophagy performs a proviral function in DENV infection of Huh7 cells (151). These results have generally been replicated in subsequent studies investigating the role of autophagy in DENV infection *in vivo* and *in vitro* (89, 125, 171, 175, 209, 267).

Multiple pro-viral roles have been proposed for DENV-induced autophagy. Initial studies observed partial co-localization between GFP-LC3 puncta and markers of viral replication complexes (NS1 and dsRNA), and suggested that DENV may hijack autophagosomes to serve as a platform or scaffold for sites of viral replication. However, high-resolution cryo-EM reconstructions of DENV replication compartments showed that these replication structures were not vesicles at all, but are actually invaginations and convolutions of the ER membrane (284). Furthermore, no other groups have replicated the association of LC3 with viral replicase machinery (89, 151, 175, 267). Autophagy has also been thought to play a role in the formation of DENV virions or serve as a cytoprotective mechanism

against viral cytopathic effect. While protection from viral CPE may be a role for DENV autophagy, the role of autophagy in DENV virion maturation is controversial.

The study that explored the role of autopagy in virion maturation utilized an autophagy inhibitor – Spautin1 – which inhibits the activities of USP10 and -13. The incubation of DENV-infected cells with Spautin-1 reduces GFP-LC3 puncta formation and intra- and extra-cellular infectious virions, without greatly affecting DENV viral RNA levels (171). Previous work in our lab demonstrated that autophagy deficiency could be overcome by supplementing free fatty acids (discussed below), and the authors showed that when they used 3-MA to block autophagy exogenous free fatty acids restored viral replication. Thus, in their own hands, lipids can complement all defective PI-3 kinase-dependent processes that are required for DENV replication, including autophagy. Exogenous lipids cannot, however, complement Spautin-1 inhibition of DENV replication. Given that exogenous lipids can complement autophagy inhibition by 3-MA (89, 171), and siRNAs that target either ATG4B, ATG12, or Beclin-1 (89), but not Spautin-1, this strongly suggests Spautin-1's inhibition of DENV virion maturation is independent of autophagy. UPS10 and USP13 regulate a broad range of autophagy-independent processes, such as p53 activity, histone modifications, and interferon signaling (19, 20, 48, 239, 295, 299, 302). Additionally, USP10 has been found to bind the 3'UTR of DENV RNA and show a moderate relocalization to sites of viral replication (279). Thus, given the potential pleiotropic effects of Spautin-1, it is unlikely that the inhibition of autophagy by Spautin-1 is what is leading to deformed virions.

As a central regulator of cellular metabolic homeostasis, autophagy is primed to be subverted by viruses for this purpose. DENV-induced autophagy modulates metabolism by initiating a selective autophagy program, termed lipophagy that preferentially targets lipid droplets (LDs), ubiquitous cytosolic stores of triglycerides and cholesterol esters (89, 253). This ultimately results in the processing of triglycerides into free fatty acids (FFAs) and their subsequent β-oxidation in mitochondria to generate ATP (253). In uninfected cells, lipophagy is induced as a starvation response to generate needed energy or as a response to lipid overload (119, 206, 253).

Initial observations noted that there was a decrease in the staining of LDs by the neutral lipid dye oil red O in DENV-infected Huh7 cells (89). Quantitation of LDs by confocal and electron microscopy indicated that the area, but not total number of LDs decreased, suggesting that they may be depleted of their lipid content. This decrease in LD staining was coincident with an increase in autophagic flux, as measured by GFP-LC3 puncta formation, such that there was a strong inverse correlation between the number of GFP-LC3 puncta per cell and the amount of LD positive area in the infected cells. GFP-LC3 autophagosomes localized to LDs in a time-dependent manner. At 24 hours post-infection the number of autophagosomes per infected cell increased four-fold, while the percent associated with LD increased three-fold, thus producing a 12-fold increase in total autophagosomes associated with LDs per cell. This increase in the percent of autophagosomes associated with LDs in DENV-infected cells suggests that DENV infection is inducing a selective autophagy (lipophagy). The depletion of LDs and the requirement for autophagy

was validated in four cell lines of hepatoma and kidney epithelial origin (Huh7, Huh-7.5, HepG2, and BHK). The inhibition of autophagy by either 3-MA or siRNAs targeting two essential components of the autophagy pathway (ATG12 and Beclin-1) prevented LD depletion in DENV-infected cells (89).

Further experiments identified that GFP-LC3 autophagosomes stained positive for oil red O in DENV-infected cells and that both autophagosomes and oil red O positive lipids were delivered to acidified lysosomes (89). The consequence of triglyceride delivery to lysosomes is their processing and the release of FFAs for β-oxidation (89, 253). DENV-infected cells displayed a much higher rate of β-oxidation over their mock-infected counterparts, and this was significantly reduced when autophagy was inhibited by 3-MA or siRNAs targeting ATG4B, ATG12, or Beclin-1. Furthermore, virus replication could be inhibited with etomoxir, a pharmacological inhibitor of β-oxidation.

Although these experiments demonstrated that DENV infection induced lipophagy, they did not show that lipophagy was the essential autophagy function for DENV replication. The requirement of lipophagy for DENV replication was demonstrated by a lipid complementation assay, wherein the requirement of autophagy for DENV replication could be supplanted by the addition of exogenous lipid. Autophagy was first inhibited by multiple means, including 3-MA or siRNAs that target either ATG4B, ATG12, or Beclin1. In each case, exogenous FFAs could complement the defect in DENV replication. Moreover, the complementation of inhibited autophagy by FFAs required β-oxidation. Treatment with etomoxir prevented DENV replication in lipid complemented cells (89). Thus, the major

requirement of autophagy for DENV replication is the stimulation of lipid catabolism. In essence, DENV is inducing a cellular response to "trick" the cell into depleting its energy stores for the benefit of the virus.

Lipophagy

Very little is known about the molecular mechanism of lipophagy. Rather, many studies have focused on the molecular mechanisms of hepatic autophagy and examined lipid droplets as a read-out for the process. This has lead to the understanding of the roles of several transcription factors important for autophagy regulation (transcription factor EB (TFEB), peroxisome proliferator-activated receptor alpha (PPARa), farsenoid X receptor (FXR), cAMP-response element binding protein (CREB)) (148, 201, 241, 242), and re-iterated the importance of several other molecules for functional autophagy/selective autophagy (e.g., Rab7, Htt, SMURF1) (205, 227, 238).

What has been uncovered recently is the role of chaperone-mediated autophagy in mediating lipophagy and lipolysis of LDs in the liver (118). While the molecular mechanisms of chaperone-mediate autophagy are largely obscure, it is known that LAMP2A (L2A) is an essential mediator of the process. Liver specific deletion of L2A from mice leads to the accumulation of LDs in oleic-acid treated cells, and this is mirrored in cultured human hepatocyte cell lines (118). While this is likely also a consequence of the lack of degradation of lipogenic enzymes, reduced VLDL synthesis, and the inability of catalytic ATGL to bind PLINs and initiate lipoplysis, the inhibtion of CMA also seems to impact the abililty of autophagosomes to assemble at the lipid droplet surface in response to lipohagic stimuli. Indeed,

subsequent inhibition of macroautophagy via 3-MA treatment does not additionally increase the lipid droplet burden of L2A-deficient cells, suggesting that these two pathways may operate together to regulate lipid droplets (118). Furthermore, the recruitment of autophagy machinery such as Beclin1, ATG5, LC3, and the adaptor molecule NBR1 to lipid droplets, which increases under starvation conditions, is significantly decreasesd in L2A deficient cells (118). Additional work by the same group showed that PLIN2 serves as a docking site for L2A, and that this is dependent on phosphorylation of PLIN2 by AMPK (117). When this phosphorylation site is mutated, CMA-lipophagy as well as macrolipophagy are blocked, further suggesting a link between the two processes.

The recruitment of NBR1 to lipid droplets suggests that lipophagy may be a ubiquitin-dependent selective autophagy, however there exists no definitive data for this. It was not tested whether deletion or knockdown of NBR1 blocks the lipophagy process (118). Additionally, the non-lipidated for of LC3 (LC3-I) can be seen on lipid droplets in the absence of autophagy induction or autophagy (ATG5-/-), suggesting that LC3 may not need to be recruited to the lipid droplet for lipophagy (253). Yet, more recent evidence suggests that LC3 on lipid droplets can be mobilized for autophagosome formation at non-lipid droplet sites (49). The selective autophagy regulator Huntingtin (Htt) interacts with p62 (and presumably other autophagy adaptors) to orchestrate the incorporation of cargo into autophagosomes (227). Given that p62 is a ubiquitin-dependent autophagy adaptor, and deletion of Htt leads to increased lipid droplets and lipid droplet size, and autophagosomes devoid of lipid droplets as cargo, one might infer lipophagy as a

ubiquitin-dependent selective autophagy (227). The mechanism remains to be elaborated.

Goals of this thesis

The goal of this thesis was to define the molecular mechanism by which dengue virus induces lipophagy. In doing so, we sought to increase basic understanding of how viruses actively reshape host metabolism and how lipophagy is controlled. We began by interrogating the role of the AMPK-mTORC1 signaling axis in controlling DENV-induced lipophagy. We found that AMPK activity and mTORC1 inihibition are required for the lipophagy induction. We next examined what are the upstream molecules that control activation through this pathway. We define transforming growth factor beta (TGFβ) as an upstream molecule that is important for DENV-induced lipophagy by signaling through TGFβ receptor (TβR) and TGFβ-activated kinase 1 (TAK1), an upstream AMPK kinase. Inhibition of TGFβ binding, TβR signaling, and TAK1 activity block lipophagy induction, however they do not inhibit ionomycin-induced autophagy (Ca^{2+}-dependent) suggesting specificity of this pathway. We then defined the molecular markers that play a role in targeting the lipid droplet for degradation. Lipid droplets accumulate ubiquitin and NBR1, hallmarks of selective autophagy, and depletion of NBR1 (but not p62) blocks DENV-induced lipophagy. Finally, we identify the proteins NS1-3 as sufficient to drive lipophagy.

Chapter II. Dengue virus activates the AMP kinase-mTOR axis to stimulate a proviral lipophagy.

Abstract

Robust dengue virus (DENV) replication requires lipophagy, a selective autophagy that targets lipid droplets. The autophagic mobilization of lipids leads to increased β-oxidation in DENV-infected cells. The mechanism by which DENV induces lipophagy is unknown. Here, we show that infection with DENV activates the metabolic regulator 5'adenosine-monophosphate activated kinase (AMPK), and that the silencing or pharmacological inhibition of AMPK activity decreases DENV replication and the induction of lipophagy. The activity of mechanistic target of rapamycin complex 1 (mTORC1), which is inhibited by AMPK, decreases in DENV-infected cells and is inversely correlated to lipophagy induction. Constitutive activation of mTORC1 by depletion of tuberous sclerosis complex 2 (TSC2) inhibits lipophagy induction in DENV-infected cells, and decreases viral replication. Thus, DENV stimulates and requires AMPK signaling to suppress mTORC1 and activate the proviral lipophagy.

Introduction

DENV is a ~11kb positive strand RNA virus of the *Flaviviridae* family that is transmitted by the *Aedes aegypti* mosquito, and is the causative agent of dengue fever. It is a global pathogen that infects ~390 million people, and causes 25,000 deaths annually. There are no therapeutics for DENV infection. Recently, a tetravalent DENV vaccine has been approved in some endemic countries, which provides protection against ~2/3 of DENV infections (73).

Macroautophagy (hereafter called "autophagy) is a catabolic process essential to cellular and organismal homeostasis (138, 180). During autophagy, de novo formed double-membrane vesicles, autophagosomes, sequester cytosolic contents and then fuse with the lysosome where the contents are degraded. The sequestration of cytosolic content into autophagosomes can be random in the case of bulk autophagy. Alternatively, autophagy can be selectively targeted towards cargo, such as aggregated proteins, damaged organelles, or nutrient stores. Autophagy also has a central role in host defense from invading pathogens, both by directly degrading the pathogen or indirectly interfacing with the larger innate and adaptive immune systems (44, 45, 153). Many pathogens have elaborated strategies to either evade detection by autophagy, or to subvert autophagy for proviral strategies (112, 141).

Multiple studies have shown that DENV induces a proviral autophagy (54, 95, 125, 150, 171, 179, 209, 210). Consistently, studies across varied cell types have shown that infection with dengue virus increases the accumulation of autophagosomes, and blockade of autophagy by either genetic approaches or pharmacological inhibitors decreases viral replication. We previously demonstrated that DENV infection elicits the selective targeting of lipid droplets (LDs) by autophagy, termed lipophagy (89). DENV infection increases both the total number of autophagosomes within the cell and the frequency of autophagosomes that localize to LDs. At 24 hours post infection, ~30% of all autophagosomes localize to LDs. When media serum conditions are low, limiting the uptake of extra-cellular lipids, DENV-induced lipophagy produces a depletion of lipid droplet volume and

triglyceride content. This results in the liberation of free fatty acids from triglycerides, which are transported to the mitochondria for b-oxidation (89, 253). Importantly, supplementation of autophagy-deficient cells with exogenous free fatty acids completely complements viral replication. This fatty acid complementation of DENV replication could be prevented by Etomoxir, which prevents the transport of fatty acids into the mitochondria for b-oxidation (89). Thus, the major requirement for autophagy in DENV replication is the stimulation of lipid metabolism.

Lipophagy is conserved from yeast to mammals, and much recent work has described conserved transcriptional requirements for lipophagy induction in *C. elegans*, mice and humans (69, 143, 148, 201, 241, 243). However, the signaling pathways that control lipophagy remain obscure. Likewise, it remains unknown how DENV triggers lipophagy during viral infection.

Integration of signaling is an important upstream regulation of autophagy, often dictating the cellular site and timing of autophagosome biogenesis (138, 229). A central node of signal integration is mammalian target of mTORC1 (115, 138). The activation of mTORC1 suppresses autophagy by antagonizing the activity of the unc51-like kinase (ULK) 1/2 complex through direct inhibitory phosphorylation of ULK1 (130). As a central sensor of nutrient homeostasis, mTORC1 integrates signals from a variety of other nutrient sensors including AMPK (reviewed in (94, 144, 240)). Activation of AMPK is tightly correlated to the cellular energy state of the cell by the differential binding affinity of AMPK to adenylate nucleotides (81, 202, 291, 292). Additionally, activation of AMPK requires its phosphorylation by several upstream kinases that integrate cell stresses (86, 92, 96, 182, 245, 286).

Activation of AMPK results in the inactivation of mTORC1. This is accomplished by the phosphorylation of tuberous sclerosis complex (TSC) 2 (101). TSC1 and TSC2 form a heterodimeric complex that functions as a GAP for the small GTPase Rheb, which is essential for mTORC1 activity (100, 157, 158, 166). Activation of TSC2 inactivates Rheb, and this leads to suppression of mTORC1 activity (100, 101). AMPK also directly phosphorylates regulatory-associated protein of mTOR (Raptor),, an essential adaptor of the mTORC1 complex (127), at Ser 722 and 792 (72). This leads to the recruitment of 14-3-3 and inhibition of mTORC1 activity (72).

In addition to its suppression of mTORC1 activity, AMPK also plays direct roles in the initiation of autophagy, through direct phosphorylation of two key complexes in autophagy (51, 129, 130, 149). AMPK directly binds and phosphorylates the ULK1/2 complex, which is essential for licensing autophagy under energy-starved conditions (51, 130). Furthermore, AMPK activation also leads to phosphorylation of the vacuolar protein sorting (Vps) 34-Beclin1 complexes to suppress their roles in vesicular trafficking, and promote the licensing of autophagosome biogenesis by Vps34-Beclin1-Atg14L complexes (129).

In this paper, we examine the role of AMPK and mTORC1 in DENV-induced lipophagy. We show that DENV infection transiently activates AMPK while inhibiting mTORC1. Inhibition of AMPK and the mTORC1 inhibitor TSC2 decrease autophagy induction, LD depletion, and DENV replication. Thus, DENV induces lipophagy via the AMPK-mTOR axis.

Materials and Methods

Cells and Virus. HepG2 cells, a human hepatoma cell line (ATCC), and HEK293T were maintained in Dulbeccco's modified Eagle medium-high-glucose, and supplemented with 5% fetal bovine serum (FBS), 0.1mM non-essential amino acids, and 1% penicillin-streptomycin (Life Technologies). Infectious DENV-2 16681 clone was used, and virus was propagated in C6/36 *Aedes albopictus* cells (ATCC) as previously described (89). Cellular viability was assayed using Cell Titer-Glo (Promega).

Antibodies and inhibitors. The antibodies used in this study include AMPKa, phospho-AMPKa Thr172, TSC2, S6K, phospho-S6K Thr389 (Cell Signaling), DENV NS3 (88)**,** b-actin (Sigma), LC3B (Novus Biologics) and goat anti-rabbit IgG (Thermo Fischer) for immunoblot analysis. For immunofluorescence analysis, the antibodies used included LC3B (Cell Signal), DENV NS3, DENV2 E (ATCC), and Alexafluor-350, -488, and -594 secondary antibodies (Life Technologies). Compound C was obtained from Cayman Chemicals.

Real-time RT-PCR. RNA was extracted from cells grown in 96-well plates by RNeasy 96 Kit (Qiagen), per manufacturers instructions. Extracts were reverse-transcribed and PCR amplified by using the Superscript III Platinum One-Step RT-PCR system with Platinum Taq (Life Technologies) as previously described (89). DENV RNAs were amplified using 300 nM forward primer (5'-TCCCAAACGCAGTGATATTACAA-3') and 300 nM reverse primer (5'-TGAGACCTTTGATCGTCAATGC-3'), and 200 nM probe (5'-6FAM-TGGTGTCCGTTTCCCCACTGCTCTT-IowaBlack-3') (Integrated DNA Technologies)

which recognizes NS2A of DENV 16881. Parallel reactions used 0.8X amount of 18s rRNA TaqMan gene expression assay as an internal loading control (Hs01021073_m1; Applied Biosystems). Reverse transcription-PCR (RT-PCR) was programmed for 50°C for 30 min, 95°C for 6 min, and then 50 cycles of 95°C for 15s, 60°C for 30s, and 72°C for 15s using an ABI 7300 system (Applied Biosystems). Data were analyzed with SDS v1.4 software (Applied Biosystems) and normalized to 18s controls. Relative quantification was calculated comparing the cycle threshold (C_T) values using 2^{DDCT}.

siRNA transfection. siRNAs were introduced into cells using Lipofectamine RNAiMax (Life Technologies) per manufacturer's instruction. 48 hours post transfection with siRNAs cells were DENV-infected for indicated times. *AMPKα1* (5'-CGGGAUCAGUUAGCAACUATT-3') and *TSC2* (TSC2-1 5'-GCACCUCUACAGGAACUUUTT-3', TSC2-2 5'-CGACGAGUCAAACAAGCCAAUUU-3') siRNAs were obtained from Life Technologies, and a scrambled negative control siRNA from Dharmacon (220).

Western Blot Analysis. Cells were plated in 12-well dishes, and at indicated times post infection washed 2x in PBS, then harvested in NP40 Lysis Buffer (50mM Tris-HCl pH 8.0, 150mM NaCl, 1% NP40, 2mM EDTA, 10% glycerol, 10mM NaF, and protease inhibitors (Roche Protease Inhibitor Cocktail)). Lysate was boiled in 1x SDS sample buffer (50mM Tris-HCl pH 6.8, 2% SDS, 10% glycerol, 1% b-mercaptoethanol, 12.5mM EDTA, 0.025% bromphenol blue). Proteins were separated by SDS-PAGE on 4-20% gradient gels (Lonza), and transferred to PVDF

membranes (Thermo Fischer). Proteins were detected using Supersignal West Femto Substrate (Thermo Fischer) and exposed to film.

Immunofluorescence. After infection for the indicated times and multiplicities of infection (MOIs), indicated cells were fixed on coverslips in either 4% PFA or methanol. Coverslips were blocked in PBS containing 30% goat serum and 0.1% saponin, and stained with antibodies in PBS containing 10% goat serum and 0.1% saponin. Lipid droplets were stained with Oil Red O (ORO, MP Biomedical) as per manufacturer's instructions. Stained coverslips were mounted with Prolong Gold with or without DAPI (Life Technologies). Images were collected with an Olympus DSU confocal microscope with a 100x oil objective. Digital images were taken with Slidebook 5.0 software and processed using ImageJ (National Institutes of Health). Analysis of images was performed with ImageJ and used a set of defined intensity thresholds on all images.

Lentivirus particle production and complementation. siRNA-resistant AMPKα1was engineered by silent mutation of the seed sequence sites in the AMPKα1 cDNA (a**gcgga**<u>**a**</u>gcgtttcaaatt; bold is seed sequence, underline is resistance mutations) into the lentivirus packaging vector pLVX-puro (Clontech) between the EcoRI and XbaI sites. HEK293T cells were transfected with empty pLVX-puro, or pLVX-puro containing siRNA resistant WT or Kinase Dead (D156A) AMPKα1 along with plasmids encoding gag/pol and VSV-G. 48 hours post transfection, the supernatants were harvested and cell debris spun down by centrifugation at 1,200xg for 5 min before filtration through a 0.22um filter. HepG2 cells were transduced with empty lentiviral pseudoparticles or those encoding an siRNA

resistant wild type or kinase-dead (D156A) AMPKα1. The following day, the cells were treated with siRNAs against AMPKα1 or an irrelevantly targeted sequence. 72 hours post siRNA treatment cells were infected and processed at subsequent indicated time points, or alternatively, protein lysates were harvested in NP-40 lysis buffer and subjected to SDS-PAGE and immunoblot analysis.

AMPK activity assay. AMPK activity was measured as previously described (37). HepG2 cells were washed 3X with warm Krebs-Hepes buffer (20 mM Na Hepes, pH 7.4, 118 mM NaCl, 3.5 mM KCl, 1.3 mM $CaCl_2$, 1.2 mM $MgSO_4$, 10 mM glucose, 1.2 mM KH_2PO_4, 0.1 % BSA) and incubated in Krebs-Hepes buffer containing for 1 h at 37°C. The buffer was aspirated and dishes were placed on ice with immediate addition of 100ml ice-cold lysis buffer (50 mM Tris/HCl, pH 7.4, 50 mM NaF, 5 mM Na pyrophosphate, 1 mM EDTA, 1 mM EGTA, 250 mM mannitol, 1 % Triton X-100, 1 mM DTT, protease inhibitors). Cells were scraped, and lysates transferred to microcentrifuge tubes and incubated on ice for 5 minutes. Lysates were then centrifuged for 30 min at 14000xg and 4 °C in preparation for use.

The AMPK activity assay was composed of a total reaction volume of 25 µl that was incubated for 10 min at 30°C. Each reaction consisted of 2.5 µl lysate assay buffer (62.5 mM Na Hepes, pH 7.0, 62.5 mM NaCl, 62.5 mM NaF, 6.25 mM Na pyrophosphate, 1.25 mM EDTA, 1.25 mM EGTA, 1 mM DTT, and protease inhibitor cocktail (Roche)), 2.5 µl of 100 µM [γ-^{32}P]-ATP (1 µCi/µl) in 25 mM $MgCl_2$, 2.5 µl of 2 mM AMP in lysate assay buffer, 5 µl of 1 mM SAMS peptide in lysate assay buffer, and 12.5 µl cell lysate. The reaction mixture was spotted on P81 phosphocellulose paper, which was washed twice with 1% phosphoric acid, and then once in water

and acetone. The radioactivity of the phosphorylated SAMS peptide was quantified by scintillation counting. Assay background was determined by incubating the lysate in the absence of SAMS peptide.

Statistical analysis. Data are presented as means ± standard error. To assess statistical significance, two-tailed, paired Student *t* tests were performed

Results

DENV induction of proviral lipophagy requires AMPK

AMPK is a central node in the cellular nutrient stress response to stress and is frequently manipulated during infection with distinct viruses (34). To investigate the role of AMPK in DENV infection, we first examined the requirement of AMPKa1 expression for DENV replication. HepG2 cells were depleted of AMPKa1 by siRNA (Fig. 1a) and then infected with DENV for 24 hours. Compared to cells treated with an irrelevant non-targeting siRNA (IRR), DENV replication was significantly impaired in cells transfected with AMPKα1 siRNA, as measured by RT-PCR quantification of viral RNA (Fig. 1B) and infectious virus production (Fig. 1C). Cell viability was unaffected by siRNA treatment (Fig. 1D).

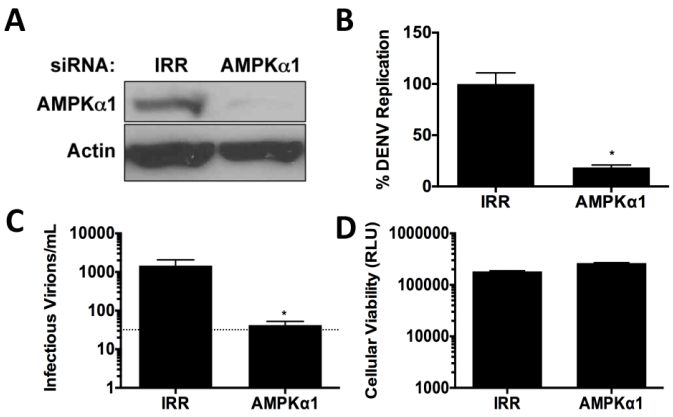

Figure 1. AMPK silencing inhibits DENV replication. (A) AMPKα1 protein levels following treatment with IRR or AMPKα1 siRNAs. (B-D). siRNA-treated cells were infected at an MOI of 1 with DENV for 24h and cellular RNA was harvested to determine viral genome replication (C), while viral supernatants were titered to determine infectious virus produced (D). (B) Cellular viability was assessed 72hrs post transfection of siRNAs.

To determine the role of AMPK in DENV-induced lipophagy, we tested the requirement of AMPKa1 for increased autophagosomes in DENV-infected cells via immunofluorescence analysis of LC3II-positive puncta. HepG2 cells were depleted of AMPKa1 by siRNA, or treated with an IRR siRNA, and then either mock- or DENV-infected for 24 hours. The infection of IRR-treated HepG2 cells with DENV increased the number of autophagosomes at 24 hpi, consistent with the induction of autophagy by DENV (Fig. 2A,B). While the silencing of AMPKa1 did not alter the number of autophagosomes in mock-infected cells, it prevented the increase in autophagosomes in DENV-infected cells. In contrast, silencing the core autophagy machinery component ATG12 decreased autophagosome number in both mock- and DENV-infected cells (Fig. 2 A,B). This

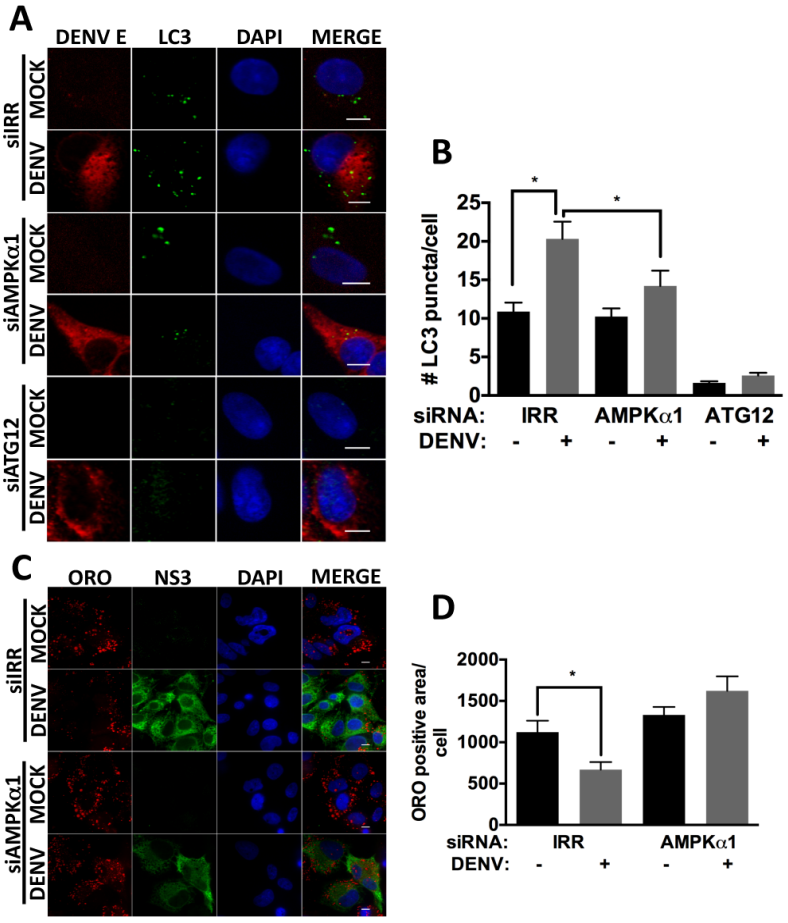

Figure 2. AMPK silencing inhibits DENV-induced lipophagy. Cells were treated with indicated siRNAs for 48h, infected with DENV at an MOI of 0.5 for 24h and 48h, and probed for DENV E and LC3-II (A) or stained with ORO (C). Nuclei were stained with DAPI. Quantification of (B) LC3-II puncta per cell and (D) LD area was performed using ImageJ. Scale bar = 8μm.

suggests that AMPK is required for DENV-induced autophagy, but not basal autophagy, in HepG2 cells.

We next examined whether AMPK is required for the mobilization of lipids from lipid droplets, as quantified by a decrease in the total area stained by the neutral lipid dye oil red O (ORO). HepG2 cells were depleted of AMPKa1 by siRNA, or treated with an IRR siRNA, and then either mock- or DENV-infected for 48 hours. DENV-infection depleted the area of lipid droplets in IRR siRNA treated cells, consistent with our previous study (89). AMPK silencing prevented the depletion of lipid droplets in DENV-infected cells (Fig. 2C,D). Thus, AMPK is required for both components of DENV-induced lipophagy: the induction of autophagosomes and the mobilization of lipid droplet stores.

DENV-induced lipophagy requires AMPK enzymatic activity

We tested the requirement of AMPK enzymatic activity for DENV-induced lipophagy and viral replication using the selective AMPK inhibitor, Compound C. HepG2 cells were infected, then treated with DMSO or Compound C for 24 hours and assayed for DENV replication (Fig. 3A) or infectious virus production (Fig. 3B). Compound C treatment significantly inhibited DENV replication and infectious virus production without compromising cellular viability (data not shown).

Similar to the AMPK silencing experiments, Compound C treatment also prevented DENV-induced lipophagy. In DMSO-treated cells, DENV infection increased autophagosome number and decreased lipid droplet area as compared to mock-infected cells. Treatment with Compound C blocked autophagy induction and lipid droplet depletion (Fig. 3C-F). Interestingly, treating mock-infected cells with

Compound C lead to an overall increase in lipid droplet area (Fig 3E,F). This suggests that AMPK regulates aspects of basal lipid metabolism that impact lipid droplet storage, in addition to DENV-induced autophagy.

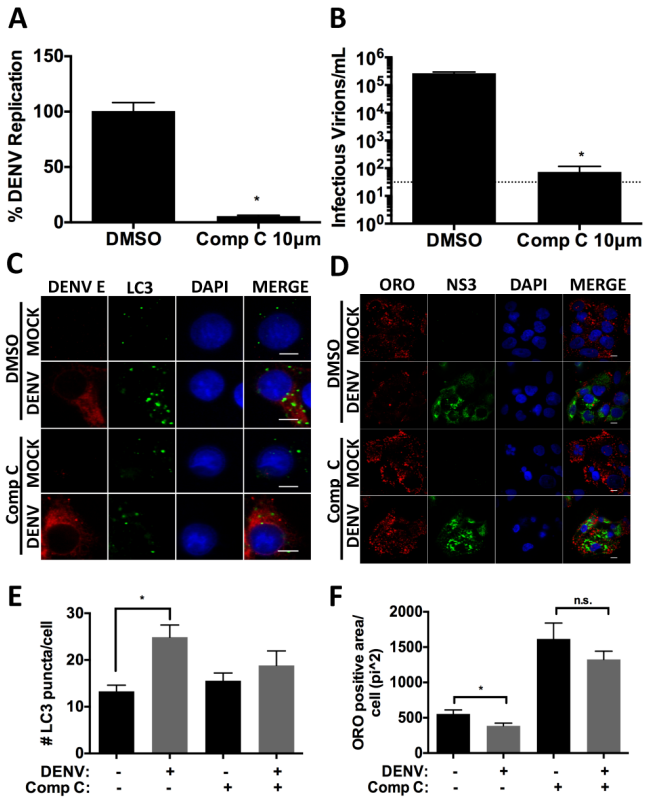

Figure 3. AMPK inhibition diminishes DENV replication and lipophagy induction. Cells were DENV infected at an MOI = 1 for 2hrs. After virus adsorption, infected cells were treated with DMSO or 10μM Compound C. At 24h post-infection, (A) cellular RNA or (B) supernatants were harvested to assess viral replication and infectious virus release, respectively. (C-D). Cells were DENV infected at an MOI = 0.2, and Compound C (2.5μM) was added after virus adsorption. Cells were fixed at 24hpi to probe for (C) DENV E and LC3-II or at 48hpi and (D) stained with DENV NS3 and ORO. Nuclei were stained with DAPI. Quantification of (E) LC3-II puncta per cell and (F) LD area was performed using ImageJ. Scale bar = 8μm.

We confirmed the requirement of AMPK enzymatic activity for DENV replication using a siRNA resistant trans-complementation approach. Replication-defective lentiviruses expressing siRNA-resistant AMPKa1 that is either wild type or enzymatically inactive (D156A) were used to infect AMPKa1 siRNA treated HepG2 cells. We confirmed that AMPKa1 siRNA treatment decreased AMPKa1 expression and that the siRNA-resistant AMPKa1-expressing lentiviruses restored AMPKa1 expression (Fig. 4A). These cells were then DENV-infected in parallel and tested for viral replication. We observe that AMPKa1 silencing decreases DENV replication, as in Fig. 1B. The enzymatically active

AMPKa1 restores DENV replication, while the enzymatically inactive AMPKa1 fails to rescue DENV replication (Fig. 4B). This confirms the requirement of AMPKa1 enzyme activity for DENV replication, in addition to ruling out off-target effects of the AMPKa1 siRNA.

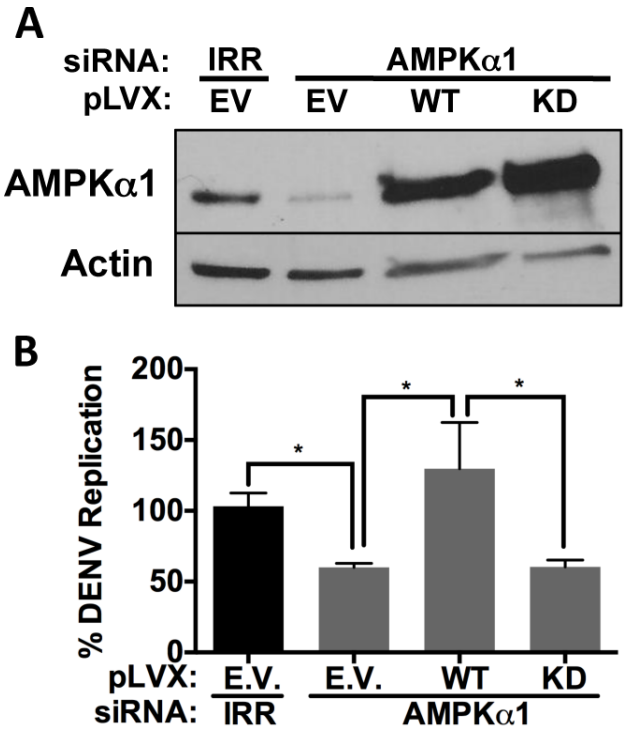

Figure 4. DENV replication requires AMPK kinase activity. HepG2 cells were transduced with lentiviruses derived from either the pLVX empty vector (EV), wild type (WT), or kinase dead (KD) AMPK, then treated with IRR or AMPK siRNAs. 72 hours post siRNA treatment, cells were infected with DENV, and (A) RNA was harvested 24hpi for qRT-PCR analysis or (B) protein lysates were harvested and subjected to immunoblot analysis for indicated proteins.

Inhibition of mTOR signaling during DENV infection is required to induce lipophagy.

Activated AMPK phosphorylates TSC2, which then inhibits mTORC1 activity (101). The requirement for AMPKa1 activity for DENV-induced lipophagy suggests that its regulation of mTORC1 activity may control this process. This model suggests that the constitutive activation of mTORC1 would prevent DENV-induced AMPK-dependent lipophagy. To test this model, we examined the effect of silencing TSC2 on DENV lipophagy. HepG2 cells were effectively depleted of TSC2 with two different siRNAs to control for off-target effects (Fig. 5A). Infection of HepG2 cells depleted of TSC2 showed a significant decrease in viral replication and

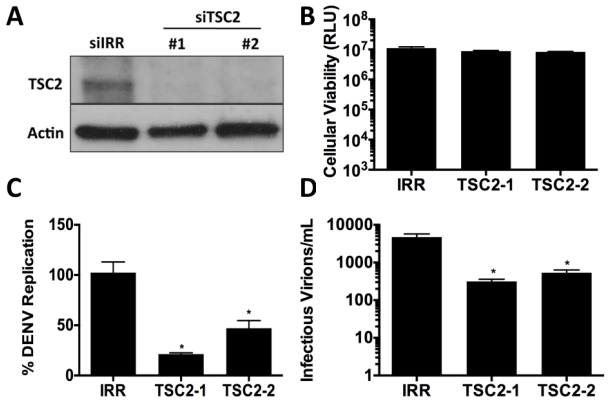

Figure 5. TSC2 silencing inhibits DENV replication. (A) TSC2 protein levels following treatment with IRR or two distinct TSC2 siRNAs. (B-D) siRNA-treated cells were DENV-infected at an MOI of 1. At 24hpi (C) RNA was harvested and analyzed for viral replication, and (D) supernatants were titered for infectious virus production. (B) HepG2 cells were assayed for cellular viability 72hrs post transfection with indicated siRNAs.

infectious virus release, with minimal effects on cellular viability, as compared with the infection of IRR siRNA-treated cells (Fig. 5B-D). Thus, depletion of TSC2 and the corresponding constitutive activation of mTORC1 inhibit DENV replication.

In parallel, we probed TSC2 silenced cells that were mock- or DENV- infected cells for markers of lipophagy. Immunofluorescent analysis of DENV-infected cells for endogenous LC3-II showed in an increase in autophagosome accumulation in IRR siRNA-treated cells as compared to mock-infected cells. This increase in autophagosome number was inhibited in TSC2-depleted DENV-infected cells (Fig. 6A,B). Additionally, TSC2 silencing blocked the significant depletion of lipid droplet area seen in DENV-infected, IRR-treated cells (Fig. 6C,D). Similar to the AMPK silencing phenotype, TSC2 silencing did not alter basal autophagy in mock-infected cells, as opposed to the positive control ATG12. Thus, TSC2 is required for robust DENV replication and the induction of lipophagy. This suggests that constitutively active mTORC1 blocks DENV-induced lipophagy and thus must be inactivated to initiate lipophagy.

DENV infection activates AMPK signaling.

Our previous experiments demonstrated a requirement of AMPK signaling for DENV-induced lipophagy. We next investigated whether DENV infection activates AMPK signaling. AMPK is a heterotrimeric complex composed of a, b, and g subunits, where the a subunit – the catalytic core of AMPK – is directly regulated by phosphorylation at threonine 172 (Thr-172) (85, 280). HepG2 cells were infected with DENV and the levels of AMPK and phospho-AMPK were probed over a time-course. We observe that although DENV infection does not alter AMPK protein levels, it results in an increase in phospho-AMPK accumulation at 12 and 24 hours post infection (Fig. 7a). Increased phospho-AMPK (Thr-172) is a correlate of AMPK activation in DENV-infected cells.

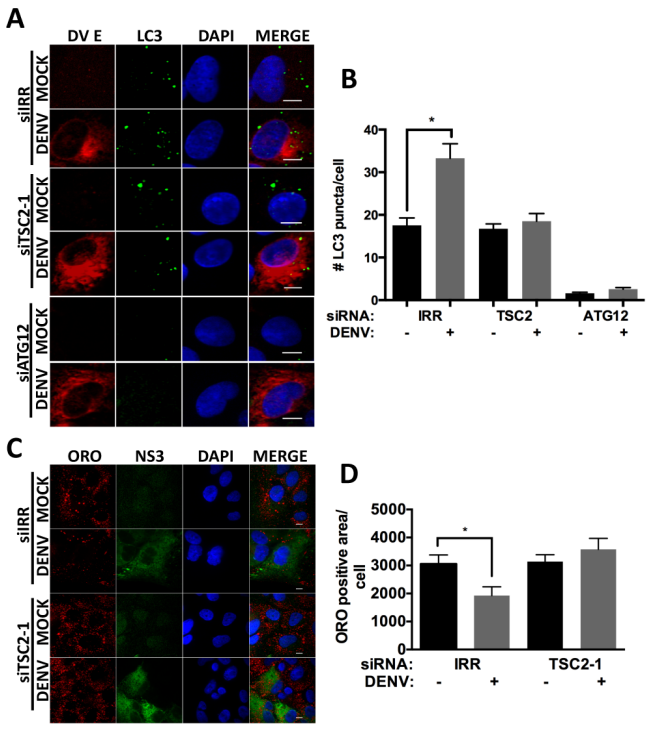

Figure 6. TSC2 silencing prevents DENV-induced lipophagy. siRNA-treated cells were DENV infected at an MOI 0.2 and fixed at 24 and 48hpi to probe for (A) DENV E LC3-II or (C) stain with ORO. Nuclei were stained with DAPI. Quantification of LC3-II puncta per cell (B) and LD area (D) was performed using ImageJ. Scale bar = 8μm.

To more directly test whether DENV infection stimulates AMPK activity, we determined the enzymatic activity of AMPK in crude cellular lysates (37). HepG2 cells were mock- or DENV-infected for 24 or 48 hours, lysed, and assayed for AMPK activation by radiolabeled phosphorylation of a peptide containing the AMPK

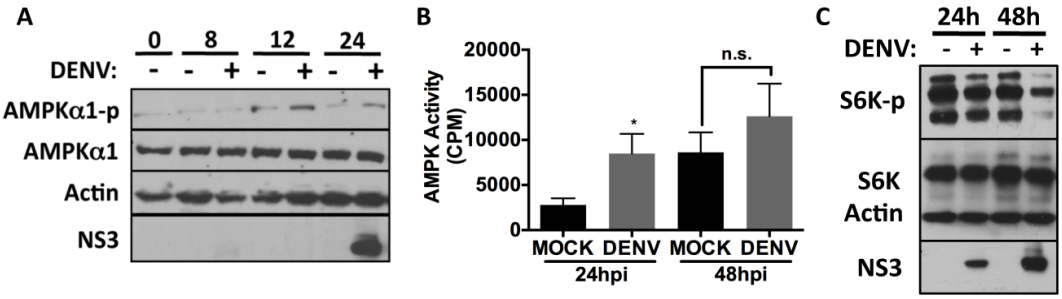

Figure 7. DENV infection activates AMPK and inhibits mTORC1 signaling. (A) HepG2 cells were infected with DENV at an MOI of 5. At the indicated times postinfection, cells were lysed and proteins extracted. Immunoblot analysis was performed to assess the levels of the indicated proteins. B) HepG2 cells were infected with DENV at an MOI of 10. Lysates (9mg) were harvested and assayed for AMPK activity. Samples were assayed in triplicate, and the mean +/- SEM was graphed. C) HepG2 cells were infected at an MOI of 5 for the indicated times and lysates were subjected to immunoblot analysis for indicated proteins.

phosphorylation site from its substrate, acetyl-coa carboxylase (ACC)) (37). Infection with DENV for 24h produced a three-fold increase in AMPK activity in DENV-infected cell lysates as compared to mock-infected cells (Fig. 7B). This activation was transient, as AMPK activity was only moderately elevated at 48 hours after DENV infection as compared the mock infected cells. Thus, DENV infection transiently enhances phospho-AMPK accumulation and AMPK enzymatic activity.

AMPK activation should inhibit mTORC1 activity. mTORC1 inhibition can regulate many processes, including the induction of autophagy and the loss of phosphorylation of the mTOR substrate p70 S6 Kinase (S6K), which regulates protein translation (26, 167). To test whether the activation of AMPK in DENV infection produced a corresponding decrease in mTORC1 activity, we examined the phosphorylation status of S6K at Thr-389 over a time course of DENV infection. We observed a decrease in phospho-S6K after 24 hours of DENV infection that further declined at 48 hours (Fig. 7C). Thus, DENV infection increases the accumulation of activated AMPK and produces a corresponding decrease in mTORC1 activity.

Cumulatively, these data demonstrate that DENV activates and requires AMPK to inactivate mTORC1, thus contributing to the induction of lipophagy.

Discussion

In this study, we investigated the role of AMPK in DENV-induced lipophagy and replication. We observed that AMPK is proviral for DENV replication. Inhibition of AMPK expression or kinase activity suppressed DENV replication and infectious virus production. Similarly, AMPK inhibition prevented the induction of lipophagy, as assayed by autophagosome number (LC3-II puncta) and lipid droplet depletion (ORO area). It is noteworthy that while AMPK inhibition prevented DENV-induced lipophagy, it did not affect basal autophagy under our experimental conditions. LC3-II puncta were unchanged in mock-infected cells by AMPK inhibition, while they were restored to basal levels in DENV-infected cells. In contrast, silencing the core autophagic component ATG12 inhibited autophagy in both mock- and DENV-infected cells.

Given the well-defined role of AMPK in mTORC1 inhibition (and the function of mTORC1 in autophagy suppression), we next tested the impact of constitutively activating mTORC1 on DENV-induced lipohagy. A common approach to studying mTORC1 activation is the silencing of the mTORC1 negative regulator TSC2. We observed that TSC2 silencing mirrored the phenotypes of AMPK inhibition. TSC2 silencing decreased DENV-induced lipophagy and replication. Similarly, TSC2 silencing did not affect basal autophagy. Thus, mTORC1 activation can inhibit DENV-induced lipophagy. The suppression of mTORC1 by AMPK is required for DENV-induced lipophagy and replication.

Our initial experiments defined a requirement for AMPK and TSC2 in DENV-induced lipophagy, but did not demonstrate that DENV activated this signaling pathway. We next examined the activation of AMPK in DENV infection in two assays. phospho-AMPK accumulation increased during DENV infection at 12 and 24h, which is consistent with the kinetics of lipophagy induction by DENV. To directly assess AMPK activity during DENV infection, we measured the AMPK activity in DENV-infected cell lysates and found it was increased during DENV infection as compared with mock-infected cells. Consistent with this data, DENV infection resulted in a decrease in mTORC1 activity. Accumulation of the mTORC1 product phospho-p70S6K decreased during DENV infection. Thus, DENV infection results in activation of AMPK and a concurrent inhibition of mTORC1. Although we demonstrate that mTORC1 inhibition is required for DENV-induced lipophagy, it is unknown how this may impact other functions of mTORC1, such as the regulation of protein translation.

As a central regulator of the cellular response to energy levels, AMPK has many known interactions with viruses (34). In some viral infections, AMPK exerts antiviral effects. AMPK is activated during Rift Valley fever virus and inhibits its replication by limiting fatty acid synthesis through inactivation of acetyl-CoA carboxylase 1 (ACC1) (188). AMPK also inhibits the replication of Sindbis virus, West Nile virus, and vesicular stomatitis virus in this manner. Hepatitis C virus and human immunodeficiency virus evade AMPK antiviral activity by preventing its activation (169, 301). Alternatively, AMPK can be proviral for many viral infections, including simian virus 40, avian reovirus, and vaccinia virus (33, 140, 187). Human

cytomegalovirus (HCMV) requires AMPK and activates it in a way that does not inhibit fatty acid synthesis, which is typically the result of AMPK activation (173). This requires the AMPK activator, calmodulin-dependent protein kinase kinase (173). CaMKKb-dependent activation of AMPK is also required for rotavirus-induced activation of autophagy (35). Interestingly, activation of AMPK was determined to be a major determinant of cellular permissiveness for rotavirus infection (68).

DENV has a sophisticated modulation of cellular lipid metabolism. Early during DENV infection, lipid droplets are reabsorbed into the endoplasmic reticulum (ER), possibly contributing to the formation of viral replication compartments (211, 265). When DENV infection proceeds under excess serum levels, lipid droplet area increases, which is consistent with an increased uptake and storage of extracellular lipids (211, 231, 265). Alternatively, when serum levels are lower, thus limiting lipid uptake, lipid droplet area decreases during DENV infection due to their depletion by lipophagy (89). This results in increased b-oxidation levels and presumably, an enhanced cellular energetic state (89). Thus, DENV appears to be enhancing lipid metabolic flux both in uptake from serum and subsequent mobilization via lipophagy resulting in increased b-oxidation levels. In parallel, DENV also induces fatty acid synthesis at sites of viral replication (the ER) (88), which would presumably be incompatible with AMPK activation (188). We envision three possibilities for the activation of both catabolic (AMPK-activated lipophagy) and anabolic (fatty acid synthesis) pathways in DENV infection. There could be mechanistic similarities between HCMV, which also activates AMPK and fatty acid

synthesis, and DENV. Alternatively, lipophagy and fatty acid biosynthesis could be either spatially separated into distinct subcellular compartments or kinetically separated at different stages of infection.

The mechanism by which DENV activates AMPK, leading to the induction of autophagy, is unknown. Lipophagy is induced by and required for subgenomic DENV replication, suggesting that the nonstructural proteins 1-5 are sufficient for its induction. However, expression of individual DENV NS proteins fails to induce lipophagy (data not shown), suggesting that either multiple viral proteins are involved or that lipophagy may be, in part, a cellular response to DENV replication. Future studies will investigate the role of DENV proteins in AMPK activation and the targeting of autophagosomes to the lipid droplet during DENV replication.

Chapter III. TGFβ-TAK1 dependence of DENV-lipophagy

Abstract

Dengue virus–induced autophagy degrades lipid droplets (LDs) in an AMPK-mTORC1 signaling-dependent fashion (Chapter II). In this chapter, we extend our studies and examine upstream molecules involved in activating this pathway. RNAi-mediated silencing and pharmacological inhibition of the upstream AMPK kinase (AMPKK) transforming growth factor beta (TGFβ)-activated kinase 1 (TAK1) blocks dengue virus-induced autophagy and LD depletion. Interestingly, silencing or inhibition of TAK1 does not block viral replication. However, the mechanism by which this occurs remains obscure. We find that infection of HepG2s activates TGFβ receptor (TβR) signaling, an upstream activator of TAK1. Inhibition of TGFβ signaling by pharmacological means or RNAi silencing of the type I and type II TβRs blocks DENV-induced lipophagy, and also compromises viral replication. Signaling through TGFβRs for DENV-lipophagy requires exogenous TGFβ, although TGFβ itself is insufficient for lipophagy induction. While inhibition of TAK1 and TGFβ signaling is sufficient to block DENV-induced lipophagy, they do not block Ca^{2+}-induced autophagy displaying the specificity of this pathway.

Introduction

As obligate intracellular pathogens, viruses must re-wire the host cell to establish an optimal niche for their replication. The evasion of host immune pathways and the physical reorganization of cellular membranes/organelles are prime examples of this manipulation. In the last decade, growing evidence has demonstrated the importance of re-wiring host metabolism for robust viral

replication (66, 226). For dengue virus to achieve robust replication the virus must modulate host glycolytic flux and lipid metabolism (55, 88, 89, 212). Previous research in our lab illustrated that the induction of autophagy was one way DENV modulates lipid metabolism (89). DENV infection leads to an induction of autophagy that degrades lipid droplets, which are cellular organelles rich in triglycerides and cholesterol esters. Degradation of these triglyceride stores results in the liberation of free fatty acids, which are then shunted to the mitochondria for fatty acid β–oxidation (89). In the previous chapter we showed that the induction of autophagy requires activation of and signaling through AMPK, however it remains unclear how AMPK is activated during DENV infection.

Signaling through AMPK is important for the integration of various cellular stresses (reviewed in (82)). Principally, AMPK is a sensor of intracellular ATP levels through its binding of AMP and ADP (67, 202, 292). Binding of these adenylate nucleotides increases the activity potential of AMPK such that increased AMP and ADP concentrations in the cell can lead to increased AMPK activity. Additionally, activation of AMPK is regulated by several post-translational modifications; among these is phosphorylation at threonine 172 (85, 280). There are three known AMPK kinases (AMPKKs) – Liver Kinase B1 (LKB1), Calmodulin kinase kinase β (CaMKKβ), and transforming growth factor β-activated kinase 1 (TAK1) – that carry out this phosphorylation. LKB1 is responsible for the activation of AMPK under conditions of low intracellular ATP concentrations, and in many cell types contributes to the majority of AMPK phosphorylation. CaMKKβ is activated by increased intracellular Ca^{2+} levels, such as ER stress, and has been shown to be important for the activation

of autophagy by rotavirus (35). HCMV activates AMPK in a CaMKKβ-dependent manner as well, though the important output is glycolytic flux and not autophagy (173, 174). Unlike CaMKKβ and LKB1 whose direct interaction with and activation of AMPK is well established, the physiological role of TAK1 as a direct activator AMPK is controversial. While initial work showed that TAK1 was sufficient to activate the yeast orthologue of AMPK, Snf1, and that TAK1 interacts with and can phosphorylate AMPK, subsequent work has suggested that the role of TAK1 in activating AMPK is LKB1-dependent (182, 293). Whether this is cell-type or signal dependent remains unresolved. Nevertheless, TAK1 has been shown to be important for TRAIL-induced autophagy in epithelial cells in an AMPK, but non-LKB1 dependent manner (90).

TAK1 is a MAPKKK whose activation is dependent upon signaling from plasma membrane cytokine receptors that activate several E3 ligases which directly ubiquitinate TAK1 (reviewed in (36, 230)). IL1βR, TNFR, and TGFβR have been shown to activate TAK1 through the recruitment and activation of TRAFs 2, 5, and 6 (230). These TRAFs ubiquitylate TAK1 with K63-linked ubiquitin chains at distinct lysine residues in a context-dependent manner. Activation of TAK1 leads to signaling through ERK, MEK, JNK, and MKK MAPK pathways, as well as activation of pro-inflammatory NFκB. TAK1 can also shift the balance between apoptosis and necroptosis in cells stimulated with TNFα and TRAIL (65). While the main roles studied for TAK1 have been related to immunity and inflammation, recent work has shown that deletion of TAK1 in mouse livers leads to decreased autophagy, lipid droplet turnover, and β-oxidation demonstrating additional roles for TAK1 in the

cell (102). Activation of TAK1 in livers has also been linked to inhibiton of the lipid homeostatic transcription factors SREBP-1 and -2 (185).

TAK1 has a complex interplay with many viruses. As a mediator of NFκB and interferon signaling in response to viral infection, TAK1 is potently antiviral and suppressing its activation is an immune evasion strategy for several viruses. Yet, for viruses such as HTLV-1, HIV-1, KSHV, and EBV activation of TAK1 can also benefit the virus (91, 164, 217, 288, 290). During HIV-1 infection, Gag, Nef, and Vpr can activate TAK1 signaling (83, 164, 217). Activation of TAK1 leads to subsequent activation of NFκB, which can drive reactivation of proviral HIV-LTRs leading to increased virus replication and production (164, 217). However, TAK1 is an important mediator of TRIM5α and Tethrin mediated restriction of HIV-1, as it is required for downstream transcription of interferon-β and establishment of the antiviral state (57, 214).

TGFβ is a pleiotropic cytokine that has diverse functions depending on the cellular context (84, 170). Binding of the mature, secreted cytokine to its heterodimeric receptor is a two-step process (287). First, dimeric TGFβ binds to two TGFβ type II receptor (TβR2) molecules. The binding of TGFβ to TβR2 induces a conformational change which allows for the binding of TβR2 to the type I TGFβ receptor (TβR1) - ALK2 or ALK5, depending on the cell type. Both TβRs I and II are serine/threonine kinase. TβR2 is constitutively active, and when TGFβ binding brings it into proximity to TβR1, TβR2 phosphorylates and activates TβR1 . Activation of TβR1 leads to kinase-dependent and independent signaling (reviewed in (84, 189)). TβR1 phosphorylation activates the SMAD2/3 transcriptional

regulators, resulting in their nuclear translocation and transcriptional activation. The TGFβ:TβR2:TβR1 complex also serves as a scaffold for the recruitment of TRAF6, which ubiquitinates and activates TAK1 to induce MAP3K signaling that occurs downstream of TGFβ binding (254). Ablation of a TRAF6 binding motif in TβR1 (ALK5 specifically) blocks the recruitment of TRAF6 and activation of TAK1 and downstream MAPK signaling (254).

In this chapter, we show that DENV-induced lipophagy depends on the AMPKK TAK1, and TGFβ signaling through the TβR complex. Inhibition of TAK1 and TβR signaling blocks DENV-induced autophagosome formation and lipid droplet depletion. The blockade of DENV-induced lipophagy is not the result of a non-specific block in the autophagy process, as inhibiting TAK1 or TβR signaling does not block Ca^{2+}-induced autophagy via ionomycin treatment. Blocking the interaction of TGFβ with its receptor also blocks DENV-induced lipophagy. However, while TGFβ is necessary for DENV-induced lipophagy, TGFβ is not sufficient to drive lipophagy. Thus, while TAK1 and TβR signaling is required for DENV-induced lipophagy, the originating signal for this process still remains obscure.

Materials and Methods

Lentivirus pseudoparticle production and transduction. pLVX-based lentivirus pseudoparticles were generated by transfecting HEK293T cells with HIV-1 gag/pol, VSV-G, and pLVX containing the transgene of interest. Briefly, ~70-80% confluent p100 dishes of HEK293Ts were transfected with 12ug of pLVX, 4ug of HIV-1 gag/pol, and 2ug of VSV-G using Lipofectamine 2000 according the manufacturer's specifications. Forty-eight hours after transfection, the supernatants were collected

and cell debris was spun down at 1,200xg for 5 minutes before filtering the clarified supernatant through a 0.22um filter. HepG2 cells were transduced with lentivirus stocks by centrifugation (4,000xg for 1 hour at 32^{o}C). Transduced cells were allowed a minimum of 24 hours before further manipulation.

Lentivirus Transcomplementation. 24 hours after transfection with siRNAs, HepG2 cells were transduced with lentivirus particles as described above. To determine successful complementation, cells were harvested and subjected to Western Blot analysis, or fixed for immunofluorescence analysis as detailed below.

Neutralizing antibody studies. TGFβ neutralizing antibody 1d11 (R&D Systems) or an IgG isotype control was added at the indicated final concentration to the mock or DENV inoculum for 5 minutes before infection of HepG2. After virus adsorption on to cells (1 hr) cells were washed with PBS and 5% media added with the same amount of TGFβ or IgG antibody. Infection proceeded, and samples were processed as required for the appropriate assay. To ensure neutralization of TGFβ was effective, HepG2 cells were seeded onto coverslips in parallel and treated with 1ng/mL of TGFβ in the presence or absence of neutralizing antibody. After 12h, cells were fixed with paraformaldehyde and examined for SMAD2 localization to the nucleus (αIgG) or retention in the cytoplasm (αTGFβ).

Plasmids. The TAK1, ALK5, and TGFβR2 expression constructs were obtained from Addgene (#23693, #19161, #19158, respectively). The TAK1 construct was cloned in-frame into pCMV-3xFLAG-HBT behind the 3xFLAG site. Briefly, the pCMV-3xFLAG-HBT plasmid was digested with BamHI and XhoI. TAK1 was amplified using the forward (5'-GATGACAAGGGATCCatgtctacagcctctgccgc-3') and reverse (5'-

gcagaaacgacaaggcacttcatgaCTCGAGTCTAGAGGG-3') primers. High-fidelity Phusion DNA polymerase (Finnzymes) was used. TAK1 inserted using the In-Fusion Cloning Kit (Clontech) making use of the BamHI and XhoI restriction sites. RNAi-resistant clones of ALK5 and TGFbR2 were prepared by PCR amplification of two segments of the gene and inserting mutations into the siRNA seed region and throughout the siRNA; ALK5: (gg**agc**gt**t**ac**g**ac**t**ac**c**t) TGFBR2: (cc**tcg**aa**c**ccc**a**ga**tc**t) bold indicates mutation. For all RNAI-resistant constructs, the amplified gene segments were combined via overlap PCR and then the In-Fusion Cloning Kit was used to insert the full-length genes into the lentivirus vector pLVX, digested with XbaI and EcoRi. Individual mutants of each gene were made on the RNAi resistant-pLVX background.

Real-time RT-PCR. RNA was extracted from cells grown in 96-well plates by RNeasy 96 Kit (Qiagen), per manufacturers instructions. Extracts were reverse-transcribed and PCR amplified by using the Superscript III Platinum One-Step RT-PCR system with Platinum Taq (Life Technologies) as previously described. DENV RNAs were amplified using 300 nM forward primer (5'-TCCCAAACGCAGTGATATTACAA-3') and 300 nM reverse primer (5'-TGAGACCTTTGATCGTCAATGC-3'), and 200 nM probe (5'-6FAM-TGGTGTCCGTTTCCCCACTGCTCTT-IowaBlack-3') (Integrated DNA Technologies) which recognizes NS2A of DENV 16881. Parallel reactions were ran with 0.8X amount of 18s rRNA TaqMan gene expression assay as a control (Hs01021073_m1; Applied Biosystems). Reverse transcription-PCR (RT-PCR) was programmed for 50^{o}C for 30 min, 95^{o}C for 6 min, and then 50 cycles of 95^{o}C for 15s, 60^{o}C for 30s, and

72°C for 15s using an ABI 7300 system (Applied Biosystems). Data were analyzed with SDS v1.4 software (Applied Biosystems) and normalized to 18s controls. Relative quantification was calculated comparing the cycle threshold (C_T) values using $2^{-\Delta\Delta CT}$.

Immunofluorescence microscopy. Glass coverslips in 24-well dishes were seeded with 70,000 cells. All washes and reagents were prepared in 1× PBS (pH 7.5) and used at room temperature. The cells were fixed with 4% paraformaldehyde (15 min) at 4°C. Cells were blocked and permeabilized with 30% Goat serum and 0.1% Saponin for 30 minutes. Primary antibodies in 10% goat serum and 0.1% saponin were incubated overnight at 4°C. anti-FLAG(M2), anti-HA, anti-6xHIS (Sigma), anti-LC3b (Cell Signal), and anti-DENV E (ATCC) antibodies were used at 1:1000, anti-NS3 antibody was used at 1:3,000, and anti-SMAD2 (Cell Signal) antibody was used at 1:400. Fluorescent-conjugated secondary antibodies were incubated with cells in 10% goat serum and 0.1% saponin for 1 hr. Alexa Fluor 488 or 594 secondary antibodies (Invitrogen) were used at 1:2,000 and Alexa Flour 350 secondary antibody was used at 1:600. When Alexa Fluor 350 was not in use, coverslips were mounted in ProLong Gold AntiFade with DAPI (4′,6′-diamidino-2-phenylindole) nuclear stain (Invitrogen). When Alexa Fluor 350 was used, coverslips were mounted in ProLong Gold Antifade (without DAPI), and no nuclei were visualized. The samples were imaged using an Olympus DSU spinning disc confocal microscope equipped with a Photometrics Evolve EMCCD camera. Digital images were taken using Slidebook v6.0 software and processed using ImageJ (National Institutes of

Health). Quantification of fluorescence intensity was determined from multiple images taken from duplicate coverslips using ImageJ.

Western blot analysis. Adherent cells were washed twice in ice-cold phosphate-buffered saline (PBS), lysed in NP-40 lysis buffer (50mM Tris-HCl pH 8.0, 150mM NaCl, 1% NP40, 2mM EDTA, 10% glycerol, 10mM NaF, and protease inhibitors (Roche Protease Inhibitor Cocktail)), proteins quantified using the BioRad Protein Quantification Dye, and boiled in SDS sample buffer. Proteins were separated on 4-20% SDS-PAGE gels (Lonza, Inc.) and transferred to PVDF. After being blocked in 10% BSA (1× PBS, 0.1% Tween 20), primary antibodies were added overnight at 4°C. Horseradish peroxidase-conjugated secondary antibodies were added for 60 min in 5% dry milk and included goat anti-rabbit (catalog no. 31462; Thermo Scientific) and rabbit anti-mouse (catalog no. 31452; Thermo Scientific), which were detected using SuperSignal-Femto or Pico chemiluminescent substrate (Pierce-Thermo Scientific) and exposure to film (HyClone). The primary antibodies used included anti-FLAG(M2), anti-HA, anti-6xHIS, anti-actin (Sigma), anti-TAK1, TAK1 pT184/187, AMPK, AMPK pT172, S6K, S6K pT139/140, anti-ALK5 (Cell Signal), anti-TBRII (abcam).

Luciferase assays. For luciferase reporter assays, the Renilla Luciferase Assay System (Promega) was used according to manufacturer's specifications and assayed in a single-read manual luminometer (Turner Biosystems).

si- and shRNAs. TAK1 (s13767, 5'-AGAUACCAAUGGAUCAGAUtt-3'), ALK5 (s229437, 5'-CCAUUGAUAUUGCUCCAAAtt-3'; s229438, 5'-GGUCUGUGACUACAACAUAtt-3'), TGFBR2 (s14077, 5'-CCAGCAATCCTGACTTG-3'),

CAMKK2 (s20925, 5'-GGCACAUCAAGAUCGCUGAtt-3'), and LKB1 (s13579, 5'-GGCUCUUACGGCAAGGUGAtt-3') siRNAs were ordered from Ambion. An shRNA targeting the 3'UTR of TAK1 (5'-CCGG**GCAGTGTATTCTTGGATTGTTT**CTCGAG**AAACAATCCAAGAATCACTGC**TTTTT T-3'; bold is TAK1 targeted sequence) was obtained from Sigma-Aldrich. shRNA pseudoparticles were generated the same as pLVX-based lentivirus pseudoparticles mentioned above.

RNA interference (RNAi) analysis. RNAi assays were performed as described previously. For immunofluoresence analysis and knockdown efficiency, 70,000 cells were transfected with 24pmol of the indicated siRNA and seeded on glass coverslips in 24-well plates. For viability, viral replication, and infectious virus release assays, 12,000 cells were transfected with 8 pmol of indicated siRNA in quadruplicate, and seeded into 96-well plates. For experiments examining cell signaling, either 100,000 cells were transfected with 48pmol of siRNAs in 12 well plates or 250,000 cells were transfected with 80pmol of siRNAs in 6-well plates. In all cases, cells were incubated with siRNAs for 72 hours before being infected with DENV or harvested for viability or Western Blot analysis.

Infectious Virus Production Assay. Cells were infected 72 hours after siRNA-treatment, or simultaneous with drug treatment at an MOI of 0.5-2 infectious DENV particles (DENV-2 16681) per cell for 2 hours, and maintained for 24 hours at 37^{o}C. Cell culture supernatants were titered by limiting dilution analysis via immuno-histochemistry using monoclonal anti-E antibody (4G2; ATCC) as described.

Statistical analysis. Data are presented as means ± the standard errors of the mean (SEM). To assess statistical significance, two-tailed, unpaired Student *t* tests were performed.

Results

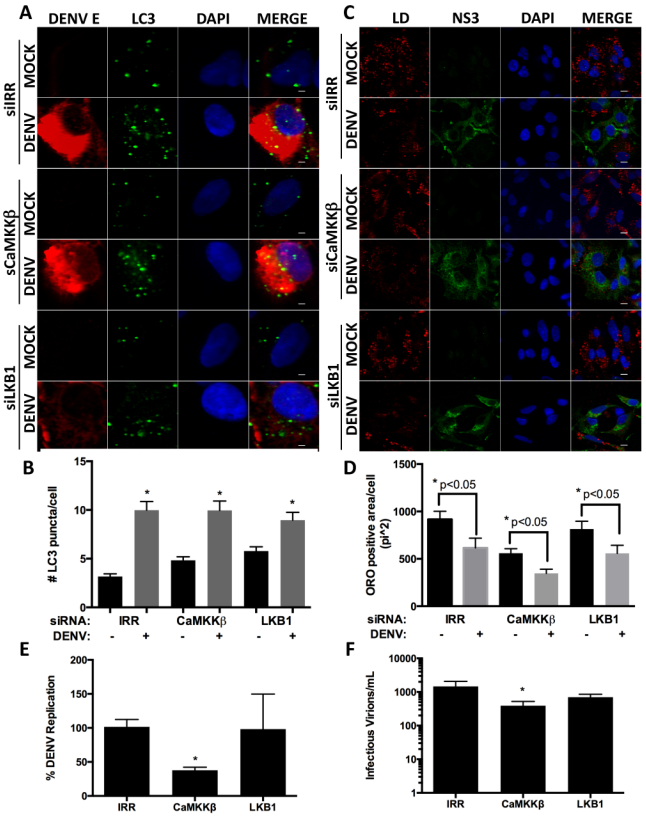

Figure 8. Knockdown of CaMKKβ and LKB1 do not impact DENV lipophagy. A and C) HepG2 cells were transfected with siRNAs against CaMKKβ and LKB1 as described in Methods section. HepG2 cells were Mock or DENV infected at an MOI of 0.5 for 24 or 48 hours, and then fixed and stained for endogenous LC3 puncta (A) or LD area (ORO; C), respectively. E-F) siRNA-treated HepG2 cells were infected with DENV at an MOI of 2. After two hours, media was changed to 5% DMEM. 24hpi RNA was harvested for TaqMan qRT-PCR assay for viral RNA levels (E) and supernatants were harvested to measure infectious virus released (F) by limiting dilution titer. Images were quantified using ImageJ and data was graphed using Prism. Error bars represent standard error.

TAK1 is required for DENV-induced lipophagy

The activation of AMPK can occur through the action of at least three upstream kinases – Liver Kinase B1 (LKB1), Calmodulin-activated kinase kinase β, (CaMKKβ) and transforming growth factor β-activated kinase 1 (TAK1). To further understand the signaling pathway DENV utilizes to initiate lipophagy induction during infection, we assessed the contribution of the known AMPK kinases to DENV replication and lipophagy. RNAi knockdown of LKB1 had no effect on autophagy induction and lipid droplet depletion in DENV-infected cells or viral replication (Fig. 8A-F). Knockdown of

CaMKKβ also did not block autophagy induction or lipid droplet depletion (Fig 8A-D), however CaMKKβ knockdown did block viral replication (Fig 8E-F). RNAi knockdown of TAK1 inhibited autophagy induction in DENV-infected cells as compared to infected cells treated with an irrelevant siRNA (Fig. 9A-B). Similarly, infected cells treated with TAK1 siRNAs were not depleted of LDs (Fig. 9C-D). Treatment of cells with the TAK1 inhibitor (5z)-7-oxozeaenol (5z7) also inhibited autophagy induction and LD depletion during DENV infection (Fig. 10A-D).

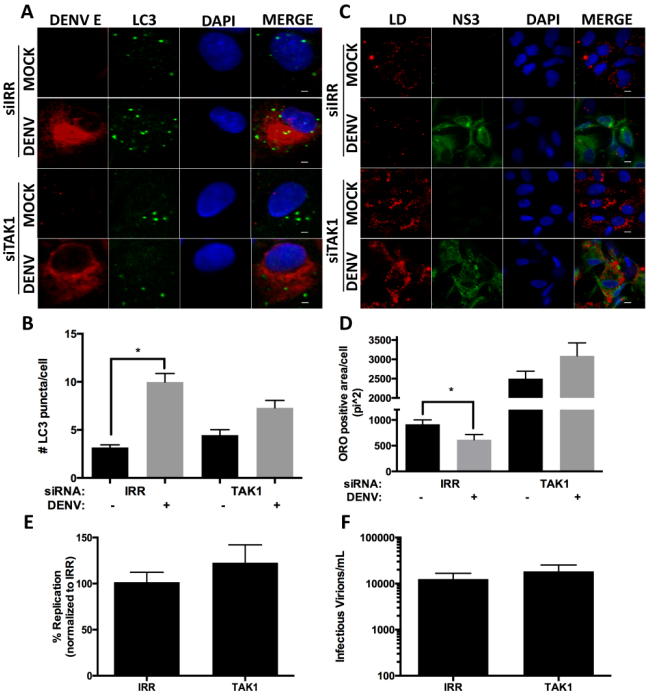

Figure 9. Knockdown of TAK1 blocks DENV lipophagy. A and C) HepG2 cells were transfected with an siRNA against TAK1 as described in Methods section. HepG2 cells were Mock or DENV infected at an MOI of 0.5 for 24 or 48 hours, and then fixed and stained for endogenous LC3 puncta (A) or LD area (ORO; C), respectively. Images were quantified for LC3 puncta (B) or LD area (D) using ImageJ and data was graphed using Prism. Error bars represent standard error. * = $p < 0.05$ E-F) HepG2 cells were transfected with siRNAs against TAK1 or an irrelevantly target sequence (IRR), and infected as described above for A and C. E) TaqMan qRT-PCR, and F) infectious virus production.

RNAi knockdown or inhibition of TAK1 in our experiments resulted in a general increase in the average LD size and total LD area in treated cells as compared to controls (Figs 9D and 10D). This is in line with recently published work that shows TAK1 plays an important role in lipid homeostasis in the liver through modulation of autophagy and β-oxidation (102). Inhibition of TAK1 can also

lead to increased activation of SREBP transcription factors, which control fatty acid (SREBP1) and cholesterol (SREBP2) biosynthesis (185).

Inhibition of TAK1 does not block DENV replication

Surprisingly, inhibiting TAK1 either by RNAi knockdown or pharmacological treatment reproducibly showed no decrease in DENV replication (Figs. 9E-F and 10E-F), and often small increases in viral replication. This suggests that other downstream targets of TAK1 may possess potent antiviral capacities that counterbalance proviral induction of lipophagy. TAK1 signaling can activate NFκB, a potent pro-inflammatory mediator. However, treatment of infected cells with the NFκB inhibitor Bay 11-7082 showed a dose-dependent inhibition in viral replication, suggesting a pro-viral role for NFκB in DENV replication (Fig. 11A-B). We next investigated other signaling pathways downstream of TAK1. TAK1 is a MAPKKK that can signal

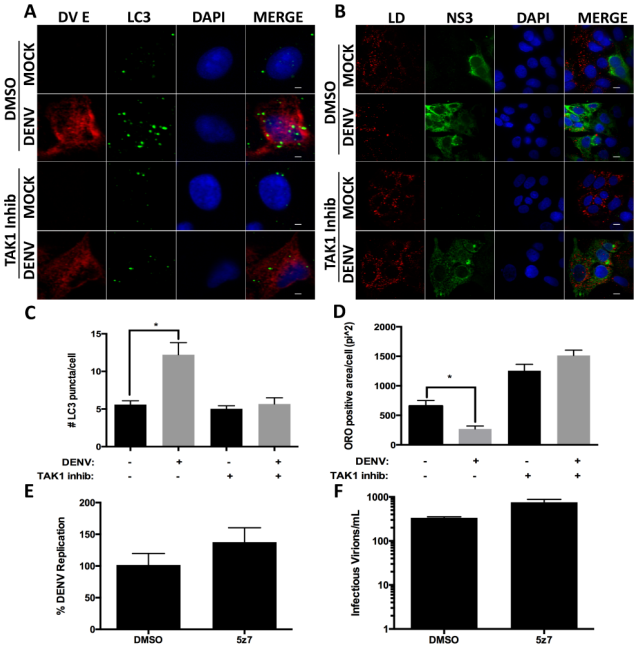

Figure 10. Inhibition of TAK1 blocks DENV lipophagy. A and C) HepG2 cells were incubated with an inhibitor of TAK1 (5z7-oxoaezenol) at 1μM for the duration of the experiment. HepG2 cells were Mock or DENV infected at an MOI of 0.5 for 24 or 48 hours, and then fixed and stained for endogenous LC3 puncta (A) or LD area (ORO; C), respectively. Images were quantified for LC3 puncta (B) or LD area (D). E-F) HepG2 cells were infected in the presence of DMSO or 5z7 (TAK1 inhibitor). After virus adsorption period (two hours), HepG2 cells were washed with PBS and media was changed to 5% DMEM. 24hpi E) RNA was harvested for TaqMan qRT-PCR of DENV RNA levels, and F) supernatants for infectious virus enumeration by limiting dilution titering. Images were quantified using ImageJ and data was graphed using Prism. Error bars represent standard error. * = $p < 0.05$

through ERK, JNK, and MEKK MAPK cascades when activated, as well as the AP-1 transcription factor. To this end, we treated cells with inhibitors to ERK, JNK, and MEKK MAPK cascades as well as an inhibitor of the AP-1 transcription factor, which is downstream of TAK1 signaling. Inhibition of these pathways did not effect DENV replication (Fig. 11C-D).

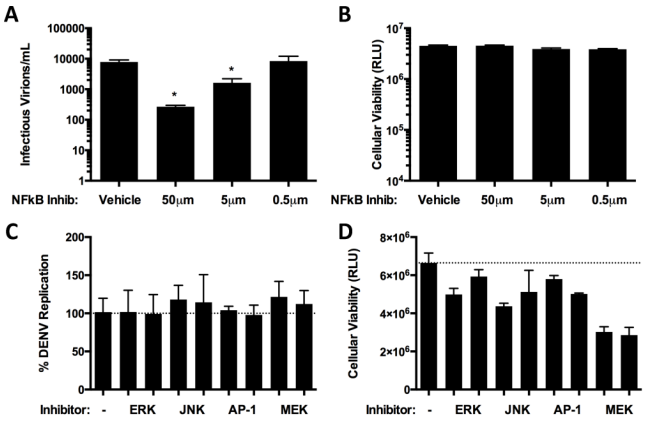

Figure 11. Effect of Inhibiting TAK1 downstream targets on DENV replication. A-B) NFκB inhibition blocks DENV replication. HepG2 cells were infected with DENV at an MOI of 1 and simultaneously treated with varying doses of the NFκB inhibitor Bay-11-7082. A) 24hpi supernatants were harvested and assessed for infectious virus release by limiting dilution titering. B) Cellular viability was assessed using Promega CellTiterGlo kit according to the manufactures instructions. C-D) TAK1 MAPK signaling does not affect viral replication. HepG2 cells were infected with DENV and simultaneoulsy treated with inhibitors to the designated targets (UO126 – MEK1/2; SP600125 – JNK 1/2; SR11302 – AP-1; FR180204 – ERK1/2). After virus adsorption, media was changed to 5% DMEM with the appropriate inhibitor. C) 24hpi RNA was harvested for TaqMan qRT-PCR of DENV RNA levels. D) Cellular viability was assessed using Promega CellTiterGlo kit according to manufacturers instructions.

TGFβ signaling is activated during DENV infection

Activation of several upstream plasma membrane cytokine receptors leads to signaling through TAK1, one of which is the TGFβ receptor (TβR) complex. Previous literature in a mouse model of cleft palate suggested that deletion of *TGFBR2* lead to a spontaneous accumulation of lipid droplets, suggesting a link between TGFβ signaling and lipid metabolism (105). Research in this model has suggested that both restoring lipid metabolism and modulating downstream MAPK signaling were sufficient to restore proper palate development (104, 105). To determine whether TGFβ signaling plays a role in DENV-induced lipophagy, we first assessed whether

TGFβ signaling activity is increased in DENV-infected cells. Activation of TGFβ leads to the activation and translocation of SMAD2/3 transcription factors to the nucleus, where they drive the expression of hundreds of genes. We transfected HepG2 cells with a luciferase reporter construct where a 4x tandem repeat of the SMAD-binding element drives luciferase expression (SBE4-luc; Fig 12A) in the presence of TGFβ, and is dependent upon signaling through the TβR complex (Fig. 12B) Infection with DENV lead to an increase in TGFβ-dependent luciferase reporter activity compared to mock infected cells (Fig. 12C). When infected cells were incubated with an inhibitor to TβR signaling, this increase was abolished

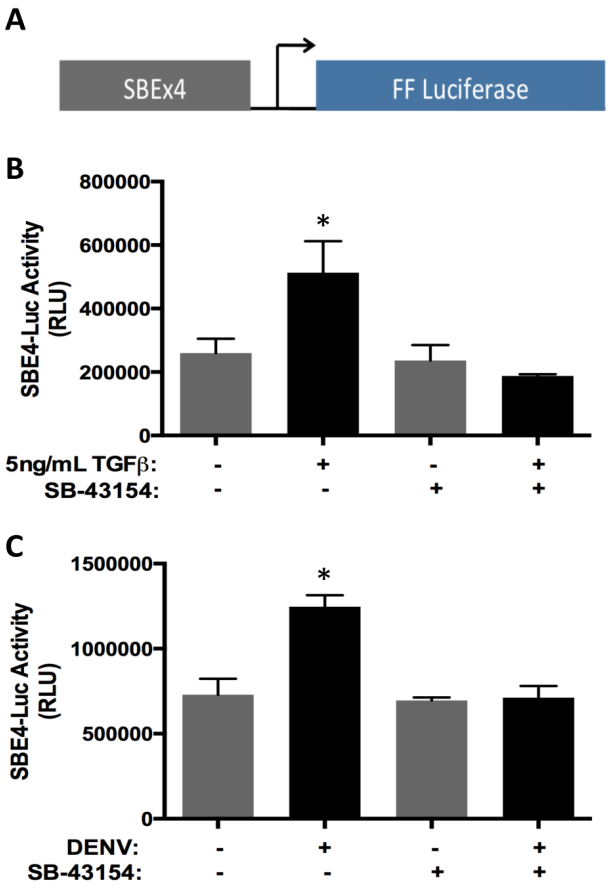

Figure 12. DENV infection increases TGFβ activity. A) Schematic representation of plasmid used. B) HepG2 cells were transfected with SBE4-Luc reporter plasmid (in A). 24hpt, HepG2 cells were treated with carrier (4mM HCl) or 5ng/mL of TGFβ in the presence or absence of SB-43154 for 12 hours. HepG2 cells were harvested and processed for luciferase readings according the Promega Luciferase Assay System kit instructions. C) HepG2 cells were infected at an MOI 5 with DENV in the presence or absence of SB-43154, and 6hpi transfected with the SBE4-Luc reporter plasmid. 30 hours post infection, HepG2 cells were harvested for luciferase readings as described above. SB-43154 was maintained throughout experiment.

demonstrating that the increased reporter activity was dependent upon TβR signaling (Fig. 12C).

*TGF*β *signaling is required for DENV-induced lipophagy*

We next assessed whether components of the TβR were important for DENV-induced lipophagy. The TβR complex is composed of two heterodimeric sets of the type I TGFβ receptor (TβR1) and type II TGFβ receptor (TβR2) (287). Both TβR1 and TβR2 are serine/threonine kinases. TβR2 is constitutively active and, upon binding TGFβ, binds and phosphorylates TβR1 leading to the latter's activation (287). The ctivated TβR1s are then competent to signal through downstream pathways (e.g., SMAD transcription factors or MAPK signaling cascades).

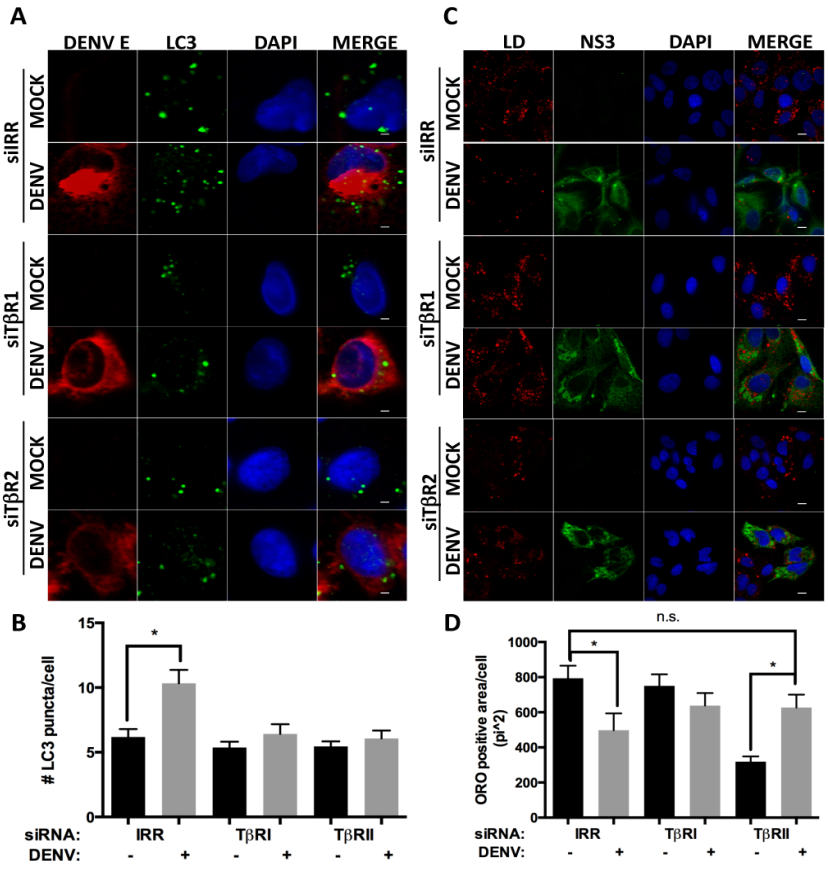

Figure 13. Knockdown of TβR1 and TβR2 block DENV lipophagy. A and C) HepG2 cells were transfected with siRNAs against TβR1, TβR2 or an irrelevantly target sequence (IRR) as described in Methods section. HepG2 cells were Mock or DENV infected at an MOI of 0.5 for 24 or 48 hours, and then fixed and stained for endogenous LC3 puncta (A) or LD area (ORO; C), respectively. Images were quantified using ImageJ and data was graphed using Prism. Error bars represent standard error. * = $p < 0.05$

To evaluate whether signaling through TβR1 is important for DENV-lipophagy, we used RNAi to knockdown TβR1, the predominant type I receptor in non-endothelial cells. Knockdown of TβR1 blocked autophagy induction during DENV infection as compared to mock-infected HepG2 cells (Fig. 13A-B). This led to an inhibition of LD depletion in DENV infected cells (Fig. 13C-D). Since there are known instances of TβR2-independent TβR1 signaling, we next asked whether TβR2 and TGFβ itself were important for DENV lipophagy. RNAi-mediated knockdown of TβR2 inhibited increases in LC3 puncta number, and LD depletion in DENV-infected cells, suggesting that TGFβ activation of TβR1 through TβR2 is involved in DENV-induced lipophagy (Fig. 13A-D). Inhibition of TβR1 activity with the inhibitor SB-43154 also blocked LC3 puncta formation and LD depletion in DENV infected cells (Fig 14A-D), further confirming the requirement of TGFβ signaling.

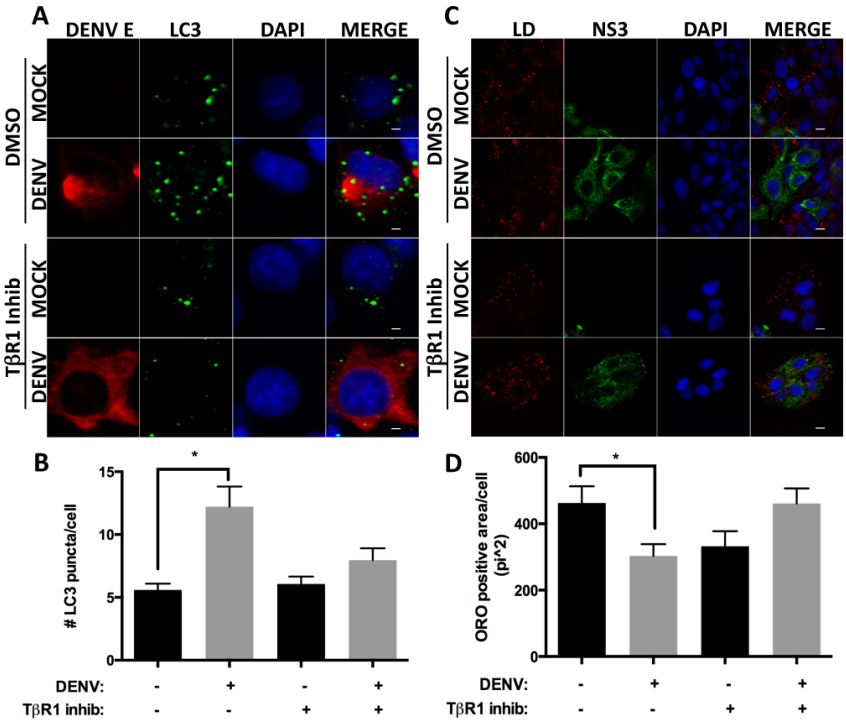

Figure 14. Inhibition of TβR1 signaling blocks DENV lipophagy. A and C) HepG2 cells were incubated with an inhibitor of TβR1 kinase activity (SB-43154) at 1mM for the duration of the experiment. HepG2 cells were Mock or DENV infected at an MOI of 0.5 for 24 or 48 hours, and then fixed and stained for endogenous LC3 puncta (A) or LD area (ORO; C), respectively. Images were quantified for LC3 puncta (B) or LD area (D) using ImageJ and data was graphed using Prism. Error bars represent standard error. * = $p < 0.05$

TGFβ is required for DENV-induced lipophagy

To directly test whether TGFβ is involved in DENV-lipophagy, we utilized a neutralizing antibody to block TGFβ interaction with TβR2. Treatment of cells with blocking antibody and TGFβ inhibits the nuclear translocation of SMAD2 that is seen when cells are treated with TGFβ and a control IgG antibody, showing that the antibody is capable of neutralizing exogenous TGFβ (Fig. 15A). TGFβ neutralizing antibody or an IgG control was added at the time of infection and maintained in the media throughout the time of the experiment. In infected cells treated with TGFβ neutralizing antibody, the number of LC3 puncta was decreased compared to IgG control antibody levels, and reduced to the level of uninfected controls. Treating cells with TGFβ neutralizing antibody also blocked the depletion of lipid droplets in infected cells (Fig. 15B-C).

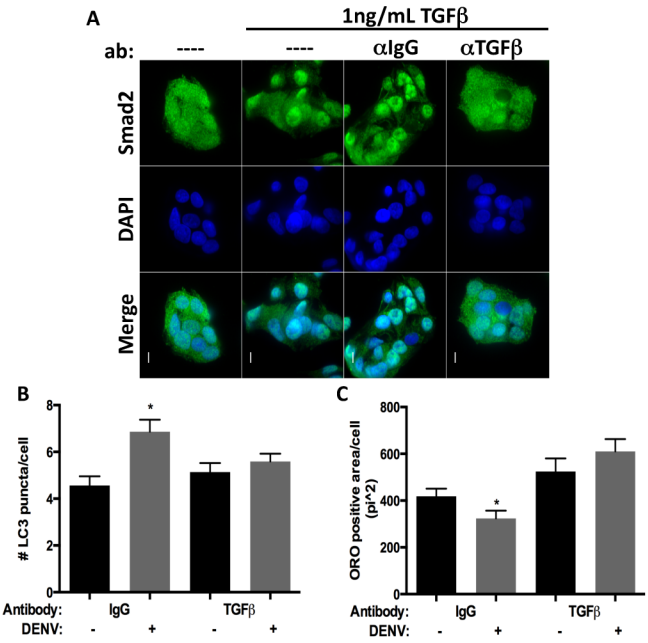

Figure 15. Neutralizing antibodies to TGFβ block DENV lipophagy. A) Carrier (4mM HCl) or 1ng/mL of TGFβ was pre-incubated with 10μg/mL of αTGFβ or αIgG aniibody in 5% DMEM for 15 minutes before addition to cells. After 6 hours of incubation, cells were fixed with PFA and stained for SMAD2 nuclear relocalization. B-C) Mock or DENV inoculum was incubated with 10μg/mL of αIgG or αTGFβ antibody for 15 minutes before addition to HepG2 cells. After two hours, media was changed to 5% DMEM with 10ug/mL of αIgG or αTGFb and maintained throughout the experiment. B) At 24hpi, HepG2 cells were fixed with MeOH, stained for DENV E and endogenous LC3, and LC3 puncta were quantified. C) At 48hpi HepG2 cells were fixed with 4% paraformaldehyde (PFA) and stained for DENV NS3 and LDs (ORO). Total area of LD staining in cells was quantified. Images were quantified for LC3 puncta or LD area using ImageJ and data was graphed using Prism. Error bars represent standard error. * = $p < 0.05$

Given that TAK1 inhibition does not block DENV replication, we were interested to see whether this was a general principle of the upstream components of the DENV-lipophagy signaling pathway, or if it was specific and intrinsic to the loss of TAK1 itself. Knockdown of TβR1 inhibited DENV replication (Fig. 16A-B). This data suggests that the uncoupling of replication and lipophagy phenotypes is specific to loss of TAK1 activity, and not an outcome of globally disrupting the upstream signaling involved in DENV-induced lipophagy.

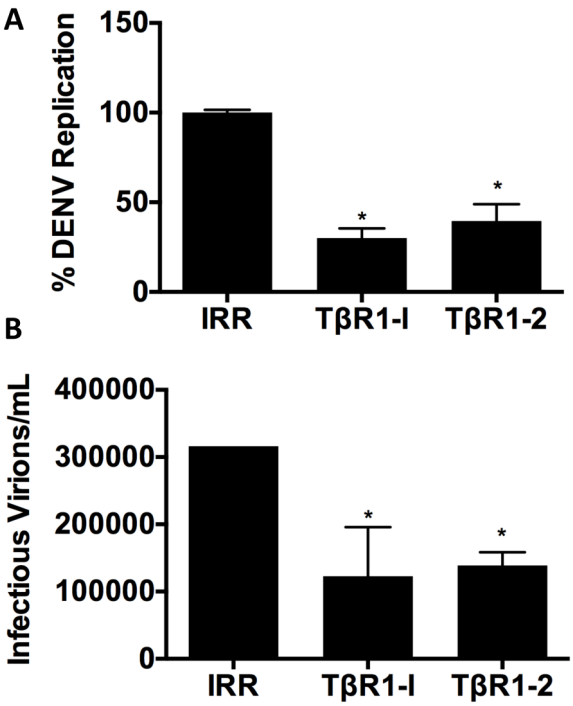

Figure 16. TβR1 knockdown blocks DENV replication. A-B) HepG2 cells were transfected with siRNAs against TβR1 (ALK5) or an irrelevantly targeted sequence (IRR). 72 hours post transfection of siRNAs, HepG2 cells were infected with DENV. 24hpi A) Intracellular RNA was harvested for TaqMan qRT-PCR quantification of DENV RNA, and B) supernatants were harvested for infectious virus quantification by limiting dilution titer.

TAK1 and TβR signaling are dispensible for Ca^{2+}-induced autophagy

We next sought to determine whether the involvement of TAK1 and TGFβ in DENV-lipophagy was specific to this pathway of autophagy induction or reflected a general role for these molecules in autophagy. To test this, we induced autophagy with ionomycin. Ionomycin is known to induce autophagy in a Ca^{2+}-dependent manner, and requires signaling through CaMKKβ and subsequent activation of AMPK. Ionomycin treatment increas LC3 puncta formation in control cells, which was abrogated in the

presence of the CaMKKβ inhibitor STO-609, and the PI3-K inhibitor 3-methyladenine (3-MA) (Fig. 17A). However, incubation of ionomycin-treated cells with either the TAK1 inhibitor (5z)-7-oxozeaenol or the TβR1 inhibitor SB-43154 did not block autophagy induction in these cells (Fig. 17A). Combined with earlier experiments, these data suggest that TAK1 and TβR1 are specifically important for this pathway of DENV-induced lipophagy, and not generally important for autophagy induction.

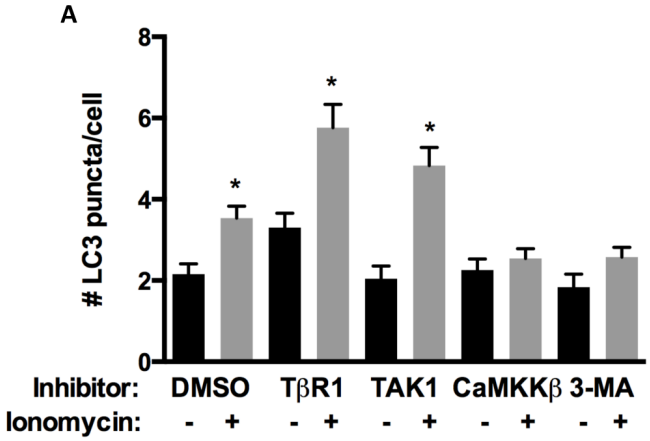

Figure 17. TAK1 and TβR do not inhibit Ca2+-dependent autophagy. A) HepG2 cells were simultaneously treated with ionomycin (1μM) or an inhibitor to the designated target (TβR1 – SB43154; TAK1 – (5z)-7-oxoaezenol; CaMKKβ – STO-609; and PI3K (Vps34) – 3-methyladenine (3-MA)). 16hpt, HepG2 cells were fixed in MeOH and stained for endogenous LC3. Images were quantified using ImageJ, and data graphed in Prism. $p < 0.05$

Exogenous TGFβ is insufficient to drive lipophagy

Given that DENV-induced lipophagy is dependent upon TGFβ, TGFβ has been shown to induce autophagy, and deficiencies in TβR signaling resulting in lipid droplet accumulation, we sought to determine whether TGFβ itself was sufficient to drive lipophagy in our system. We treated HepG2 cells with increasing concentrations of TGFβ for 48hrs. To determine whether the TGFβ was bioactive, in parallel, we assessed the nuclear translocation of SMAD2. To determine whether lipid droplets were depleted, we assessed the LD number and area and saw no difference between vehicle treatment and any concentration of TGFβ added (data not shown). Upon TGFβ treatment we noticed that the SMAD2 nuclear translocation

was not uniform across the population. Thus, we decided to repeat the experiment and also stain for SMAD2 localization, and focus on those cells with high SMAD2 nuclear localization (Fig 16A). With this, we utilized the strength of SMAD2 nuclear localization as proxy for the strength of the inducing signal in that cell. However, separating out the cells in this fashion did not show a trend of LD depletion (Fig 16A). Additionally, at no concentration of, or time point after, TGFβ addition did we see an increase in LC3 puncta formation per cell as compared to the vehicle control (Fig 16B). Because of incompatibility of the LC3 and SMAD2 antibody, we could not look into cells stained for both and separate out the groups as we did with the LD samples, but given that there was no decrease in LD area/number previously we infer that any change in autophagosome number would not be indicative of lipophagy. While negative, these data suggest that in our system TGFβ does not induce autophagy, nor is it sufficient to drive lipophagy.

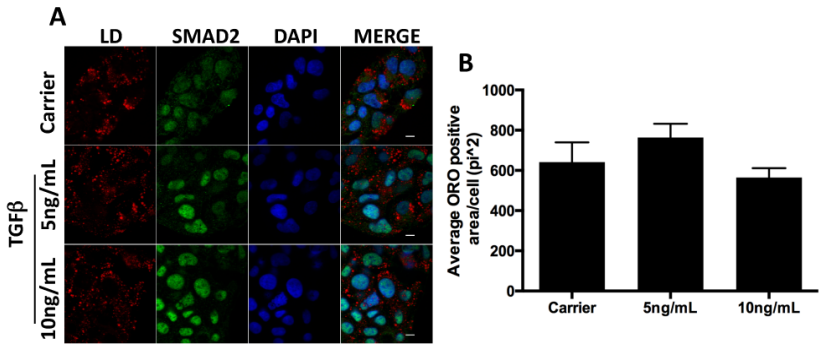

Figure 18. TGFβ does not induce lipophagy. A) HepG2 cells were treated with Carrier (4mM HCl) or 5 and 10 ng/mL of TGFβ for 48 hours. 48hpt, cells were fixed in 4% PFA and stained for SMAD2 re-localization and LDs (ORO). B) In TGFβ samples, cells with strong nuclear localization of SMAD2 (a proxy of TGFβ activity) were analyzed for LD area. In carrier-treated HepG2 cells, there was no discrimination based on SMAD2 localization. Images were quantified for LC3 puncta or LD area using ImageJ and data was graphed using Prism. Error bars represent standard error. * = $p < 0.05$

Discussion

We have demonstrated that DENV-induced lipophagy relies on a TGFβ and TAK1-dependent signaling pathway. Although we have been unable to display the direct link between these molecules and the downstream signaling identified earlier, substantial evidence in the literature connects them. Importantly, inhibitors of the TβRI kinase activity are known to block SMAD-dependent signaling through the TβRs, but not TAK1 suggesting a possible synergistic role for both arms of TβR signaling. Rather, a TβR-TRAF6 complex that leads to polyubiqutination, and subsequent activation of TAK1 orchestrates TGFβ-dependent TAK1 activation (254). While we have not specifically tested whether this complex is involved, our results suggest TGFβ signaling as being important for TAK1 activation in this context.

TAK1 has been shown to control lipid metabolism in mouse livers through the modulation of autophagy and lipid β-oxidation, as well as through control of SREBP proteins (102, 185). In mouse livers, TAK1 was suggested to control autophagy and lipid metabolism partially through LKB1-dependent activation of AMPK (102), which is at odds with our study where knockdown of LKB1 does not impact DENV-lipophagy. Rather, our results suggest that TAK1 maybe acting directly to activate AMPK as happens in the TRAIL-induced cytoprotective autophagy in epithelial cells (90). Future work will be needed to address whether TAK1 is directly activating AMPK during DENV-lipophagy.

Our research indicates that like HIV-1, DENV has evolved to activate TAK1 both for its benefit and to its detriment. Knockdown and inhibition of TAK1 suggest that overall it's impact is antiviral for DENV. This antiviral capacity is not related to

autophagy as autophagy induction does not occur during TAK1-inhibited, DENV-infected cells, and inhibition or knockdown of TAK1 when inhibiting AMPK, TSC2, or BECN1 boosts viral replication to a similar degree (~3-fold, data not shown). Since TAK1's primary influence on innate immunity is the activation of NFκB, we utilized the NFκB the inhibitor Bay-11-7082 to assess the role of NFκB signaling in viral infection. However, this showed a strong dose-dependent decrease in DENV replication suggesting that dengue requires NFκB activation for replication.

TAK1 is a MAPKKK that signals through ERK, MKK, JNK, and MEK signaling cascades to alter various aspects of the cellular state (36, 230). However, inhibition of signaling through these molecules also did not enhance viral replication, suggesting no role for these pathways in controlling dengue virus. It is possible that the antiviral capacity of TAK1 may lie outside of its canonical roles, and be amplified by the combination of autophagy inhibition which comes with TAK1 and whatever enigmatic signaling results from DENV-dependent TAK1 activation. Recent work with TAK1 has shown that loss of TAK1 can switch a TNFα/TRAIL-induced apoptotic cell death program to necroptotic (65, 184). However, this switch is mediated by the presence of several autophagy proteins, though not the process of autophagy itself (65). Thus, there may be potential for similar synergistic effects of downstream TAK1 signaling in the absence of autophagy during DENV replication.

Our results have also identified a novel proviral role for TGFβ signaling during DENV infection. *In vivo*, as well as *in vitro*, DENV infection has been shown to upregulate TGFβ expression, and increases the amount of active TGFβ circulating (5, 32, 208, 213). However, the focus of TGFβ activity has been on its

immunosuppressive effects, and the possible link of polymorphisms in TGFβ to susceptibility of severe dengue hemorrhagic fever (5, 32, 208, 213). We demonstrate that in infected hepatocytes, the activation of TGFβ signaling is important, at least, for the induction of lipophagy by DENV. Failure to signal through TβRs results in the inihibition of viral replication, autophagy induction, and LD depletion. Thus, TGFβ signaling is important for viral modulation of the host cellular metabolism.

TGFβ can be an important modulator of host lipid metabolism in a tissue dependent context, adding to the pleiotropic function of this cytokine. Interestingly, however, TGFβ, while necessary, is not sufficient to induce the process of lipophagy. This suggests that TGFβ is not the originating stimulus for lipophagy induction, and that there is still yet another upstream molecule(s) that coordinates this process. Future work will be focused on determining the role of viral proteins and upstream activators of TGFβ in lipophagy induction.

Chapter IV. Targeting of the lipid droplet during DENV-induced lipophagy.

Abstract

In the previous chapters, we have established a signaling pathway for dengue virus-induced lipophagy. In this chapter, we seek to examine how the lipid droplet (LD) is targeted for depletion and to identify the viral proteins involved in lipophagy. Mass spectrometry analysis of LD-associated fractions showed enrichment in ubiquitin peptides in fractions from DENV-infected cells. Ubiquitin is an important marker of autophagy cargo in many forms of selective autophagy. In dengue virus infected cells, LDs accumulate K63-linked chains of ubiquitin (K63-ub). Furthermore, disruption of the TβR-dependent signaling pathway does not block accumulation of K63-ub at the LD. Co-localization analysis and RNAi silencing experiments suggest a role for the autophagy adaptor NBR1 in lipophagy, but not other autophagy adaptors. Expression of individual viral proteins was insufficient to induce lipophagy, although NS3 with and without its cofactor NS2B was able to induce autophagy. Expression of NS1-3 was the minimal requirement for induction of lipophagy, suggesting a synergistic activity of two or more viral proteins for lipophagy induction.

Introduction

We have shown that DENV induces a LD specific selective autophagy program that results in increased β-oxidation of free fatty acids imported into the mitochondria (89). The previous chapters of this thesis have focused on the signaling pathways that drive dengue virus induced-lipophagy. In this chapter we will focus on expanding our understanding of what occurs at the lipid droplet

surface that leads to the specific targeting of LD during dengue virus-induced lipophagy.

Selective autophagy is a form of autophagy in which a specific cargo is targeted for degradation. Selective autophagy is employed to degrade damaged organelles, misfolded proteins, and invasive pathogens (109). The molecular mechanisms of selective autophagy are as variant as the cargo that is engulfed, however they broadly fall under two categories: ubiquitin-dependent and ubiquitin-independent (126).

The most well studied form of ubiquitin-dependent selective autophagy is PARKIN-PINK1 mitochondrial autophagy (mitophagy). Genetic deficiencies in both PINK1 and PARKIN lead to the accumulation of damaged mitochondria that are thought to be associated with Parkinson's disease. Briefly, as mitochondria lose their membrane potential over time, PARL, a protease in the intermembrane space, is deactivated and no longer cleaves the kinase PINK1 (38, 107, 178). This allows for the deposition of PINK1 on the mitochondrial surface where it recruits Parkin to the mitochondrial outer surface and phosphorylates Parkin, leading to its activation (116, 248). Activation of Parkin's E3 ligase activity leads to the decoration of the mitochondrial surface with ubiquitin moieties with K27, -63, and -48 linkages that are phosphorylated at S65 by PINK1 (59, 136, 236). Although all five major receptors (p62, OPTN, NDP52, NBR1, and TAX1BP1) have been shown to be recruited to damaged mitochondria during PINK1-PARKIN mitophagy, only OPTN and NDP52 individually have been shown to be necessary and sufficient to restore mitophagy in the absence of all other receptors (145). In other forms of ubiquitin

dependent selective autophagy (e.g., xenophagy) the autophagy receptors show distinct localizations on the cargo, but ultimately semi-redundant roles in the process.

Cargo can also be marked for degradation in ubiquitin-independent ways (126). Several forms of mitophagy can be ubiquitin-independent (163, 197). In these cases, organelle resident proteins have LC3-interacting regions (LIRs) that become exposed and are able to bind LC3 after a post-translational modification to the proteins. For example, during conditions of hypoxia, multiple phosphorylations of FUNDC1 near and in the LIR domain regulate its ability to bind to LC3 and coordinate mitophagy (139, 163, 289). Similarly, the mitochondrial protein Nix/BNIP3L is essential for mitochondrial clearance during erythrocyte maturation in a LIR-dependent manner (197).

The molecular mechanism for targeting lipid droplets for autophagic degradation is unclear. Recent research has shown that lipophagy is dependent upon the outer protein shell of the lipid droplet being broken by chaperone-mediated autophagy and ATGL-mediated lipolysis (118). Additionally, accumulation of the autophagy receptor NBR1 has been observed at lipid droplets in cells undergoing lipophagy, however it is unknown whether this protein is essential for lipophagy (118).

In this chapter we show that ubiquitin accumulates on lipid droplets during DENV infection, suggesting that DENV-induced lipophagy is ubquitin-dependent. Ubiquitin, specifically K63-linked chain linkages, and NBR1 accumulate on lipid droplet during DENV infection. Depletion of NBR1 inhibits DENV induction of

autophagy and lipid droplet depletion. RNAi-mediated knockdown of TAK1, AMPK, and TSC2 does not inhibit the accumulation of K63-ub at the lipid droplet. Additionally, we identify NS1-3 as the minimal viral protein sufficient for lipophagy induction. Together, these data suggest that DENV-induced lipophagy is a ubiquitin-dependent selective autophagy process that is driven by NS1-3.

Materials and Methods

Plasmids. The myc-ubiquitin K48R vectorwas a gift from Daniel Boone. Generation of V5-tagged DENV nonstructural proteins were previously described (88). NS1-3, NS1-4B, and NS2B-4A were generated by PCR amplification of the relevant genome sections, with overhangs for InFusion Cloning into pCMV-myc-N between the EcoRI and NotI. Overhangs for forward primers (5'-TGGAGGCCCGAATTCgg-3') and reverse primers (5'- GCGGCCGCGGGGATC-3').

Immunofluorescence microscopy. Glass coverslips in 24-well dishes were seeded with 70,000 cells. All washes and reagents were prepared in 1× PBS (pH 7.5) and used at room temperature. The cells were fixed with 4% paraformaldehyde (15 min) at 4^{o}C. For measurement of LC3 puncta, coverslips were fixed in methanol at -20^{o}C for 10 minutes. Cells were blocked and permeabilized with 30% Goat serum and 0.1% Saponin for 30 minutes. Primary antibodies in 10% goat serum and 0.1% Saponin were incubated overnight at 4°C. anti-NBR1 (Cell Signal), anti-p62 (Sigma), anti-OPTN (Sigma), anti-K63-ubiquitin (EMDMillipore) and anti-DENV NS3 antibodies were used at 1:1000, anti-NS3 antibody was used at 1:3,000, and anti-SMAD2 (Cell Signal) antibody was used at 1:400. Fluorescent-conjugated secondary antibodies were incubated with cells in 10% goat serum and 0.1% saponin for 1 hr.

Alexa Fluor-488 and -594, secondary antibodies (Invitrogen) were used at 1:2,000 and Alexa Flour 350 secondary antibody was used at 1:600. When Alexa Fluor 350, coverslips were mounted in ProLong Gold AntiFade with DAPI (4′,6′-diamidino-2-phenylindole) nuclear stain (Invitrogen). When Alexa Fluor 350 was used, coverslips were mounted in ProLong Gold Antifade (without DAPI), and no nuclei were visualized. The samples were imaged using an Olympus DSU spinning disc confocal microscope equipped with a Photometrics Evolve EMCCD camera. Digital images were taken using Slidebook v6.0 software and processed using ImageJ (National Institutes of Health). Quantification of fluorescence intensity was determined from multiple images taken from duplicate coverslips using ImageJ.

RNA interference (RNAi) analysis. RNAi assays were performed as described previously. For immunofluoresence analysis and knockdown efficiency, 70,000 cells were transfected with 24pmol of the indicated siRNA and seeded on glass coverslips in 24-well plates. For viability, viral replication, and infectious virus release assays, 12,000 cells were transfected with 8 pmol of indicated siRNA in quadruplicate, and seeded into 96-well plates. For experiments examining cell signaling, either 100,000 cells were transfected with 48pmol of siRNAs in 12 well plates or 250,000 cells were transfected with 80pmol of siRNAs in 6-well plates. In all cases, cells were incubated with siRNAs for 72 hours before being infected with DENV or harvested for viability or Western Blot analysis.

siRNAs. siRNAs for TALDO1, p62, and NBR1 were ordered from Ambion. TALDO1 (5'-GCAAGGACCGAAUUCUUAUtt-3'); p62 (5'-GGAGCAGGAGGGAAAAGAtt-3'); NBR1 (5'-GTATCATAGTAGATCCTTTtt-3').

Infectious Virus Production Assay. Cells were infected 72 hours after siRNA-treatment, or simultaneous with drug treatment at an MOI of 0.5-2 infectious DENV particles (DENV-2 16681) per cell for 2 hours, and maintained for 24 hours at 37^{o}C. Cell culture supernatants were titered by limiting dilution analysis via immuno-histochemistry using monoclonal anti-E antibody (4G2; ATCC) as described.

Statistical analysis. Data are presented as means ± the standard errors of the mean (SEM). To assess statistical significance, two-tailed, unpaired Student *t* tests were performed.

Results

Ubiquitin is enriched at the lipid droplet during DENV infection.

To determine the differences in protein composition of lipid droplets in DENV infection, we harvested lipid droplet fractions from mock- and DENV-infected cells 24hpi. The harvested fractions were subjected to SDS-PAGE and silver staining to determine differences in the protein profile of the LDs. We cut out several bands corresponding to observed differences in banding patterns and identified them by tandem LC/MS/MS (Fig. 19A). We identified several proteins enriched in lipid droplet fractions from DENV-infected cells. Of interest to us were the accumulation of transaldolase 1 (TALDO1), ancient ubiquitous protein 1 (AUP1), and ubiquitin (Fig. 19B).

Transaldolase 1 is an enzyme involved in the pentose phosphate pathway, and mutation leads to early on set hepatocellular carcinoma and other liver defects in children (146, 270, 275). TALDO1 has been found in previous lipid droplet proteomes, and deletion of TALDO1 in mice leads to an accumulation of lipid

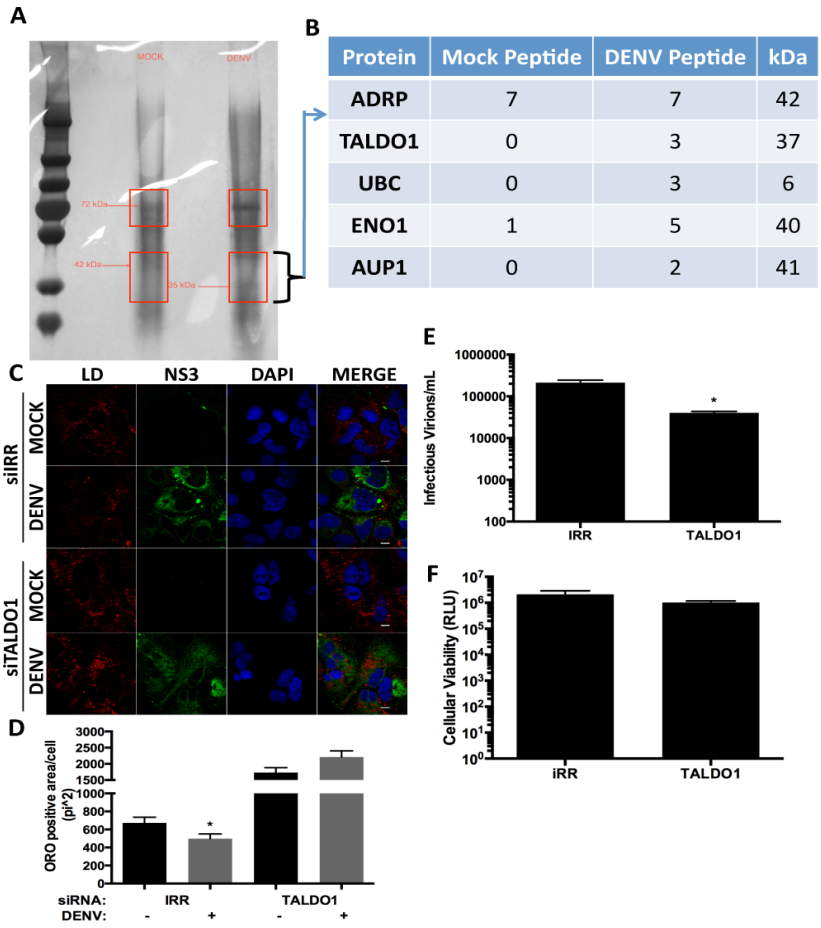

Figure 19. LD mass spec identifies proteins enriched in DENV LD-associated fractions. A) Silver stain gel of isolated LD fractions. $1.4x10^8$ Huh7s were infected at an MOI of 2 for 24 hours. LDs were isolated as indicated in Methods section, and ran on an SDS-PAGE gel for silver stain. The red boxes correspond to the sections of the gel with the most significant visible differences in banding pattern that were cut out. The bands were sent for LC/MS/MS-Tandem mass spectroscopy for protein identification. B) Proteins that were enriched in the 35-46 kDa section of the gel in LD preps from DENV infected cells. ADRP serves as a control to show that equivalent protein was loaded into each lane. C-F) TALDO1 knockdown compromises DENV replication and lipophagy. Huh7s were transfected with siRNAs against TALDO1 or an irrelevantly targeted sequence (IRR). C) siRNA-treated Huh7s were infected with DENV at an MOI of 0.5, fixed with 4% PFA at 48hpi, and stained for DENV NS3, LDs (ORO), and DAPI. D) Quantification of ORO area in mock and DENV infected Huh7s treated with either IRR or TALDO1 siRNAs. E) siRNA-treated cells were infected with DENV at an MOI of 1. 48hpi supernatants were harvested to assess infectious virus release by limiting dilution titer. F) Cellular viability was measured using the Promega CellTiterGlo kit according to manufacturers instructions. * = $p < 0.05$. Error bars = standard error. Images were analyzed in ImageJ, and data graphed in Prism.

droplets (among other defects) (79). We tested whether TALDO1 knockdown would inhibit DENV lipophagy. Infection of IRR treated cells decreased lipid droplet area as compared to their mock counterparts. However, depletion of TALDO1 inhibited this process, and in addition lead to a large basal increase of LD area in knockdown cells (Fig. 19C-D).

Knockdown of TALDO1 also reduced viral replication (Fig. 19E) with no significant impact on cellular viability (Fig. 19F). Immunoflouresnce studies of TALDO1 found that staining was overwhelmingly nuclear (data not shown) with little evidence for cytoplasmic or lipid droplet localization. However, a recent report demonstrated that the gene encoding TALDO1 has an alternative start site, and expression of this gene produces a cytoplasmic protein (186).

Given a potential role for ubiquitin in selective autophagies, we were intrigued by AUP1, a widely conserved protein with unknown function that is known to bind and recruit E2 ubiquitin conjugation enzymes to the LD (108, 133, 165, 255, 258). AUP1 has been detected in LD proteomes previously, and E2 recruitment by AUP1 is important for the ER-associated degradation (ERAD) pathway (108, 133, 255). Knockdown of AUP1, however, did not affect the ability of DENV to deplete LDs in infected cells (data not shown).

The accumulation of ubiqutin in the DENV-associated LD fractions was encouraging. Ubiquitin has been shown to accumulate at the lipid droplet during the ERAD-mediated degradation of apolipoprotein B, and that this is a K48-linkage dependent process (204, 261), whereas the predominant chain linkage involved in selective autophagy is K63-linked. To separate whether this accumulation of ubiquitin is distinct from ERAD, we infected cells with DENV at a high MOI (~5), and 6hrs later transfected the cells with myc-ub-K48R. 30hpi, we fixed the cells and stained for myc-ubiquitin and LDs (ORO) (Fig. 20A). We observed that in DENV-infected cells, myc-ub-K48R still accumulated at the LD surface (Figure 20A), suggesting that the ubquitin accumulation during DENV was not dependent upon

ERAD. We then examined whether endogenous K63-linked ubiquitin chains (K63ub) increased in localization to LDs during DENV infection. Examining mock and DENV infected cells 24hpi revealed that DENV infected cells displayed more co-localization of K63ub and LDs than their mock counterparts (Fig. 20B-C). Together these data validate our MS data, and suggest that ubiquitination of the LD proteins is increased during DENV infection.

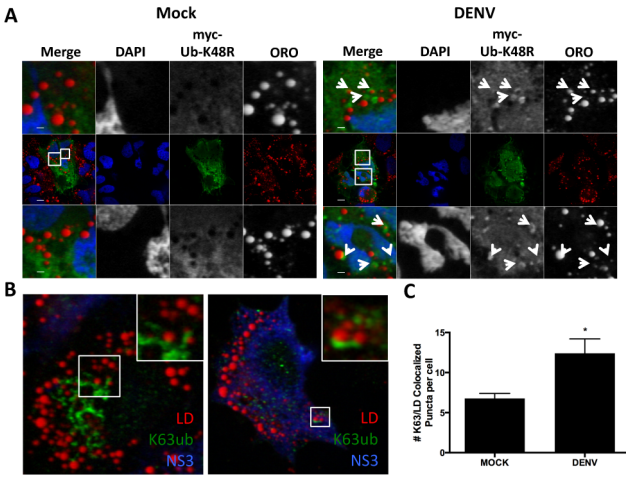

Figure 20. K63-linked ubiquitin chains accumulate at the lipid droplet during DENV infection. A) HepG2 cells were Mock or DENV infected at an MOI 5 for 6 hours before transfection with a myc-tagged K48R ubiquitin. 30hpi, cells were fixed with PFA and stained for myc-K48R ubiquitin and LDs (ORO). B) HepG2 cells were mock or DENV infected at an MOI of 0.5 for 24 hours, fixed in 4% PFA, and stained for endogenous K63-ub, DENV NS3, and LDs (ORO). C) Colocalization of K63ub and LDs was quantified using ImageJ and graphed in Prism.

Evidence for NBR1 as the autophagosome adaptor for DENV-induced lipophagy.

The accumulation of ubiquitin on LDs at regions associated with autophagosomes suggests a ubiquitin-dependent mechanism of selective autophagy. As mentioned earlier, this pathway is mediated by recruitment of autophagy adaptors that harbor ubiquitin binding domains and an LC3-interacting region (LIR). Previous work has shown that depletion of the autophagy adaptors NDP52 and TAX1BP1 does not affect viral replication (124), and thus we assume are not essential for DENV lipophagy; however the role of other selective autophagy adaptors remains unclear. To assess whether additional receptors might play a role in DENV-induced lipophagy, we first examined which

receptors accumulated at the LD surface during DENV infection via immunofluorescence microscopy. p62 is the prototypical, and most studied, autophagy adaptor. However, during DENV infection we do not see an increase in the amount of p62 associated with LDs in infected cells, and we found similar results for OPTN (Fig. 21A-D). However, when we assessed the localization of NBR1 at LDs in DENV-infected cells, we found that NBR1 accumulated at LDs (Fig. 21E-F). This concurs with a previous recent report (118).

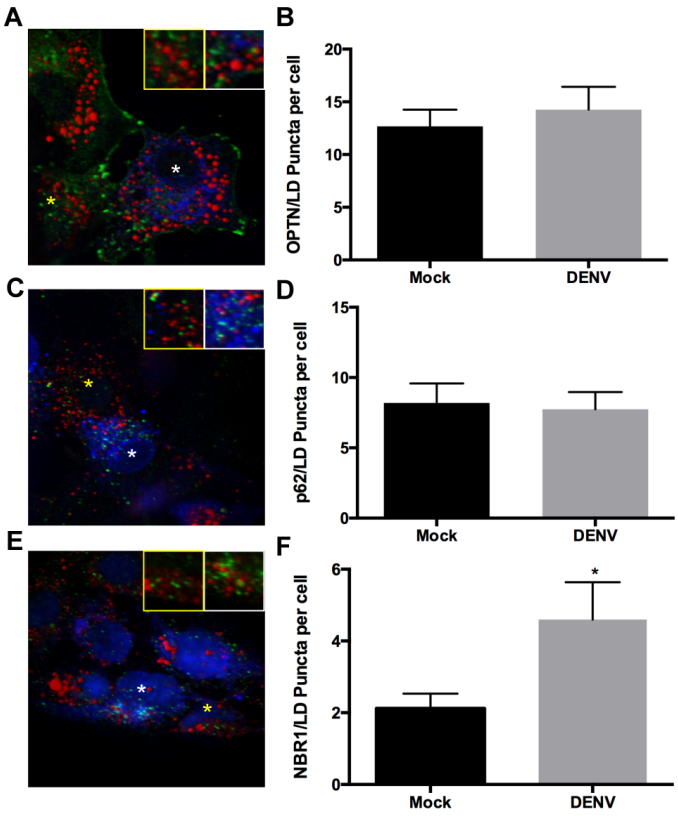

Figure 21. NBR1, but not p62 or OPTN, is recruited to LDs during DENV infection. HepG2 cells were infected at an MOI of 0.5. 24hpi, HepG2 cells were fixed in 4% PFA and stained for endogenous p62 and DENV NS3 (A), endogenous OPTN and DENV NS3 (C), or endogenous NBR1 and DENV E, and LDs (ORO). Colocalization was between p62 (B), OPTN (D), or NBR1 (F) and LDs was analyzed using ImageJ Colocalization Highlighter. Yellow asterisk and box = uninfected cells; white asterisk and box = DENV infected cell. Insets for all are the same size, and come from HepG2 cells with asterisk.

We next tested the requirement of NBR1 for DENV replication and lipophagy. To determine the effect of NBR1 on DENV lipophagy, we infected HepG2 cells transduced with control or NBR1 shRNAs, and then fixed cells at 24 and 48hpi to stain for endogenous LC3 and LDs, respectively. As expected, DENV infection increased autophagosome number and depleted lipid droplets in cells expressing an IRR targeting shRNA (Fig. 22A-B). However, knockdown of NBR1

inhibited autophagy induction in DENV cells (Fig. 22A-B). Suggesting that NBR1 may be the critical adaptor for DENV-induced lipophagy. Interestingly, while testing the requirement of p62, we saw that depletion of p62 lead to a basal increase in LD area when compared to cells treated with an irrelevenat siRNA, which we also saw with NBR1 (Fig 22 B-C). However, unlike NRB1 Knockdown, infection with DENV was still able to greatly reduce the LD area in infected cells (Fig 22C). Thus, simply increasing the basal LD number in cells (e.g., knockdown of NBR1, TAK1, or TALDO1) in and of itself is not sufficient to block DENV lipophagy.

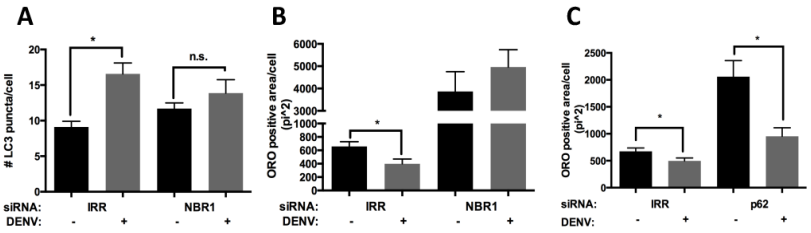

Figure 22. Knockdown of NBR1, not p62, blocks DENV lipophagy. A and C) HepG2 cells were transfected with an siRNA against NBR1 or an irrelevantly targeted sequence (IRR) as described in Methods section. HepG2 cells were Mock or DENV infected at an MOI of 0.5 for 24 or 48 hours, and then fixed, stained, and quantified for endogenous LC3 puncta (A) or LD area (ORO; B), respectively. C) HepG2 cells were transfected with an siRNA against p62 or IRR, and infected at an MOI 0.5 for 48hrs. HepG2 cells were fixed 48hpi, stained for DENV NS3 and LDs (ORO), and the area of LDs in mock and uninfected cells was analzyed. Error bars represent standard error. * = $p < 0.05$. Images were quantified in Image J.

The TβR-dependent signaling pathway is not required for K63-ub accumulation at LDs.

We sought next to understand the relation between the TβR-dependent signaling pathway described previously, and the deposition of the lipid droplet surface with K63-ub. Cells were depleted of each signaling molecule by RNAi, and then infected with DENV for 24 hours, at which time the cells were fixed on coverslips and stained for endogenous K63-ub, DENV NS3 protein, and LDs (Oil Red O) (Fig. 23A). In the case of each signaling molecule tested, we found that inhibiting

signaling through the pathway did not decrease the number of LDs that accumulated K63-linked ubiquitin in DENV-infected cells (Fig. 23B). Indeed, following DENV infection of cells silenced for AMPK, TSC2, or TAK1, the total area of K63-ub on the LD actually increased (Fig 23C). Similarly, DENV infection of BECN1 knockdown cells led to an increase in both the number of LDs associated with K63-ubiquitin and the area that K63-ubiquitin occupies on LDs, as compared to IRR treated mock- or DENV-infected cells (Fig. 23B-C). The increase in K63-ubiquitin at the LD in autophagy deficient conditions suggests that autophagy mediates clearance of these ubiquitin chains. Together with previous data, this supports our model that DENV-induced lipophagy is a ubiquitin-dependent form of selective autophagy. It also suggests that DENV-induced lipophagy has two distinct steps: the induction of autophagy via AMPK-dependent signaling and the AMPK-independent stimulation of K63-linked ubiquitination of LD proteins.

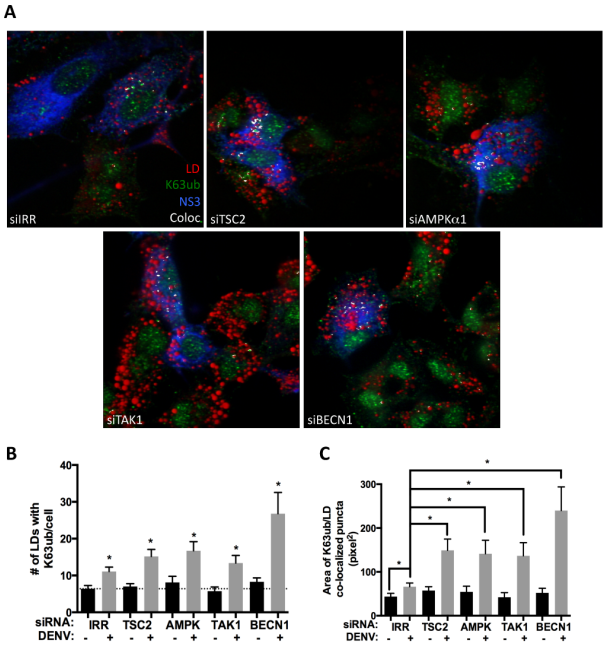

Figure 23. Knockdown of lipophagy signaling molecules does not block K63-linked ubiquitin chains accumulate at the LD during DENV infection. A) HepG2 cells were transfected with siRNAs against TSC2, AMPK, TAK1, BECN1 or an irrelevantly targeted sequence (IRR) as described in the Methods section. HepG2 cells were then infected with DENV at an MOI of 0.5. 24hpi, HepG2 cells were fixed with 4% PFA and stained for K63-ub, DENV NS3, and LDs (ORO). Representative images are shown in with co-localization (Coloc) of K63ub and LDs highlighted in white. B) The number of LDs co-localized with K63ub/cell was quantified using ImageJ. C) The area of K63ub and LD co-localization was analyzed and graphed in DENV and un-infected HepG2s. * = $p < 0.05$. Data graphed in Prism.

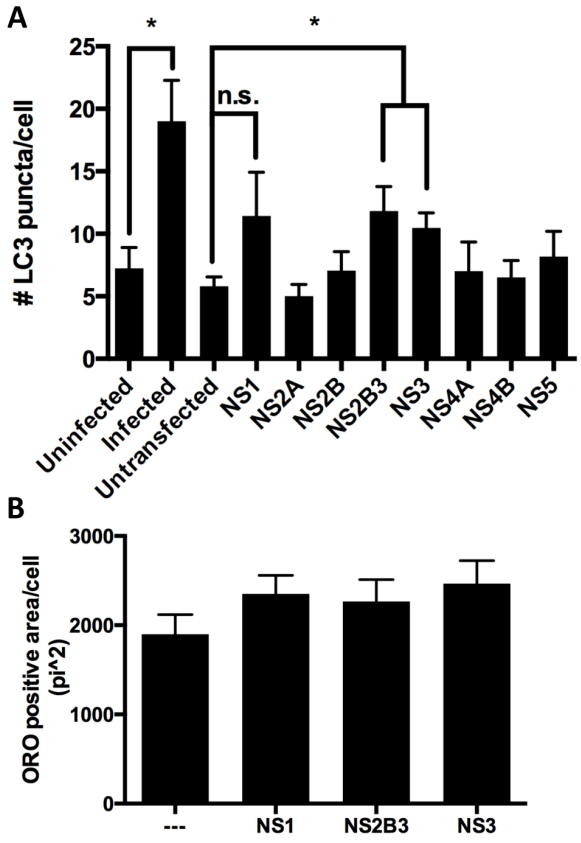

Figure 24. Single DENV proteins do not induce lipophagy. A) HepG2 cells were either infected at an MOI of 0.5 or transfected with 1.2ug of plasmid encoding single C-terminally V5-tagged DENV nonstructural (NS) proteins. 24hp infection and transfection HepG2 cells were fixed and stained for DENV E or V5 and endogenous LC3. The number of LC3 puncta per cell was analyzed in ImageJ. B) HepG2 cells were transfected with plasmids encoding NS1-V5, NS2B3-V5, or NS3-V5 and fixed 48hpt with 4% PFA. HepG2 cells were stained for V5 and LDs (ORO), and the LD area in transfected and untransfected cells was measured.

NS1-3 is required for DENV-lipophagy

We were interested in understanding the viral components necessary to induce lipophagy. Previous work has shown that electroporating the DENV replicon was sufficient to induce lipophagy, and so we focused our efforts on the nonstructural proteins. HepG2 cells were transfected with plasmids encoding single nonstructural proteins, and assayed for their ability to induce autophagy or deplete lipid droplets. Expression of NS2B3 or NS3 was sufficient to induce a modest autophagic response, although this was not as robust as DENV infection (Fig. 24A). Surprisingly, we did not see evidence for NS4A induction of autophagy, which has been described previously for DENV as well as Modoc and Zika viruses (160, 175). Because lipophagy requires autophagy induction, we focused our analysis of LD depletion on NS2B3 and NS3. Since NS1 showed a trend

in autophagy induction we also included this in the test as well. However, transfection of none of these was sufficient to drive the depletion of LD (Fig. 24B).

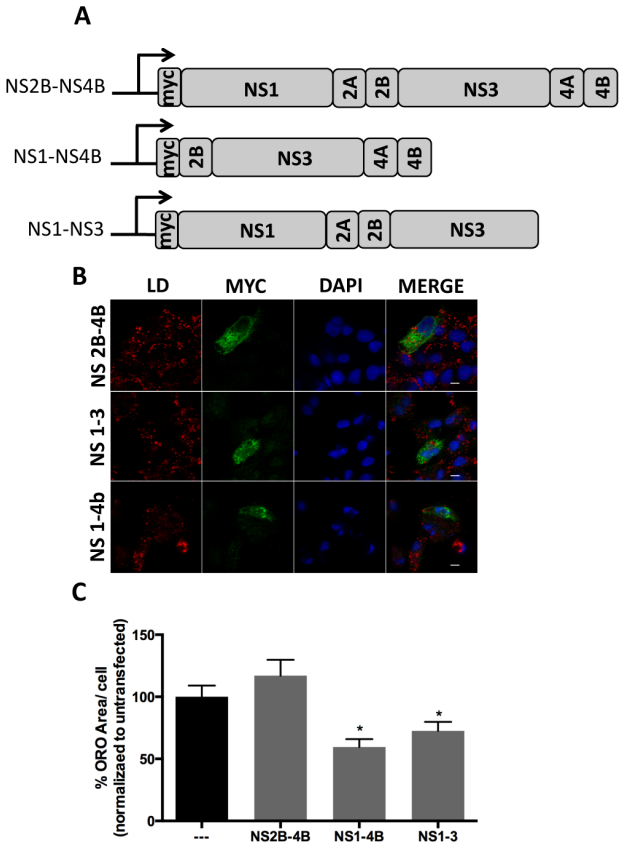

Figure 25. DENV NS1-3 is sufficient to induce lipophagy. A) Schematic of constructs used. B) HepG2 cells were transduced with myc-NS1-3, myc-NS1-4b, and myc-2B-4B for 48hrs and then fixed with 4% PFA. Fixed cells were stained for myc-tag and LDs (ORO), and the area of LD was measured in each cell. C) Data is normalized to the average ORO area of untransfected cells * = $p < 0.05$. Error bars = standard error of measure.

Transfection of single genes has limitations – the most obvious of which is expression outside of the context of the rest of the virus. Thus, we expressed overlapping multi-protein coding fragments of the viral genome in order to identify the minimal requirement for DENV-induced lipophagy. We generated plasmids encoding NS1-3, NS1-4B, and NS2B-4A, individually transfected them or a GFP control plasmid into HepG2 cells, and monitored lipid droplet depletion at 48 hours post transfection (Fig 25A-C). Cells expressing NS2B-4A did not deplete lipid droplets when compared to untransfected control cells (Fig. 25C). However, cells expressing NS1-3 or NS1-4B strongly depleted lipid droplets (Fig. 25C). Taken together, these data suggest that NS1-3 expression is sufficient to induce lipophagy.

Discussion

In this chapter, we have described the requirements of the selective autophagy machinery and DENV virus that are required for DENV-induced lipophagy. Our initial proteomic approaches identified ubiquitin as being enriched in LD-associated fractions in DENV-infected cells, leading us to hypothesize that DENV-lipophagy proceeds through a ubiquitin-dependent mechanism. This was supported by our immunofluoresence that showed an increase in K63-linked ubiquitin chains and NBR1 at LDs in DENV-infected cells. Depletion of NBR1 demonstrated its necessity for DENV-induced lipophagy, both the induction of autophagy and depletion of lipid droplets. Interestingly, while depletion of p62 did not block DENV-induced lipophagy, there was a significant increase in the basal amount of lipid droplets in p62-deficient cells. The accumulation of LDs can be a byproduct of several events, thus we cannot say whether or not p62 has a direct role in the turnover of LDs in the basal state. Our proteomics approach also identified at least one other protein that seems to be involved in DENV lipophagy, TALDO1. However, it's unclear where and how it fits into the pathway of lipophagy.

One may expect that depletion of the autophagy adaptor would lead to a decrease in LD depletion, but not autophagosome number. However what has been borne out by much research in selective autophagy is that the autophagosome forms around the cargo *de novo*, rather than the adaptors recruiting nascent phagophores (reviewed in (300)). Yet, depletion of autophagy adaptors does not inhibit the lipidation of LC3 demonstrating that, while linked at the sight of engulfment, these

processes are separately controlled (145). Instead, what remains inhibited in the absence of the adaptors is the recruitment of the machinery required to drive *de novo* formation of the autophagosome to the cargo to be degraded (145). This makes intuitive sense when examining electron micrographs of autophagosomes engulfing lipid droplets, or time-lapse microscopy of autophagosomes engulfing mitochondria.

How upstream signaling for autophagosome biogenesis links with the marking of cargo for degradation is unclear for many forms of selective autophagy. In PINK1-PARKIN mediated mitophagy it is clear that assembling the autophagy receptors at the mitochondrial surface is important for recruitment of ULK1 and other autophagy initiating molecules, but the reverse has yet to be explored (145). Utilizing DENV we have demonstrated that, at least so far upstream as we have identified, the signaling pathway that initiates autophagosome biogenesis does not impact the activation of the lipophagy E3 ligase, and the deposition of K63-ub at the LD surface. Rather, when inhibited, the K63-linked chains took up more area on LDs in infected cells suggesting that since autophagy was compromised the K63-linked ubiquitin marking was not cleared from the LD. In support of this, a similar trend is seen when Beclin1 is knocked down.

This leads us to a model of hierarchy that is similar to other forms of selective autophagy, wherein the marking of the target is the initiating event in selective autophagy. This marking specifies the assembly site of the autophagosomal membrane, and is important for the recruitment of the machinery to do so. In this model, a spatial question becomes immediately apparent - how does assembling NBR1 at the LD signal through TGFβ at the plasma membrane to induce lipophagy?

TGFβ is constitutively secreted from the cell, and held inactive in the extracellular matrix as a latent complex that can be activated as needed. One might envision that the initiating signal is sufficient to set off NBR1 recruitment and TGFβ activation, however this does not resolve the spatial problem. Future work will be required to understand how signaling for autophagy and targeting the LD are coordinated.

Several inputs influence the specificity of selective autophagy adaptors for their cargo. While we can only speculate at this point, it is noteworthy to point out that NBR1 contains an amphipathic J domain that is necessary for NBR1 targeting of peroxisomes for pexophagy (43). Transplanting this domain into an orthologous position in p62 allows p62 to complement a NBR1 deficient cell's ability to degrade peroxisomes, while wildtype p62 cannot (43). Many LD proteins are targeted to the organelle through an amphipathic helix or other hydrophobic domains (135). Future experimentation will be required to determine whether this J domain serves a similar function in lipophagy as it does in pexophagy.

The DENV replicon is sufficient to induce autophagy and deplete lipid droplets (data not shown), suggesting that the structural proteins play no role in lipophagy. Previous work had shown a role for DENV and modoc, a murine flavivirus, NS4A was sufficient to induce autophagy, and a recent study shows that Zika NS4A and NS4B singly and combined can induce autophagy (160, 175). Thus, we were initially surprised when single transfection experiments showed that NS3 was sufficient to induce an autophagic response in our hands. However, this response was not as pronounced as *bona fide* infection, and subsequent analysis of

lipid droplets showed that neither NS3 nor any other DENV nonstructural protein depleted lipid droplets. Rather, depletion of LDs required expression of NS1-3.

Given that (i) NS(2B)3 expression is sufficient to induce autophagy, (ii) AMPK signaling is required for autophagy induction but not K63-linked ubiquitination of LD proteins, and (iii) NS1-3, but not NS2B-4A, expression is sufficient to induce lipophagy, we propose the following model for DENV-induced lipophagy (Figure 26). NS(2B)3 stimulates the AMPK-dependent induction of autophagy, likely by increasing TGFβ signaling, which we showed in the prior chapter is implicated in DENV-induced lipophagy. NS1 then promotes autophagosomal targeting of the LD by stimulating the K63-linked ubiquitylation of LD proteins. This recruits the selective autophagy adaptor NBR1 to the LD, which binds to autophagosomes, resulting in lipophagy.

The mechanism by which NS1 promotes K63-linked ubiquitination of LD proteins is unknown. NS1 does not contain obvious E3 ubiquitin ligase domains, suggesting that it may act by recruiting a cellular E3 ligase to LDs. Proteomic analysis of NS1 immunoprecipitations from infected HepG2 cells showed that during DENV infection NS1 binds to the E3 ligase UBE3B (39). UBE3B is poorly studied, but its mutation is associated with severe developmental defects and low serum cholesterol (11). Future studies will test the requirement of UBE3B for DENV-induced lipophagy.

Both NS1 and NS3 modulate host cellular metabolism (7, 88). NS1 increases glycolytic flux, whereas NS3 increases *de novo* fatty acid synthesis (7, 88). In HCMV infection, the driving of glycolytic flux is essential for fueling the *de novo* fatty acid

synthesis HCMV infection requires, and so it is not unreasonable to speculate a parallel action here (173, 174, 256). Increased fatty acid synthesis can lead to increases of lipid droplet content, and it is possible the cell may sense this lipid overload and initiate lipophagy in response. Indeed, in many experimental inductions of lipophagy, lipid overload is the stimulus for lipophagy. While NS3 alone is sufficient to increase FASN activity, we do not know if this is as robust an increase as with the full virus. Thus, one might speculate that the induction of lipophagy is a larger response to the metabolic rewiring of the DENV infected cell, and that inhibition at various points along this process would block autophagy. Whether or not this is the case is yet to be defined.

Chapter V. Conclusions

The modulation of cellular metabolism is a critical component of a viral replication strategy. For example, HCV replication increases ATP concentrations at replication complexes to fuel the demand of ATP for viral replication (8); HCMV activates glycolytic flux to increase precurors for fatty acid synthesis, whose downstream products become incorporated in the viral envelope (173, 174, 256), and increases flux through UDP-sugar pathway for glycosylation of viral proteins (46); and DENV, and many other positive strand viruses, must re-wire host lipid metabolism in order to generate their viral replication complexes (88, 212). The coordination of these outcomes requires sophisticated manipulation of host cell metabolism in order for the virus to ensure a robust replicative niche, and successfully produce infectious progeny.

The induction of lipophagy by DENV is but one of several strategies the virus utilizes to re-wire host cell metabolism for its own benefit (111). Yet, the underlying pathway for how this process was triggered, both in DENV infection and as a natural process of the cell was unknown. In this thesis, we expanded our understanding of DENV-induced lipophagy and elucidated a defined signaling pathway by which lipophagy is triggered, and identified key molecules that mark the LD for selective degradation. Furthermore, we have also identified a region of the viral genome that is required for DENV-induced lipophagy. Our results have lead us to the model in Figure 26.

DENV activates a central hub of cellular signaling, AMPK, in order to induce autophagy. DENV activation of AMPK leads to activation of TSC2, a negative

regulator of the mTORC1 kinase complex, and subsequent licensing of autophagsome induction. AMPK and mTORC1 are crucial to sensing the cellular energy, nutrient, and stress state, and as such have a multitude of outputs in addition to autophagy, several of which are modulated by other viral infections. While we are able to show the inhibition of AMPK, and activation of mTORC1 block DENV-induced lipophagy and viral replication, we were unable to rule out whether modulating these pathways may also impair viral replication for other reasons.

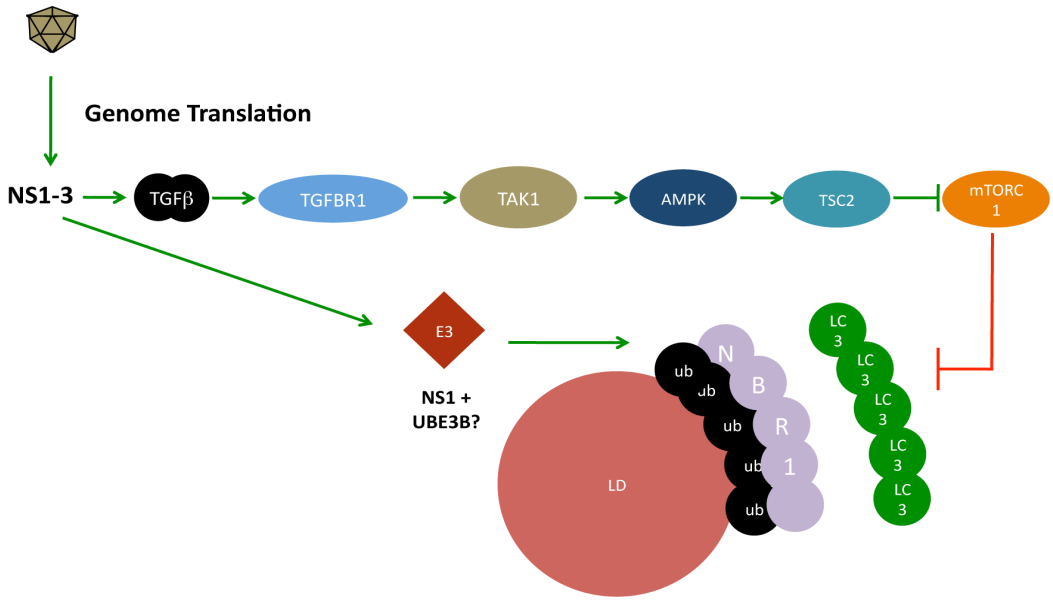

Figure 26. Model for Mechanism of DENV-induced Lipophagy. We propose this current model of DENV-induced lipophagy. Translation of DENV genome results in the expression of NS proteins 1-3, which initiate lipophagy. This initiation bifurcates, and we propose a possible where NS1 is responsible for the deposition of ubiquitin at the lipid droplet (possibly through its interaction with UBE3B), and NS3 initiates autophagy induction through a TGFβ-dependent pathway. Deposition of ubiquitin at the lipid droplet leads to the recruitment of NBR1 to the LD surface to mark the LDs destined for lipophagic degradation. TGFβ-dependent activation of TAK1 and AMPK leads to the licensing of autophagosomal biogenesis, and degradation of LDs.

The requirement of DENV to activate AMPK to achieve robust replication is intriguing as the AMPK pathway can be potently antiviral (188). Indeed, this could be said of multiple parts of this pathway (e.g., TAK1, discussed below). AMPK was

identified as the major kinase that phosphorylates and inactivates acetyl-CoA carboxylase (ACC), the rate-limiting step in *de novo* fatty acid biosynthesis (27, 190, 252). Many decades later, this was realized to be not only an important metabolic check for the cell, but a form of "intrinsic" immunity in response to viral pathogens (188). Yet, many viruses have evolved to utilize AMPK signaling for their benefit (168). HCMV and DENV both activate AMPK, at least in part, to modulate host metabolism, but both encode evasion strategies to avoid the shutdown of *de novo* lipid synthesis by AMPK (88, 173, 174, 256). DENV NS3 recruits FASN to sites of viral replication and increases its activity (208), and results in our lab have also suggested ACC1 is similarly recruited and stimulated. HCMV infection increases both the expression and specific activity of ACC1, although through an unknown mechanism (256). Similarly, rotavirus infection requires both the activation of AMPK and maintenance of fatty acid biosynthesis for robust viral infection (35, 58, 68). Thus, for at least some viruses modulation of AMPK comes along with subversion strategies to drive *de novo* fatty acid synthesis.

Exploring the known kinases upstream of AMPK for their impact on DENV-lipophagy led to several interesting findings. First, knockdown and inhibition of TAK1 was sufficient to block DENV-lipophagy without inhibiting viral replication, while inhibition of CaMKKβ inhibited viral replication but not DENV-lipophagy. Although it remains unclear why TAK1 inhibition uncouples viral replication and lipophagy induction, combined with the CaMKKβ data it is evidence that generic inhibition of viral replication does not simply block autophagy induction. It is important to emphasize the superiority of immunfluorescence analysis of single

cells rather than whole cell assays, e.g. Western blot analysis or thin layer chromatography, etc. These bulk population assays cannot discriminate between decreased infection rates leading to fewer cells undergoing lipophagy, and the specific inhibition of lipophagy in infected cells.

Our data also indicate that TAK1 does not require LKB1 as an intermediary for AMPK activation during DENV-induced lipophagy. If this were so, we would expect to see both TAK1 and LKB1 required for lipophagy, but we do not. TRAIL induces a cytoprotective autophagy via TAK1 that is LKB1-independent, and while LKB1 has been suggested to be the intermediary between TAK1 and AMPK in TAK1 control of lipid metabolism, the data for this is only correlative (90, 102). Primary hepatocytes from TAK1 deficient mice showed decreased phosphorylation of LKB1 and AMPK under starvation conditions as compared to their wildtype counterparts (102).

Our studies are the first to suggest an AMPK-dependent role of TAK1 in viral replication. Viral interaction with TAK1 has focused largely on its signaling through NFκB or various mitogen-activated protein kinase (MAPK) cascades. Even more so than AMPK, the activation of TAK1 presents a conundrum for DENV, as TAK1 functions primarily as a restriction factor for DENV. We tested the obvious candidate for a TAK1 antiviral effector, NFκB activation, however the NFκB inhibitor decreased viral replication, suggesting NFκB activation is proviral for DENV replication. Exploration of the major downstream MAPK pathways showed no effect on viral replication either, and so the antiviral activity of TAK1 will require more detailed study. Using a microarray to determine genes differentially regulated by

TAK1 during DENV infection may be an initial start point. Additionally, proteomic analysis has identified two DENV NS proteins (NS1 and NS2B) that can interact with TAB2, an adaptor molecule important for TAK1 activation (124). Interrogation of how this affects TAK1 signaling might also be telling.

Both TAK1 and TβR2 have been demonstrated to influence lipid metabolism, and this falls in line with our data (102, 105, 185). The depletion of TAK1 in mouse livers leads to increased lipid droplets (steatosis), brought about by a decrease in hepatic autophagy and β-oxidation. Activation of PPARα or inhibition of mTORC1 (both of which induce autophagy) leads to a decrease in lipid burden in the livers (102, 185). In the case of TGFβ signaling, depletion of TβR2 in epithelial cells of the palate leads to a spontaneous accumulation of lipid droplets in these cells (105). While this is thought to be dependent in large part on defective lipolysis, we now know efficient lipolysis is also required for lipophagy (118). Together with our results, this suggests that DENV may manipulate an existing pathway for the degradation of LDs, and not constructing a pathway from scratch. Thus, a principal importance of this work has been to utilize DENV as a tool to elucidate the natural cellular pathways that control lipophagy.

To understand the machinery involved in targeting the lipid droplet, we began with a semi-unbiased approach. Detection of ubiquitin peptides in DENV, but not mock, infected LD samples suggested that lipophagy might be signaled in a ubiquitin-dependent manner. Immunofluorescence analysis of infected cells further supported this model, as infected cells showed increased localization of ubiquitin, as well as the ubiquitin-dependent autophagy adaptor NBR1, at the LD. NBR1 is one of

five canonical autophagy adaptors. NBR1 has distinct roles in the autophagy of peroxisomes, focal adhesions, and is dispensable for mitophagy (43, 123, 145, 247). Validating the ubiquitin-dependence of lipophagy will require the reconstitution of NBR1-deficient cells with WT NBR1 and ΔUBA NBR1 constructs to determine whether lipid droplets are depleted when NBR1 cannot bridge the ubiquitinated LD surface to the nascent autophagosome.

Antagonism of the TβR-dependent signaling pathway demonstrated that this signaling pathway does not control ubiquitin deposition at the lipid droplet surface. There is at least one other signaling pathway that must activate the E3 ligase responsible for ubiquitination of the LD surface; and if this ligase is not LD-resident, recruit the ligase to the LD. This data also suggests that TGFβ is not the originating signal for lipophagy, a point further supported by the inability of exogenous TGFβ to induce lipophagy. Identifying this ligase will be important for understanding this second signal, and determining the initiating signal for lipophagy. In PINK1/PARKIN mitophagy, this signal is the depolarization of the intermitochondrial space. This leads to the PINK1-dependent phosphorylation of ubiquitin, recruitment of autophagy adaptors (NDP52 and OPTN), increased PARKIN E3 ligase activity, ubiquitin deposition, and further ubiquitin phosphorylation by PINK1 (29, 38, 59, 98, 107, 116, 120, 121, 136, 145, 177, 178, 248). This continues in a feed-forward mechanism, recruiting more PARKIN and autophagy adaptors to the mitochondrial surface. For forms of xenophagy, endosomal rupture exposes luminal sugars that are then bound by galectins (31, 156, 268). These galectins then orchestrate the initiation of xenophagy (31, 268).

One of the largest remaining questions of DENV- induced lipophagy is the identity of the E3 ligase for lipophagy. Our proteomics attempts to date have been biased towards the recruitment of an E3 ligase, but recent work in pexophagy has shown that organelle resident E3 ligases can also be involved in selective autophagies (235). To this day, there has not yet been identified a resident E3 ligase of lipid droplets and so we have leaned towards the recruitment hypothesis. Addressing this question using proteomics of the LD has had little success, and this is largely for two reasons: the low protein content of lipid droplets (and thus large number of viruses and cells required) and relatively few number of lipid droplets undergoing lipophagy at any one time. However, we now have the tools to overcome these issues.

These limitations can be circumvented by a combination of TAK1 knockdown (or pharmacological inhibition) and a cell line that inducibly expresses NS1-3. Inducing NS1-3 expression allows us to expand to as many cells as we desire without limits on how much virus we can produce. Furthermore, depletion or inhibition of TAK1 will allow us to let the marking of lipid droplets proceed in the absence of autophagic clearance. What is evident from mitophagy and xenophagy is that the E3 ligase that ubiquitinates the cargo remains associated with the cargo. Thus, allowing the marking to accumlate should also allow the ligase to accumulate. Technically, this strategy could be utilized with any of the signaling molecules although inhibition of TAK1 has the least effect on cell growth after several passages. Stable isotope labeling of amino acids in culture (SILAC) or another quantitative proteomics approach of the lipid droplet associated fraction would be

the best choice in these circumstances, as one could examine both differentially localized proteins as well as resident proteins for a potential E3 ligase.

The validation of the E3 ligase should focus on complementing knockdown cells with a mutant deficient in ligase activity, and the subsequent monitoring of LDs for depletion, K63-linked ubiquitin, and NBR1 recruitment as compared to the WT ligase. After that, focusing on the viral proteins involved in recruiting and activating the ligase would be worth examining. If a viral protein did bind the E3 ligase, it would be interesting to see what other substrates the ligase might ubiquitinate during DENV infection. Substrates of E3 ligases have been notoriously hard to identify, however, a recently described technique (UBAIT) takes advantage of ubiquitination chemistry to trap ligase-ubiquitin-substrate complexes covalently, reportedly yielding more substrates than simple co-immunoprecipitation strategies (198).

NS1-3 is sufficient to induce lipophagy, yet how they induce lipophagy remains unknown. Obvious starting points to resolve this focus on the enzymatic activities of NS3 and the hydrophobic interface of NS1 hexamers. It should be emphasized that the finding that these proteins were important for lipophagy was entirely unexpected based on the fact that they were specifically tested for co-localization with autophagosomes in DENV infected cells (89). However, since that publication both NS3 and NS1 (in addition to the capsid protein) have been either shown or suggested to associate with lipid droplets, respectively (70, 265). NS1 hexamers are secreted from infected cells as lipoprotein-like molecules with a core rich in triglycerides, the main constituent of lipid droplets (70). Since lipophagy

results in increased β-oxidation, and it is inhibition of this β-oxidation that is essential for viral replication (89) it seems unlikely that the formation of NS1-hexameric lipoproteins would be an initiating event in lipophagy. In pursuit of the functional domain/amino acids of NS1 in lipophagy, the second approach would be the more conventional mutational analysis, beginning with large deletions and fine-tuning down to amino acid substitutions. Deleting the region of NS1 that interacts with the TAK1 adaptor TAB2 might be a usefull starting point (124).

For NS3, if mutating the enzymatic activities has no effect, an additional approach would be testing mutants that are unable to bind FASN or the RNAi-mediated depletion of Rab18. Together, these would render the virus able to activate and, possibly, relocalize FASN to LDs, respecitively (88, 265). This strategy pursues the hypothesis that lipophagy may be a cellular response to the increase in fatty acid synthesis driven by viral replication. Indeed, a major way of inducing lipophagy in other experimental systems relies on overloading the cells with fatty acids. In the third part of his thesis, Nick Heaton mapped the binding of FASN and NS3 to two stretches of amino acids on the N and C-terminus of NS3. These residues were essential for DENV replication, limiting our ability to test the functional consequences of their mutation on modulated lipid metabolism. The ability to induce lipophagy by transfecting NS1-3 now allows the mutations to be characterized outside of the context of the virus. Directly inhibiting FASN should be avoided, since the inhibition of FASN can decrease the number of lipid droplets in the cell, complicating the interpretation of the experiment.

While the above has focused on NS1 and NS3, it is formally possible that NS2A plays a role in initiating lipophagy, and this should be ruled out experimentally. Either by the simple quantification of LD area in cells co-transfected with NS1 and NS3 vs those with NS2A and NS3. Given that NS2b-4a does not induce this process, we can reason that NS2B itself, or in combination with NS3, is insufficient for lipophagy.

Two final questions of interest extend beyond deeper mechanistic understanding of the pathway of lipophagy, and focus on how lipophagy benefits viral infection. The first deals with the cell-intrinsic benefit DENV derives from lipophagy, which is to say – what does β-oxidation provide for the virus? We have presumed that the relevant output for β-oxidation is the production of ATP, yet we have not thoroughly tested this. In this sense a metabolomics approach may be most useful. Rather than simply quantifying the change in metabolites between mock or DENV infected cells in the presence and absence of etomixir, it might be beneficial to also trace label lipids so that one could monitor their flux during viral infection. This approach has proved successful in studying the metabolic reorganization of the cell by HCMV (191). After metabolic profiling, a more nuanced analysis of the major metabolites changed could identify what in particular is important for DENV. The why, however, may remain elusive.

The second question examines lipophagy with a view towards the emerging intersection of metabolism and immunity. The activation and effector function of immune cells is heavily shaped by their metabolic landscape. Principally this has been described in understanding T-cell biology, but work has been done in other

immune cell types with each subset requiring different metabolic needs (reviewed in (196, 199, 200)). One of the principal cell targets of DENV is dendritic cells. AMPK is a metablic switch point for dendritic cells (28, 53). Immature myeloid DCs drive an AMPK-active, lipid-oxidation dependent metabolic program, and upon activation switch over to an AMPK-inactive, glycolysis-dependent metabolism for maturation (53). Forced activation of AMPK inhibits the maturation of myeloid DCs, and deletion or inhibition of AMPK leads to hyperactivation of immature DCs in response to stimuli (28, 53). DENV suppresses DC activation and the ability of infected DCs to stimulate T-cells (207, 224, 225). While the suppression of RIG-I translocation to the mitochondria by NS3 plays an important role in suppressing DC activation (30), it remains possible that the activation of an AMPK-dependent, lipid-oxidation end point autophagy program in infected immature DCs helps to enforce an immature phenotype.

The experimental proof of principle would be fairly straightforward since we can induce AMPK-dependent lipophagy independent of viral replication/infection. CD14- monocytes can be transduced with lentivirus pseudoparticles encoding NS1-3 and differentiated into immature DCs using a standard cocktail of GM-CSF and IL-4. To determine whether NS1-3 expression affects DC maturation, DCs can be induced by the addition of several different ligands – TNFa, LPS, polyI:C, etc – and maturation can be assessed by staining for CD80 and CD86 surface markers, as well as their ability to stimulate the proliferation and activation (IFN-γ production) of T-cells. In addition to being an initial study into viruses modulating metabolism to evade the immune system, it could provide further explanation as to why the virus

has evolved a mechanism to activate the AMPK pathway when its activation shuts down fatty acid synthesis, a process upon which the viral lifecycle heavily depends. It may further explain why the virus evolved a mechanism to specifically recruit FASN as a spatial attempt in resolving this AMPK activation paradox.

REFERENCES

1. 2010. Locally acquired Dengue--Key West, Florida, 2009-2010. MMWR. Morbidity and mortality weekly report 59:577-581.
2. 2012. West nile virus disease and other arboviral diseases - United States, 2011. MMWR. Morbidity and mortality weekly report 61:510-514.
3. Abrahamsen, H., H. Stenmark, and H. W. Platta. 2012. Ubiquitination and phosphorylation of Beclin 1 and its binding partners: Tuning class III phosphatidylinositol 3-kinase activity and tumor suppression. FEBS letters 586:1584-1591.
4. Acosta, E. G., V. Castilla, and E. B. Damonte. 2008. Functional entry of dengue virus into Aedes albopictus mosquito cells is dependent on clathrin-mediated endocytosis. J Gen Virol 89:474-484.
5. Agarwal, R., E. A. Elbishbishi, U. C. Chaturvedi, R. Nagar, and A. S. Mustafa. 1999. Profile of transforming growth factor-beta 1 in patients with dengue haemorrhagic fever. International journal of experimental pathology 80:143-149.
6. Alers, S., A. S. Loffler, S. Wesselborg, and B. Stork. 2012. Role of AMPK-mTOR-Ulk1/2 in the regulation of autophagy: cross talk, shortcuts, and feedbacks. Molecular and cellular biology 32:2-11.
7. Allonso, D., I. S. Andrade, J. N. Conde, D. R. Coelho, D. C. Rocha, M. L. da Silva, G. T. Ventura, E. M. Silva, and R. Mohana-Borges. 2015. Dengue Virus NS1 Protein Modulates Cellular Energy Metabolism by Increasing Glyceraldehyde-3-Phosphate Dehydrogenase Activity. J Virol 89:11871-11883.
8. Ando, T., H. Imamura, R. Suzuki, H. Aizaki, T. Watanabe, T. Wakita, and T. Suzuki. 2012. Visualization and measurement of ATP levels in living cells replicating hepatitis C virus genome RNA. PLoS Pathog 8:e1002561.
9. Axe, E. L., S. A. Walker, M. Manifava, P. Chandra, H. L. Roderick, A. Habermann, G. Griffiths, and N. T. Ktistakis. 2008. Autophagosome formation from membrane compartments enriched in phosphatidylinositol 3-phosphate and dynamically connected to the endoplasmic reticulum. J Cell Biol 182:685-701.
10. Bai, F., K. F. Kong, J. Dai, F. Qian, L. Zhang, C. R. Brown, E. Fikrig, and R. R. Montgomery. 2010. A paradoxical role for neutrophils in the pathogenesis of West Nile virus. The Journal of infectious diseases 202:1804-1812.
11. Basel-Vanagaite, L., R. Yilmaz, S. Tang, M. S. Reuter, N. Rahner, D. K. Grange, M. Mortenson, P. Koty, H. Feenstra, K. D. Farwell Gonzalez, H. Sticht, N. Boddaert, J. Desir, K. Anyane-Yeboa, C. Zweier, A. Reis, C. Kubisch, T. Jewett, W. Zeng, and G. Borck. 2014. Expanding the clinical and mutational spectrum of Kaufman oculocerebrofacial syndrome with biallelic UBE3B mutations. Human genetics 133:939-949.
12. Beasley, D. W., L. Li, M. T. Suderman, and A. D. Barrett. 2002. Mouse neuroinvasive phenotype of West Nile virus strains varies depending upon virus genotype. Virology 296:17-23.

13. Beasley, D. W., M. C. Whiteman, S. Zhang, C. Y. Huang, B. S. Schneider, D. R. Smith, G. D. Gromowski, S. Higgs, R. M. Kinney, and A. D. Barrett. 2005. Envelope protein glycosylation status influences mouse neuroinvasion phenotype of genetic lineage 1 West Nile virus strains. J Virol 79:8339-8347.
14. Beatman, E., R. Oyer, K. D. Shives, K. Hedman, A. C. Brault, K. L. Tyler, and J. D. Beckham. 2012. West Nile virus growth is independent of autophagy activation. Virology 433:262-272.
15. Ben-Nathan, D., I. Huitinga, S. Lustig, N. van Rooijen, and D. Kobiler. 1996. West Nile virus neuroinvasion and encephalitis induced by macrophage depletion in mice. Archives of virology 141:459-469.
16. Bhatt, S., P. W. Gething, O. J. Brady, J. P. Messina, A. W. Farlow, C. L. Moyes, J. M. Drake, J. S. Brownstein, A. G. Hoen, O. Sankoh, M. F. Myers, D. B. George, T. Jaenisch, G. R. Wint, C. P. Simmons, T. W. Scott, J. J. Farrar, and S. I. Hay. 2013. The global distribution and burden of dengue. Nature 496:504-507.
17. Birgisdottir, A. B., T. Lamark, and T. Johansen. 2013. The LIR motif - crucial for selective autophagy. Journal of cell science 126:3237-3247.
18. Blackley, S., Z. Kou, H. Chen, M. Quinn, R. C. Rose, J. J. Schlesinger, M. Coppage, and X. Jin. 2007. Primary human splenic macrophages, but not T or B cells, are the principal target cells for dengue virus infection in vitro. J Virol 81:13325-13334.
19. Bomberger, J. M., R. L. Barnaby, and B. A. Stanton. 2010. The deubiquitinating enzyme USP10 regulates the endocytic recycling of CFTR in airway epithelial cells. Channels (Austin) 4:150-154.
20. Bomberger, J. M., R. L. Barnaby, and B. A. Stanton. 2009. The deubiquitinating enzyme USP10 regulates the post-endocytic sorting of cystic fibrosis transmembrane conductance regulator in airway epithelial cells. J Biol Chem 284:18778-18789.
21. Boonnak, K., K. M. Dambach, G. C. Donofrio, B. Tassaneetrithep, and M. A. Marovich. 2011. Cell type specificity and host genetic polymorphisms influence antibody-dependent enhancement of dengue virus infection. J Virol 85:1671-1683.
22. Boonnak, K., B. M. Slike, T. H. Burgess, R. M. Mason, S. J. Wu, P. Sun, K. Porter, I. F. Rudiman, D. Yuwono, P. Puthavathana, and M. A. Marovich. 2008. Role of dendritic cells in antibody-dependent enhancement of dengue virus infection. J Virol 82:3939-3951.
23. Boya, P., F. Reggiori, and P. Codogno. 2013. Emerging regulation and functions of autophagy. Nat Cell Biol 15:713-720.
24. Brandt, W. E., J. M. McCown, M. K. Gentry, and P. K. Russell. 1982. Infection enhancement of dengue type 2 virus in the U-937 human monocyte cell line by antibodies to flavivirus cross-reactive determinants. Infection and immunity 36:1036-1041.
25. Buescher, E. L., and W. F. Scherer. 1959. Ecologic studies of Japanese encephalitis virus in Japan. IX. Epidemiologic correlations and conclusions. The American journal of tropical medicine and hygiene 8:719-722.

26. Burnett, P. E., R. K. Barrow, N. A. Cohen, S. H. Snyder, and D. M. Sabatini. 1998. RAFT1 phosphorylation of the translational regulators p70 S6 kinase and 4E-BP1. Proc Natl Acad Sci U S A 95:1432-1437.
27. Carling, D., P. R. Clarke, V. A. Zammit, and D. G. Hardie. 1989. Purification and characterization of the AMP-activated protein kinase. Copurification of acetyl-CoA carboxylase kinase and 3-hydroxy-3-methylglutaryl-CoA reductase kinase activities. European journal of biochemistry / FEBS 186:129-136.
28. Carroll, K. C., B. Viollet, and J. Suttles. 2013. AMPKalpha1 deficiency amplifies proinflammatory myeloid APC activity and CD40 signaling. Journal of leukocyte biology 94:1113-1121.
29. Caulfield, T. R., F. C. Fiesel, E. L. Moussaud-Lamodiere, D. F. Dourado, S. C. Flores, and W. Springer. 2014. Phosphorylation by PINK1 releases the UBL domain and initializes the conformational opening of the E3 ubiquitin ligase Parkin. PLoS computational biology 10:e1003935.
30. Chan, Y. K., and M. U. Gack. 2016. A phosphomimetic-based mechanism of dengue virus to antagonize innate immunity. Nat Immunol 17:523-530.
31. Chauhan, S., S. Kumar, A. Jain, M. Ponpuak, M. H. Mudd, T. Kimura, S. W. Choi, R. Peters, M. Mandell, J. A. Bruun, T. Johansen, and V. Deretic. 2016. TRIMs and Galectins Globally Cooperate and TRIM16 and Galectin-3 Co-direct Autophagy in Endomembrane Damage Homeostasis. Developmental cell.
32. Chen, R. F., L. Wang, J. T. Cheng, H. Chuang, J. C. Chang, J. W. Liu, I. C. Lin, and K. D. Yang. 2009. Combination of CTLA-4 and TGFbeta1 gene polymorphisms associated with dengue hemorrhagic fever and virus load in a dengue-2 outbreak. Clin Immunol 131:404-409.
33. Chi, P. I., W. R. Huang, I. H. Lai, C. Y. Cheng, and H. J. Liu. 2013. The p17 nonstructural protein of avian reovirus triggers autophagy enhancing virus replication via activation of phosphatase and tensin deleted on chromosome 10 (PTEN) and AMP-activated protein kinase (AMPK), as well as dsRNA-dependent protein kinase (PKR)/eIF2alpha signaling pathways. J Biol Chem 288:3571-3584.
34. Chukkapalli, V., N. S. Heaton, and G. Randall. 2012. Lipids at the interface of virus-host interactions. Current opinion in microbiology 15:512-518.
35. Crawford, S. E., J. M. Hyser, B. Utama, and M. K. Estes. 2012. Autophagy hijacked through viroporin-activated calcium/calmodulin-dependent kinase kinase-beta signaling is required for rotavirus replication. Proc Natl Acad Sci U S A 109:E3405-3413.
36. Dai, L., C. Aye Thu, X. Y. Liu, J. Xi, and P. C. Cheung. 2012. TAK1, more than just innate immunity. IUBMB life 64:825-834.
37. Davies, S. P., D. Carling, and D. G. Hardie. 1989. Tissue distribution of the AMP-activated protein kinase, and lack of activation by cyclic-AMP-dependent protein kinase, studied using a specific and sensitive peptide assay. European journal of biochemistry / FEBS 186:123-128.
38. Deas, E., H. Plun-Favreau, S. Gandhi, H. Desmond, S. Kjaer, S. H. Loh, A. E. Renton, R. J. Harvey, A. J. Whitworth, L. M. Martins, A. Y. Abramov, and N. W.

Wood. 2011. PINK1 cleavage at position A103 by the mitochondrial protease PARL. Human molecular genetics 20:867-879.
39. Dechtawewat, T., A. Paemanee, S. Roytrakul, P. Songprakhon, T. Limjindaporn, P. T. Yenchitsomanus, S. Saitornuang, C. Puttikhunt, W. Kasinrerk, P. Malasit, and S. Noisakran. 2016. Mass spectrometric analysis of host cell proteins interacting with dengue virus nonstructural protein 1 in dengue virus-infected HepG2 cells. Biochimica et biophysica acta 1864:1270-1280.
40. Dejnirattisai, W., A. Jumnainsong, N. Onsirisakul, P. Fitton, S. Vasanawathana, W. Limpitikul, C. Puttikhunt, C. Edwards, T. Duangchinda, S. Supasa, K. Chawansuntati, P. Malasit, J. Mongkolsapaya, and G. Screaton. 2010. Cross-reacting antibodies enhance dengue virus infection in humans. Science 328:745-748.
41. Delgado, M. A., R. A. Elmaoued, A. S. Davis, G. Kyei, and V. Deretic. 2008. Toll-like receptors control autophagy. Embo J 27:1110-1121.
42. Denizot, M., M. Varbanov, L. Espert, V. Robert-Hebmann, S. Sagnier, E. Garcia, M. Curriu, R. Mamoun, J. Blanco, and M. Biard-Piechaczyk. 2008. HIV-1 gp41 fusogenic function triggers autophagy in uninfected cells. Autophagy 4:998-1008.
43. Deosaran, E., K. B. Larsen, R. Hua, G. Sargent, Y. Wang, S. Kim, T. Lamark, M. Jauregui, K. Law, J. Lippincott-Schwartz, A. Brech, T. Johansen, and P. K. Kim. 2013. NBR1 acts as an autophagy receptor for peroxisomes. Journal of cell science 126:939-952.
44. Deretic, V. 2011. Autophagy in immunity and cell-autonomous defense against intracellular microbes. Immunol Rev 240:92-104.
45. Deretic, V., T. Saitoh, and S. Akira. 2013. Autophagy in infection, inflammation and immunity. Nature reviews. Immunology 13:722-737.
46. DeVito, S. R., E. Ortiz-Riano, L. Martinez-Sobrido, and J. Munger. 2014. Cytomegalovirus-mediated activation of pyrimidine biosynthesis drives UDP-sugar synthesis to support viral protein glycosylation. Proc Natl Acad Sci U S A 111:18019-18024.
47. Dong, X., and B. Levine. 2013. Autophagy and viruses: adversaries or allies? Journal of innate immunity 5:480-493.
48. Draker, R., E. Sarcinella, and P. Cheung. 2011. USP10 deubiquitylates the histone variant H2A.Z and both are required for androgen receptor-mediated gene activation. Nucleic acids research 39:3529-3542.
49. Dupont, N., S. Chauhan, J. Arko-Mensah, E. F. Castillo, A. Masedunskas, R. Weigert, H. Robenek, T. Proikas-Cezanne, and V. Deretic. 2014. Neutral lipid stores and lipase PNPLA5 contribute to autophagosome biogenesis. Current biology : CB 24:609-620.
50. Egan, D., J. Kim, R. J. Shaw, and K. L. Guan. 2011. The autophagy initiating kinase ULK1 is regulated via opposing phosphorylation by AMPK and mTOR. Autophagy 7:643-644.
51. Egan, D. F., D. B. Shackelford, M. M. Mihaylova, S. Gelino, R. A. Kohnz, W. Mair, D. S. Vasquez, A. Joshi, D. M. Gwinn, R. Taylor, J. M. Asara, J. Fitzpatrick, A. Dillin, B. Viollet, M. Kundu, M. Hansen, and R. J. Shaw. 2011. Phosphorylation

of ULK1 (hATG1) by AMP-activated protein kinase connects energy sensing to mitophagy. Science 331:456-461.
52. Espert, L., M. Denizot, M. Grimaldi, V. Robert-Hebmann, B. Gay, M. Varbanov, P. Codogno, and M. Biard-Piechaczyk. 2006. Autophagy is involved in T cell death after binding of HIV-1 envelope proteins to CXCR4. J Clin Invest 116:2161-2172.
53. Everts, B., E. Amiel, S. C. Huang, A. M. Smith, C. H. Chang, W. Y. Lam, V. Redmann, T. C. Freitas, J. Blagih, G. J. van der Windt, M. N. Artyomov, R. G. Jones, E. L. Pearce, and E. J. Pearce. 2014. TLR-driven early glycolytic reprogramming via the kinases TBK1-IKKvarepsilon supports the anabolic demands of dendritic cell activation. Nat Immunol 15:323-332.
54. Fang, Y. T., S. W. Wan, Y. T. Lu, J. H. Yao, C. F. Lin, L. J. Hsu, M. G. Brown, J. S. Marshall, R. Anderson, and Y. S. Lin. 2014. Autophagy facilitates antibody-enhanced dengue virus infection in human pre-basophil/mast cells. PloS one 9:e110655.
55. Fontaine, K. A., E. L. Sanchez, R. Camarda, and M. Lagunoff. 2015. Dengue virus induces and requires glycolysis for optimal replication. J Virol 89:2358-2366.
56. Fujita, N., T. Itoh, H. Omori, M. Fukuda, T. Noda, and T. Yoshimori. 2008. The Atg16L complex specifies the site of LC3 lipidation for membrane biogenesis in autophagy. Molecular biology of the cell 19:2092-2100.
57. Galao, R. P., A. Le Tortorec, S. Pickering, T. Kueck, and S. J. Neil. 2012. Innate sensing of HIV-1 assembly by Tetherin induces NFkappaB-dependent proinflammatory responses. Cell Host Microbe 12:633-644.
58. Gaunt, E. R., W. Cheung, J. E. Richards, A. Lever, and U. Desselberger. 2013. Inhibition of rotavirus replication by downregulation of fatty acid synthesis. J Gen Virol 94:1310-1317.
59. Geisler, S., K. M. Holmstrom, D. Skujat, F. C. Fiesel, O. C. Rothfuss, P. J. Kahle, and W. Springer. 2010. PINK1/Parkin-mediated mitophagy is dependent on VDAC1 and p62/SQSTM1. Nat Cell Biol 12:119-131.
60. Geng, J., and D. J. Klionsky. 2008. The Atg8 and Atg12 ubiquitin-like conjugation systems in macroautophagy. 'Protein modifications: beyond the usual suspects' review series. EMBO reports 9:859-864.
61. Getts, D. R., R. L. Terry, M. T. Getts, M. Muller, S. Rana, B. Shrestha, J. Radford, N. Van Rooijen, I. L. Campbell, and N. J. King. 2008. Ly6c+ "inflammatory monocytes" are microglial precursors recruited in a pathogenic manner in West Nile virus encephalitis. The Journal of experimental medicine 205:2319-2337.
62. Gilfoy, F. D., and P. W. Mason. 2007. West Nile virus-induced interferon production is mediated by the double-stranded RNA-dependent protein kinase PKR. J Virol 81:11148-11158.
63. Gollins, S. W., and J. S. Porterfield. 1985. Flavivirus infection enhancement in macrophages: an electron microscopic study of viral cellular entry. J Gen Virol 66 (Pt 9):1969-1982.

64. Gollins, S. W., and J. S. Porterfield. 1986. pH-dependent fusion between the flavivirus West Nile and liposomal model membranes. J Gen Virol 67 (Pt 1):157-166.
65. Goodall, M. L., B. E. Fitzwalter, S. Zahedi, M. Wu, D. Rodriguez, J. M. Mulcahy-Levy, D. R. Green, M. Morgan, S. D. Cramer, and A. Thorburn. 2016. The Autophagy Machinery Controls Cell Death Switching between Apoptosis and Necroptosis. Developmental cell 37:337-349.
66. Goodwin, C. M., S. Xu, and J. Munger. 2015. Stealing the Keys to the Kitchen: Viral Manipulation of the Host Cell Metabolic Network. Trends in microbiology 23:789-798.
67. Gowans, G. J., S. A. Hawley, F. A. Ross, and D. G. Hardie. 2013. AMP is a true physiological regulator of AMP-activated protein kinase by both allosteric activation and enhancing net phosphorylation. Cell metabolism 18:556-566.
68. Green, V. A., and L. Pelkmans. 2016. A Systems Survey of Progressive Host-Cell Reorganization during Rotavirus Infection. Cell Host Microbe 20:107-120.
69. Guo, B., X. Huang, P. Zhang, L. Qi, Q. Liang, X. Zhang, J. Huang, B. Fang, W. Hou, J. Han, and H. Zhang. 2014. Genome-wide screen identifies signaling pathways that regulate autophagy during Caenorhabditis elegans development. EMBO reports 15:705-713.
70. Gutsche, I., F. Coulibaly, J. E. Voss, J. Salmon, J. d'Alayer, M. Ermonval, E. Larquet, P. Charneau, T. Krey, F. Megret, E. Guittet, F. A. Rey, and M. Flamand. 2011. Secreted dengue virus nonstructural protein NS1 is an atypical barrel-shaped high-density lipoprotein. Proc Natl Acad Sci U S A 108:8003-8008.
71. Guzman, M. G., M. Alvarez, and S. B. Halstead. 2013. Secondary infection as a risk factor for dengue hemorrhagic fever/dengue shock syndrome: an historical perspective and role of antibody-dependent enhancement of infection. Archives of virology 158:1445-1459.
72. Gwinn, D. M., D. B. Shackelford, D. F. Egan, M. M. Mihaylova, A. Mery, D. S. Vasquez, B. E. Turk, and R. J. Shaw. 2008. AMPK phosphorylation of raptor mediates a metabolic checkpoint. Mol Cell 30:214-226.
73. Hadinegoro, S. R., J. L. Arredondo-Garcia, M. R. Capeding, C. Deseda, T. Chotpitayasunondh, R. Dietze, H. I. Muhammad Ismail, H. Reynales, K. Limkittikul, D. M. Rivera-Medina, H. N. Tran, A. Bouckenooghe, D. Chansinghakul, M. Cortes, K. Fanouillere, R. Forrat, C. Frago, S. Gailhardou, N. Jackson, F. Noriega, E. Plennevaux, T. A. Wartel, B. Zambrano, and M. Saville. 2015. Efficacy and Long-Term Safety of a Dengue Vaccine in Regions of Endemic Disease. The New England journal of medicine 373:1195-1206.
74. Hale, A. N., D. J. Ledbetter, T. R. Gawriluk, and E. B. Rucker, 3rd. 2013. Autophagy: Regulation and role in development. Autophagy 9:951-972.
75. Halstead, S. B., and E. J. O'Rourke. 1977. Antibody-enhanced dengue virus infection in primate leukocytes. Nature 265:739-741.
76. Halstead, S. B., and E. J. O'Rourke. 1977. Dengue viruses and mononuclear phagocytes. I. Infection enhancement by non-neutralizing antibody. The Journal of experimental medicine 146:201-217.

77. Hamel, R., O. Dejarnac, S. Wichit, P. Ekchariyawat, A. Neyret, N. Luplertlop, M. Perera-Lecoin, P. Surasombatpattana, L. Talignani, F. Thomas, V. M. Cao-Lormeau, V. Choumet, L. Briant, P. Despres, A. Amara, H. Yssel, and D. Misse. 2015. Biology of Zika Virus Infection in Human Skin Cells. J Virol 89:8880-8896.
78. Hanada, T., N. N. Noda, Y. Satomi, Y. Ichimura, Y. Fujioka, T. Takao, F. Inagaki, and Y. Ohsumi. 2007. The Atg12-Atg5 conjugate has a novel E3-like activity for protein lipidation in autophagy. J Biol Chem 282:37298-37302.
79. Hanczko, R., D. R. Fernandez, E. Doherty, Y. Qian, G. Vas, B. Niland, T. Telarico, A. Garba, S. Banerjee, F. A. Middleton, D. Barrett, M. Barcza, K. Banki, S. K. Landas, and A. Perl. 2009. Prevention of hepatocarcinogenesis and increased susceptibility to acetaminophen-induced liver failure in transaldolase-deficient mice by N-acetylcysteine. J Clin Invest 119:1546-1557.
80. Hanna, R. A., M. N. Quinsay, A. M. Orogo, K. Giang, S. Rikka, and A. B. Gustafsson. 2012. Microtubule-associated protein 1 light chain 3 (LC3) interacts with Bnip3 protein to selectively remove endoplasmic reticulum and mitochondria via autophagy. The Journal of biological chemistry 287:19094-19104.
81. Hardie, D. G., D. Carling, and S. J. Gamblin. 2011. AMP-activated protein kinase: also regulated by ADP? Trends in biochemical sciences 36:470-477.
82. Hardie, D. G., F. A. Ross, and S. A. Hawley. 2012. AMPK: a nutrient and energy sensor that maintains energy homeostasis. Nat Rev Mol Cell Biol 13:251-262.
83. Hashimoto, M., H. Nasser, T. Chihara, and S. Suzu. 2014. Macropinocytosis and TAK1 mediate anti-inflammatory to pro-inflammatory macrophage differentiation by HIV-1 Nef. Cell death & disease 5:e1267.
84. Hata, A., and Y. G. Chen. 2016. TGF-beta Signaling from Receptors to Smads. Cold Spring Harbor perspectives in biology 8.
85. Hawley, S. A., M. Davison, A. Woods, S. P. Davies, R. K. Beri, D. Carling, and D. G. Hardie. 1996. Characterization of the AMP-activated protein kinase kinase from rat liver and identification of threonine 172 as the major site at which it phosphorylates AMP-activated protein kinase. J Biol Chem 271:27879-27887.
86. Hawley, S. A., D. A. Pan, K. J. Mustard, L. Ross, J. Bain, A. M. Edelman, B. G. Frenguelli, and D. G. Hardie. 2005. Calmodulin-dependent protein kinase kinase-beta is an alternative upstream kinase for AMP-activated protein kinase. Cell metabolism 2:9-19.
87. He, C., Y. Wei, K. Sun, B. Li, X. Dong, Z. Zou, Y. Liu, L. N. Kinch, S. Khan, S. Sinha, R. J. Xavier, N. V. Grishin, G. Xiao, E. L. Eskelinen, P. E. Scherer, J. L. Whistler, and B. Levine. 2013. Beclin 2 functions in autophagy, degradation of G protein-coupled receptors, and metabolism. Cell 154:1085-1099.
88. Heaton, N. S., R. Perera, K. L. Berger, S. Khadka, D. J. Lacount, R. J. Kuhn, and G. Randall. 2010. Dengue virus nonstructural protein 3 redistributes fatty acid synthase to sites of viral replication and increases cellular fatty acid synthesis. Proc Natl Acad Sci U S A 107:17345-17350.
89. Heaton, N. S., and G. Randall. 2010. Dengue virus-induced autophagy regulates lipid metabolism. Cell Host Microbe 8:422-432.

90. Herrero-Martin, G., M. Hoyer-Hansen, C. Garcia-Garcia, C. Fumarola, T. Farkas, A. Lopez-Rivas, and M. Jaattela. 2009. TAK1 activates AMPK-dependent cytoprotective autophagy in TRAIL-treated epithelial cells. Embo J 28:677-685.
91. Ho, Y. K., H. Zhi, T. Bowlin, B. Dorjbal, S. Philip, M. A. Zahoor, H. M. Shih, O. J. Semmes, B. Schaefer, J. N. Glover, and C. Z. Giam. 2015. HTLV-1 Tax Stimulates Ubiquitin E3 Ligase, Ring Finger Protein 8, to Assemble Lysine 63-Linked Polyubiquitin Chains for TAK1 and IKK Activation. PLoS Pathog 11:e1005102.
92. Hong, S. P., M. Momcilovic, and M. Carlson. 2005. Function of mammalian LKB1 and Ca2+/calmodulin-dependent protein kinase kinase alpha as Snf1-activating kinases in yeast. J Biol Chem 280:21804-21809.
93. Hosokawa, N., T. Hara, T. Kaizuka, C. Kishi, A. Takamura, Y. Miura, S. Iemura, T. Natsume, K. Takehana, N. Yamada, J. L. Guan, N. Oshiro, and N. Mizushima. 2009. Nutrient-dependent mTORC1 association with the ULK1-Atg13-FIP200 complex required for autophagy. Molecular biology of the cell 20:1981-1991.
94. Howell, J. J., and B. D. Manning. 2011. mTOR couples cellular nutrient sensing to organismal metabolic homeostasis. Trends in endocrinology and metabolism: TEM 22:94-102.
95. Huang, J., Y. Li, Y. Qi, Y. Zhang, L. Zhang, Z. Wang, X. Zhang, and L. Gui. 2014. Coordinated regulation of autophagy and apoptosis determines endothelial cell fate during Dengue virus type 2 infection. Molecular and cellular biochemistry 397:157-165.
96. Hurley, R. L., K. A. Anderson, J. M. Franzone, B. E. Kemp, A. R. Means, and L. A. Witters. 2005. The Ca2+/calmodulin-dependent protein kinase kinases are AMP-activated protein kinase kinases. The Journal of biological chemistry 280:29060-29066.
97. Ichimura, Y., T. Kirisako, T. Takao, Y. Satomi, Y. Shimonishi, N. Ishihara, N. Mizushima, I. Tanida, E. Kominami, M. Ohsumi, T. Noda, and Y. Ohsumi. 2000. A ubiquitin-like system mediates protein lipidation. Nature 408:488-492.
98. Iguchi, M., Y. Kujuro, K. Okatsu, F. Koyano, H. Kosako, M. Kimura, N. Suzuki, S. Uchiyama, K. Tanaka, and N. Matsuda. 2013. Parkin-catalyzed ubiquitin-ester transfer is triggered by PINK1-dependent phosphorylation. J Biol Chem 288:22019-22032.
99. Inoki, K., J. Kim, and K. L. Guan. 2012. AMPK and mTOR in cellular energy homeostasis and drug targets. Annual review of pharmacology and toxicology 52:381-400.
100. Inoki, K., Y. Li, T. Xu, and K. L. Guan. 2003. Rheb GTPase is a direct target of TSC2 GAP activity and regulates mTOR signaling. Genes & development 17:1829-1834.
101. Inoki, K., T. Zhu, and K. L. Guan. 2003. TSC2 mediates cellular energy response to control cell growth and survival. Cell 115:577-590.
102. Inokuchi-Shimizu, S., E. J. Park, Y. S. Roh, L. Yang, B. Zhang, J. Song, S. Liang, M. Pimienta, K. Taniguchi, X. Wu, K. Asahina, W. Lagakos, M. R. Mackey, S. Akira, M. H. Ellisman, D. D. Sears, J. M. Olefsky, M. Karin, D. A. Brenner, and E. Seki.

2014. TAK1-mediated autophagy and fatty acid oxidation prevent hepatosteatosis and tumorigenesis. J Clin Invest 124:3566-3578.
103. Ishak, R., D. G. Tovey, and C. R. Howard. 1988. Morphogenesis of yellow fever virus 17D in infected cell cultures. J Gen Virol 69 (Pt 2):325-335.
104. Iwata, J., J. G. Hacia, A. Suzuki, P. A. Sanchez-Lara, M. Urata, and Y. Chai. 2012. Modulation of noncanonical TGF-beta signaling prevents cleft palate in Tgfbr2 mutant mice. J Clin Invest 122:873-885.
105. Iwata, J., A. Suzuki, R. C. Pelikan, T. V. Ho, P. A. Sanchez-Lara, and Y. Chai. 2014. Modulation of lipid metabolic defects rescues cleft palate in Tgfbr2 mutant mice. Human molecular genetics 23:182-193.
106. Jin, R., W. Zhu, S. Cao, R. Chen, H. Jin, Y. Liu, S. Wang, W. Wang, and G. Xiao. 2013. Japanese encephalitis virus activates autophagy as a viral immune evasion strategy. PLoS One 8:e52909.
107. Jin, S. M., M. Lazarou, C. Wang, L. A. Kane, D. P. Narendra, and R. J. Youle. 2010. Mitochondrial membrane potential regulates PINK1 import and proteolytic destabilization by PARL. J Cell Biol 191:933-942.
108. Jo, Y., I. Z. Hartman, and R. A. DeBose-Boyd. 2013. Ancient ubiquitous protein-1 mediates sterol-induced ubiquitination of 3-hydroxy-3-methylglutaryl CoA reductase in lipid droplet-associated endoplasmic reticulum membranes. Molecular biology of the cell 24:169-183.
109. Johansen, T., and T. Lamark. 2011. Selective autophagy mediated by autophagic adapter proteins. Autophagy 7:279-296.
110. Johnston, L. J., G. M. Halliday, and N. J. King. 2000. Langerhans cells migrate to local lymph nodes following cutaneous infection with an arbovirus. The Journal of investigative dermatology 114:560-568.
111. Jordan, T. X., and G. Randall. 2016. Flavivirus modulation of cellular metabolism. Current opinion in virology 19:7-10.
112. Jordan, T. X., and G. Randall. 2012. Manipulation or capitulation: virus interactions with autophagy. Microbes and infection / Institut Pasteur 14:126-139.
113. Joubert, P. E., G. Meiffren, I. P. Gregoire, G. Pontini, C. Richetta, M. Flacher, O. Azocar, P. O. Vidalain, M. Vidal, V. Lotteau, P. Codogno, C. Rabourdin-Combe, and M. Faure. 2009. Autophagy induction by the pathogen receptor CD46. Cell Host Microbe 6:354-366.
114. Jounai, N., F. Takeshita, K. Kobiyama, A. Sawano, A. Miyawaki, K. Q. Xin, K. J. Ishii, T. Kawai, S. Akira, K. Suzuki, and K. Okuda. 2007. The Atg5 Atg12 conjugate associates with innate antiviral immune responses. Proc Natl Acad Sci U S A 104:14050-14055.
115. Jung, C. H., S. H. Ro, J. Cao, N. M. Otto, and D. H. Kim. 2010. mTOR regulation of autophagy. FEBS letters 584:1287-1295.
116. Kane, L. A., M. Lazarou, A. I. Fogel, Y. Li, K. Yamano, S. A. Sarraf, S. Banerjee, and R. J. Youle. 2014. PINK1 phosphorylates ubiquitin to activate Parkin E3 ubiquitin ligase activity. J Cell Biol 205:143-153.
117. Kaushik, S., and A. M. Cuervo. 2016. AMPK-dependent phosphorylation of lipid droplet protein PLIN2 triggers its degradation by CMA. Autophagy 12:432-438.

118. Kaushik, S., and A. M. Cuervo. 2015. Degradation of lipid droplet-associated proteins by chaperone-mediated autophagy facilitates lipolysis. Nat Cell Biol 17:759-770.
119. Kaushik, S., J. A. Rodriguez-Navarro, E. Arias, R. Kiffin, S. Sahu, G. J. Schwartz, A. M. Cuervo, and R. Singh. 2011. Autophagy in hypothalamic AgRP neurons regulates food intake and energy balance. Cell metabolism 14:173-183.
120. Kazlauskaite, A., C. Kondapalli, R. Gourlay, D. G. Campbell, M. S. Ritorto, K. Hofmann, D. R. Alessi, A. Knebel, M. Trost, and M. M. Muqit. 2014. Parkin is activated by PINK1-dependent phosphorylation of ubiquitin at Ser65. The Biochemical journal 460:127-139.
121. Kazlauskaite, A., R. J. Martinez-Torres, S. Wilkie, A. Kumar, J. Peltier, A. Gonzalez, C. Johnson, J. Zhang, A. G. Hope, M. Peggie, M. Trost, D. M. van Aalten, D. R. Alessi, A. R. Prescott, A. Knebel, H. Walden, and M. M. Muqit. 2015. Binding to serine 65-phosphorylated ubiquitin primes Parkin for optimal PINK1-dependent phosphorylation and activation. EMBO reports 16:939-954.
122. Ke, P. Y., and S. S. Chen. 2011. Activation of the unfolded protein response and autophagy after hepatitis C virus infection suppresses innate antiviral immunity in vitro. J Clin Invest 121:37-56.
123. Kenific, C. M., S. J. Stehbens, J. Goldsmith, A. M. Leidal, N. Faure, J. Ye, T. Wittmann, and J. Debnath. 2016. NBR1 enables autophagy-dependent focal adhesion turnover. J Cell Biol 212:577-590.
124. Khadka, S., A. D. Vangeloff, C. Zhang, P. Siddavatam, N. S. Heaton, L. Wang, R. Sengupta, S. Sahasrabudhe, G. Randall, M. Gribskov, R. J. Kuhn, R. Perera, and D. J. LaCount. 2011. A physical interaction network of dengue virus and human proteins. Molecular & cellular proteomics : MCP 10:M111 012187.
125. Khakpoor, A., M. Panyasrivanit, N. Wikan, and D. R. Smith. 2009. A role for autophagolysosomes in dengue virus 3 production in HepG2 cells. J Gen Virol 90:1093-1103.
126. Khaminets, A., C. Behl, and I. Dikic. 2016. Ubiquitin-Dependent And Independent Signals In Selective Autophagy. Trends in cell biology 26:6-16.
127. Kim, D. H., D. D. Sarbassov, S. M. Ali, J. E. King, R. R. Latek, H. Erdjument-Bromage, P. Tempst, and D. M. Sabatini. 2002. mTOR interacts with raptor to form a nutrient-sensitive complex that signals to the cell growth machinery. Cell 110:163-175.
128. Kim, H. J., S. Lee, and J. U. Jung. 2010. When autophagy meets viruses: a double-edged sword with functions in defense and offense. Seminars in immunopathology 32:323-341.
129. Kim, J., Y. C. Kim, C. Fang, R. C. Russell, J. H. Kim, W. Fan, R. Liu, Q. Zhong, and K. L. Guan. 2013. Differential regulation of distinct Vps34 complexes by AMPK in nutrient stress and autophagy. Cell 152:290-303.
130. Kim, J., M. Kundu, B. Viollet, and K. L. Guan. 2011. AMPK and mTOR regulate autophagy through direct phosphorylation of Ulk1. Nat Cell Biol 13:132-141.
131. Kirisako, T., Y. Ichimura, H. Okada, Y. Kabeya, N. Mizushima, T. Yoshimori, M. Ohsumi, T. Takao, T. Noda, and Y. Ohsumi. 2000. The reversible modification

regulates the membrane-binding state of Apg8/Aut7 essential for autophagy and the cytoplasm to vacuole targeting pathway. J Cell Biol 151:263-276.
132. Kirkin, V., D. G. McEwan, I. Novak, and I. Dikic. 2009. A role for ubiquitin in selective autophagy. Mol Cell 34:259-269.
133. Klemm, E. J., E. Spooner, and H. L. Ploegh. 2011. Dual role of ancient ubiquitous protein 1 (AUP1) in lipid droplet accumulation and endoplasmic reticulum (ER) protein quality control. J Biol Chem 286:37602-37614.
134. Klomporn, P., M. Panyasrivanit, N. Wikan, and D. R. Smith. 2011. Dengue infection of monocytic cells activates ER stress pathways, but apoptosis is induced through both extrinsic and intrinsic pathways. Virology 409:189-197.
135. Kory, N., R. V. Farese, Jr., and T. C. Walther. 2016. Targeting Fat: Mechanisms of Protein Localization to Lipid Droplets. Trends in cell biology 26:535-546.
136. Koyano, F., K. Okatsu, H. Kosako, Y. Tamura, E. Go, M. Kimura, Y. Kimura, H. Tsuchiya, H. Yoshihara, T. Hirokawa, T. Endo, E. A. Fon, J. F. Trempe, Y. Saeki, K. Tanaka, and N. Matsuda. 2014. Ubiquitin is phosphorylated by PINK1 to activate parkin. Nature 510:162-166.
137. Krishnan, M. N., B. Sukumaran, U. Pal, H. Agaisse, J. L. Murray, T. W. Hodge, and E. Fikrig. 2007. Rab 5 is required for the cellular entry of dengue and West Nile viruses. J Virol 81:4881-4885.
138. Kroemer, G., G. Marino, and B. Levine. 2010. Autophagy and the integrated stress response. Mol Cell 40:280-293.
139. Kuang, Y., K. Ma, C. Zhou, P. Ding, Y. Zhu, Q. Chen, and B. Xia. 2016. Structural Basis for the Phosphorylation of FUNDC1 LIR as a Molecular Switch of Mitophagy. Autophagy:0.
140. Kumar, S. H., and A. Rangarajan. 2009. Simian virus 40 small T antigen activates AMPK and triggers autophagy to protect cancer cells from nutrient deprivation. J Virol 83:8565-8574.
141. Kyei, G. B., C. Dinkins, A. S. Davis, E. Roberts, S. B. Singh, C. Dong, L. Wu, E. Kominami, T. Ueno, A. Yamamoto, M. Federico, A. Panganiban, I. Vergne, and V. Deretic. 2009. Autophagy pathway intersects with HIV-1 biosynthesis and regulates viral yields in macrophages. J Cell Biol 186:255-268.
142. Kyle, J. L., and E. Harris. 2008. Global spread and persistence of dengue. Annual review of microbiology 62:71-92.
143. Lapierre, L. R., C. D. De Magalhaes Filho, P. R. McQuary, C. C. Chu, O. Visvikis, J. T. Chang, S. Gelino, B. Ong, A. E. Davis, J. E. Irazoqui, A. Dillin, and M. Hansen. 2013. The TFEB orthologue HLH-30 regulates autophagy and modulates longevity in Caenorhabditis elegans. Nature communications 4:2267.
144. Laplante, M., and D. M. Sabatini. 2012. mTOR signaling in growth control and disease. Cell 149:274-293.
145. Lazarou, M., D. A. Sliter, L. A. Kane, S. A. Sarraf, C. Wang, J. L. Burman, D. P. Sideris, A. I. Fogel, and R. J. Youle. 2015. The ubiquitin kinase PINK1 recruits autophagy receptors to induce mitophagy. Nature 524:309-314.
146. Leduc, C. A., E. E. Crouch, A. Wilson, J. Lefkowitch, M. M. Wamelink, C. Jakobs, G. S. Salomons, X. Sun, Y. Shen, and W. K. Chung. 2014. Novel association of

early onset hepatocellular carcinoma with transaldolase deficiency. JIMD reports 12:121-127.
147. Lee, H. K., J. M. Lund, B. Ramanathan, N. Mizushima, and A. Iwasaki. 2007. Autophagy-dependent viral recognition by plasmacytoid dendritic cells. Science 315:1398-1401.
148. Lee, J. M., M. Wagner, R. Xiao, K. H. Kim, D. Feng, M. A. Lazar, and D. D. Moore. 2014. Nutrient-sensing nuclear receptors coordinate autophagy. Nature 516:112-115.
149. Lee, J. W., S. Park, Y. Takahashi, and H. G. Wang. 2010. The association of AMPK with ULK1 regulates autophagy. PLoS One 5:e15394.
150. Lee, Y. R., H. Y. Hu, S. H. Kuo, H. Y. Lei, Y. S. Lin, T. M. Yeh, C. C. Liu, and H. S. Liu. 2013. Dengue virus infection induces autophagy: an in vivo study. Journal of biomedical science 20:65.
151. Lee, Y. R., H. Y. Lei, M. T. Liu, J. R. Wang, S. H. Chen, Y. F. Jiang-Shieh, Y. S. Lin, T. M. Yeh, C. C. Liu, and H. S. Liu. 2008. Autophagic machinery activated by dengue virus enhances virus replication. Virology 374:240-248.
152. Levine, B., and G. Kroemer. 2008. Autophagy in the pathogenesis of disease. Cell 132:27-42.
153. Levine, B., N. Mizushima, and H. W. Virgin. 2011. Autophagy in immunity and inflammation. Nature 469:323-335.
154. Li, J. K., J. J. Liang, C. L. Liao, and Y. L. Lin. 2012. Autophagy is involved in the early step of Japanese encephalitis virus infection. Microbes and infection / Institut Pasteur 14:159-168.
155. Li, L., S. M. Lok, I. M. Yu, Y. Zhang, R. J. Kuhn, J. Chen, and M. G. Rossmann. 2008. The flavivirus precursor membrane-envelope protein complex: structure and maturation. Science 319:1830-1834.
156. Li, S., M. P. Wandel, F. Li, Z. Liu, C. He, J. Wu, Y. Shi, and F. Randow. 2013. Sterical hindrance promotes selectivity of the autophagy cargo receptor NDP52 for the danger receptor galectin-8 in antibacterial autophagy. Science signaling 6:ra9.
157. Li, Y., K. Inoki, and K. L. Guan. 2004. Biochemical and functional characterizations of small GTPase Rheb and TSC2 GAP activity. Molecular and cellular biology 24:7965-7975.
158. Li, Y., K. Inoki, H. Vikis, and K. L. Guan. 2006. Measurements of TSC2 GAP activity toward Rheb. Methods in enzymology 407:46-54.
159. Liang, C., J. S. Lee, K. S. Inn, M. U. Gack, Q. Li, E. A. Roberts, I. Vergne, V. Deretic, P. Feng, C. Akazawa, and J. U. Jung. 2008. Beclin1-binding UVRAG targets the class C Vps complex to coordinate autophagosome maturation and endocytic trafficking. Nat Cell Biol 10:776-787.
160. Liang, Q., Z. Luo, J. Zeng, W. Chen, S. S. Foo, S. A. Lee, J. Ge, S. Wang, S. A. Goldman, B. V. Zlokovic, Z. Zhao, and J. U. Jung. 2016. Zika Virus NS4A and NS4B Proteins Deregulate Akt-mTOR Signaling in Human Fetal Neural Stem Cells to Inhibit Neurogenesis and Induce Autophagy. Cell stem cell.
161. Lim, P. Y., M. J. Behr, C. M. Chadwick, P. Y. Shi, and K. A. Bernard. 2011. Keratinocytes are cell targets of West Nile virus in vivo. J Virol 85:5197-5201.

162. Littaua, R., I. Kurane, and F. A. Ennis. 1990. Human IgG Fc receptor II mediates antibody-dependent enhancement of dengue virus infection. J Immunol 144:3183-3186.
163. Liu, L., D. Feng, G. Chen, M. Chen, Q. Zheng, P. Song, Q. Ma, C. Zhu, R. Wang, W. Qi, L. Huang, P. Xue, B. Li, X. Wang, H. Jin, J. Wang, F. Yang, P. Liu, Y. Zhu, S. Sui, and Q. Chen. 2012. Mitochondrial outer-membrane protein FUNDC1 mediates hypoxia-induced mitophagy in mammalian cells. Nat Cell Biol 14:177-185.
164. Liu, R., Y. Lin, R. Jia, Y. Geng, C. Liang, J. Tan, and W. Qiao. 2014. HIV-1 Vpr stimulates NF-kappaB and AP-1 signaling by activating TAK1. Retrovirology 11:45.
165. Lohmann, D., J. Spandl, A. Stevanovic, M. Schoene, J. Philippou-Massier, and C. Thiele. 2013. Monoubiquitination of ancient ubiquitous protein 1 promotes lipid droplet clustering. PLoS One 8:e72453.
166. Long, X., Y. Lin, S. Ortiz-Vega, K. Yonezawa, and J. Avruch. 2005. Rheb binds and regulates the mTOR kinase. Current biology : CB 15:702-713.
167. Magnuson, B., B. Ekim, and D. C. Fingar. 2012. Regulation and function of ribosomal protein S6 kinase (S6K) within mTOR signalling networks. The Biochemical journal 441:1-21.
168. Mankouri, J., and M. Harris. 2011. Viruses and the fuel sensor: the emerging link between AMPK and virus replication. Reviews in medical virology 21:205-212.
169. Mankouri, J., P. R. Tedbury, S. Gretton, M. E. Hughes, S. D. Griffin, M. L. Dallas, K. A. Green, D. G. Hardie, C. Peers, and M. Harris. 2010. Enhanced hepatitis C virus genome replication and lipid accumulation mediated by inhibition of AMP-activated protein kinase. Proc Natl Acad Sci U S A 107:11549-11554.
170. Massague, J. 2012. TGFbeta signalling in context. Nat Rev Mol Cell Biol 13:616-630.
171. Mateo, R., C. M. Nagamine, J. Spagnolo, E. Mendez, M. Rahe, M. Gale, Jr., J. Yuan, and K. Kirkegaard. 2013. Inhibition of cellular autophagy deranges dengue virion maturation. J Virol 87:1312-1321.
172. Matsunaga, K., T. Saitoh, K. Tabata, H. Omori, T. Satoh, N. Kurotori, I. Maejima, K. Shirahama-Noda, T. Ichimura, T. Isobe, S. Akira, T. Noda, and T. Yoshimori. 2009. Two Beclin 1-binding proteins, Atg14L and Rubicon, reciprocally regulate autophagy at different stages. Nat Cell Biol 11:385-396.
173. McArdle, J., N. J. Moorman, and J. Munger. 2012. HCMV targets the metabolic stress response through activation of AMPK whose activity is important for viral replication. PLoS Pathog 8:e1002502.
174. McArdle, J., X. L. Schafer, and J. Munger. 2011. Inhibition of calmodulin-dependent kinase kinase blocks human cytomegalovirus-induced glycolytic activation and severely attenuates production of viral progeny. J Virol 85:705-714.
175. McLean, J. E., A. Wudzinska, E. Datan, D. Quaglino, and Z. Zakeri. 2011. Flavivirus NS4A-induced autophagy protects cells against death and enhances virus replication. J Biol Chem 286:22147-22159.

176. Medigeshi, G. R., A. M. Lancaster, A. J. Hirsch, T. Briese, W. I. Lipkin, V. Defilippis, K. Fruh, P. W. Mason, J. Nikolich-Zugich, and J. A. Nelson. 2007. West Nile virus infection activates the unfolded protein response, leading to CHOP induction and apoptosis. J Virol 81:10849-10860.
177. Meissner, C., H. Lorenz, B. Hehn, and M. K. Lemberg. 2015. Intramembrane protease PARL defines a negative regulator of PINK1- and PARK2/Parkin-dependent mitophagy. Autophagy 11:1484-1498.
178. Meissner, C., H. Lorenz, A. Weihofen, D. J. Selkoe, and M. K. Lemberg. 2011. The mitochondrial intramembrane protease PARL cleaves human Pink1 to regulate Pink1 trafficking. Journal of neurochemistry 117:856-867.
179. Metz, P., A. Chiramel, L. Chatel-Chaix, G. Alvisi, P. Bankhead, R. Mora-Rodriguez, G. Long, A. Hamacher-Brady, N. R. Brady, and R. Bartenschlager. 2015. Dengue Virus Inhibition of Autophagic Flux and Dependency of Viral Replication on Proteasomal Degradation of the Autophagy Receptor p62. Journal of virology 89:8026-8041.
180. Mizushima, N., B. Levine, A. M. Cuervo, and D. J. Klionsky. 2008. Autophagy fights disease through cellular self-digestion. Nature 451:1069-1075.
181. Mizushima, N., T. Noda, T. Yoshimori, Y. Tanaka, T. Ishii, M. D. George, D. J. Klionsky, M. Ohsumi, and Y. Ohsumi. 1998. A protein conjugation system essential for autophagy. Nature 395:395-398.
182. Momcilovic, M., S. P. Hong, and M. Carlson. 2006. Mammalian TAK1 activates Snf1 protein kinase in yeast and phosphorylates AMP-activated protein kinase in vitro. J Biol Chem 281:25336-25343.
183. Monastyrska, I., M. Ulasli, P. J. Rottier, J. L. Guan, F. Reggiori, and C. A. de Haan. 2013. An autophagy-independent role for LC3 in equine arteritis virus replication. Autophagy 9:164-174.
184. Morioka, S., P. Broglie, E. Omori, Y. Ikeda, G. Takaesu, K. Matsumoto, and J. Ninomiya-Tsuji. 2014. TAK1 kinase switches cell fate from apoptosis to necrosis following TNF stimulation. J Cell Biol 204:607-623.
185. Morioka, S., K. Sai, E. Omori, Y. Ikeda, K. Matsumoto, and J. Ninomiya-Tsuji. 2016. TAK1 regulates hepatic lipid homeostasis through SREBP. Oncogene 35:3829-3838.
186. Moriyama, T., S. Tanaka, Y. Nakayama, M. Fukumoto, K. Tsujimura, K. Yamada, T. Bamba, Y. Yoneda, E. Fukusaki, and M. Oka. 2016. Two isoforms of TALDO1 generated by alternative translational initiation show differential nucleocytoplasmic distribution to regulate the global metabolic network. Scientific reports 6:34648.
187. Moser, T. S., R. G. Jones, C. B. Thompson, C. B. Coyne, and S. Cherry. 2010. A kinome RNAi screen identified AMPK as promoting poxvirus entry through the control of actin dynamics. PLoS Pathog 6:e1000954.
188. Moser, T. S., D. Schieffer, and S. Cherry. 2012. AMP-activated kinase restricts Rift Valley fever virus infection by inhibiting fatty acid synthesis. PLoS Pathog 8:e1002661.
189. Mu, Y., S. K. Gudey, and M. Landstrom. 2012. Non-Smad signaling pathways. Cell and tissue research 347:11-20.

190. Munday, M. R., and D. G. Hardie. 1986. The role of acetyl-CoA carboxylase phosphorylation in the control of mammary gland fatty acid synthesis during the starvation and re-feeding of lactating rats. The Biochemical journal 237:85-91.
191. Munger, J., S. U. Bajad, H. A. Coller, T. Shenk, and J. D. Rabinowitz. 2006. Dynamics of the cellular metabolome during human cytomegalovirus infection. PLoS Pathog 2:e132.
192. Nakamoto, M., R. H. Moy, J. Xu, S. Bambina, A. Yasunaga, S. S. Shelly, B. Gold, and S. Cherry. 2012. Virus recognition by Toll-7 activates antiviral autophagy in Drosophila. Immunity 36:658-667.
193. Nawa, M. 1998. Effects of bafilomycin A1 on Japanese encephalitis virus in C6/36 mosquito cells. Archives of virology 143:1555-1568.
194. Ng, M. L., and L. C. Lau. 1988. Possible involvement of receptors in the entry of Kunjin virus into Vero cells. Archives of virology 100:199-211.
195. Noda, T., K. Matsunaga, N. Taguchi-Atarashi, and T. Yoshimori. 2010. Regulation of membrane biogenesis in autophagy via PI3P dynamics. Seminars in cell & developmental biology 21:671-676.
196. Norata, G. D., G. Caligiuri, T. Chavakis, G. Matarese, M. G. Netea, A. Nicoletti, L. A. O'Neill, and F. M. Marelli-Berg. 2015. The Cellular and Molecular Basis of Translational Immunometabolism. Immunity 43:421-434.
197. Novak, I., V. Kirkin, D. G. McEwan, J. Zhang, P. Wild, A. Rozenknop, V. Rogov, F. Lohr, D. Popovic, A. Occhipinti, A. S. Reichert, J. Terzic, V. Dotsch, P. A. Ney, and I. Dikic. 2010. Nix is a selective autophagy receptor for mitochondrial clearance. EMBO reports 11:45-51.
198. O'Connor, H. F., N. Lyon, J. W. Leung, P. Agarwal, C. D. Swaim, K. M. Miller, and J. M. Huibregtse. 2015. Ubiquitin-Activated Interaction Traps (UBAITs) identify E3 ligase binding partners. EMBO reports 16:1699-1712.
199. O'Neill, L. A., R. J. Kishton, and J. Rathmell. 2016. A guide to immunometabolism for immunologists. Nat Rev Immunol 16:553-565.
200. O'Neill, L. A., and E. J. Pearce. 2016. Immunometabolism governs dendritic cell and macrophage function. The Journal of experimental medicine 213:15-23.
201. O'Rourke, E. J., and G. Ruvkun. 2013. MXL-3 and HLH-30 transcriptionally link lipolysis and autophagy to nutrient availability. Nat Cell Biol 15:668-676.
202. Oakhill, J. S., R. Steel, Z. P. Chen, J. W. Scott, N. Ling, S. Tam, and B. E. Kemp. 2011. AMPK is a direct adenylate charge-regulated protein kinase. Science 332:1433-1435.
203. Ogata, M., S. Hino, A. Saito, K. Morikawa, S. Kondo, S. Kanemoto, T. Murakami, M. Taniguchi, I. Tanii, K. Yoshinaga, S. Shiosaka, J. A. Hammarback, F. Urano, and K. Imaizumi. 2006. Autophagy is activated for cell survival after endoplasmic reticulum stress. Molecular and cellular biology 26:9220-9231.
204. Ohsaki, Y., J. Cheng, A. Fujita, T. Tokumoto, and T. Fujimoto. 2006. Cytoplasmic lipid droplets are sites of convergence of proteasomal and autophagic degradation of apolipoprotein B. Molecular biology of the cell 17:2674-2683.

205. Orvedahl, A., R. Sumpter, Jr., G. Xiao, A. Ng, Z. Zou, Y. Tang, M. Narimatsu, C. Gilpin, Q. Sun, M. Roth, C. V. Forst, J. L. Wrana, Y. E. Zhang, K. Luby-Phelps, R. J. Xavier, Y. Xie, and B. Levine. 2011. Image-based genome-wide siRNA screen identifies selective autophagy factors. Nature 480:113-117.
206. Ouimet, M., V. Franklin, E. Mak, X. Liao, I. Tabas, and Y. L. Marcel. 2011. Autophagy regulates cholesterol efflux from macrophage foam cells via lysosomal acid lipase. Cell metabolism 13:655-667.
207. Palmer, D. R., P. Sun, C. Celluzzi, J. Bisbing, S. Pang, W. Sun, M. A. Marovich, and T. Burgess. 2005. Differential effects of dengue virus on infected and bystander dendritic cells. J Virol 79:2432-2439.
208. Pandey, N., A. Jain, R. K. Garg, R. Kumar, O. P. Agrawal, and P. V. Lakshmana Rao. 2015. Serum levels of IL-8, IFNgamma, IL-10, and TGF beta and their gene expression levels in severe and non-severe cases of dengue virus infection. Archives of virology 160:1463-1475.
209. Panyasrivanit, M., A. Khakpoor, N. Wikan, and D. R. Smith. 2009. Co-localization of constituents of the dengue virus translation and replication machinery with amphisomes. J Gen Virol 90:448-456.
210. Panyasrivanit, M., A. Khakpoor, N. Wikan, and D. R. Smith. 2009. Linking dengue virus entry and translation/replication through amphisomes. Autophagy 5:434-435.
211. Pena, J., and E. Harris. 2012. Early dengue virus protein synthesis induces extensive rearrangement of the endoplasmic reticulum independent of the UPR and SREBP-2 pathway. PLoS One 7:e38202.
212. Perera, R., C. Riley, G. Isaac, A. S. Hopf-Jannasch, R. J. Moore, K. W. Weitz, L. Pasa-Tolic, T. O. Metz, J. Adamec, and R. J. Kuhn. 2012. Dengue virus infection perturbs lipid homeostasis in infected mosquito cells. PLoS Pathog 8:e1002584.
213. Perez, A. B., B. Sierra, G. Garcia, E. Aguirre, N. Babel, M. Alvarez, L. Sanchez, L. Valdes, H. D. Volk, and M. G. Guzman. 2010. Tumor necrosis factor-alpha, transforming growth factor-beta1, and interleukin-10 gene polymorphisms: implication in protection or susceptibility to dengue hemorrhagic fever. Human immunology 71:1135-1140.
214. Pertel, T., S. Hausmann, D. Morger, S. Zuger, J. Guerra, J. Lascano, C. Reinhard, F. A. Santoni, P. D. Uchil, L. Chatel, A. Bisiaux, M. L. Albert, C. Strambio-De-Castillia, W. Mothes, M. Pizzato, M. G. Grutter, and J. Luban. 2011. TRIM5 is an innate immune sensor for the retrovirus capsid lattice. Nature 472:361-365.
215. Petersen, L. R., A. C. Brault, and R. S. Nasci. 2013. West Nile virus: review of the literature. JAMA : the journal of the American Medical Association 310:308-315.
216. Pham, A. M., R. A. Langlois, and B. R. TenOever. 2012. Replication in cells of hematopoietic origin is necessary for Dengue virus dissemination. PLoS Pathog 8:e1002465.
217. Postler, T. S., and R. C. Desrosiers. 2012. The cytoplasmic domain of the HIV-1 glycoprotein gp41 induces NF-kappaB activation through TGF-beta-activated kinase 1. Cell Host Microbe 11:181-193.

218. Radke, E. G., C. J. Gregory, K. W. Kintziger, E. K. Sauber-Schatz, E. A. Hunsperger, G. R. Gallagher, J. M. Barber, B. J. Biggerstaff, D. R. Stanek, K. M. Tomashek, and C. G. Blackmore. 2012. Dengue outbreak in Key West, Florida, USA, 2009. Emerging infectious diseases 18:135-137.
219. Ramos, M. M., H. Mohammed, E. Zielinski-Gutierrez, M. H. Hayden, J. L. Lopez, M. Fournier, A. R. Trujillo, R. Burton, J. M. Brunkard, L. Anaya-Lopez, A. A. Banicki, P. K. Morales, B. Smith, J. L. Munoz, and S. H. Waterman. 2008. Epidemic dengue and dengue hemorrhagic fever at the Texas-Mexico border: results of a household-based seroepidemiologic survey, December 2005. The American journal of tropical medicine and hygiene 78:364-369.
220. Randall, G., M. Panis, J. D. Cooper, T. L. Tellinghuisen, K. E. Sukhodolets, S. Pfeffer, M. Landthaler, P. Landgraf, S. Kan, B. D. Lindenbach, M. Chien, D. B. Weir, J. J. Russo, J. Ju, M. J. Brownstein, R. Sheridan, C. Sander, M. Zavolan, T. Tuschl, and C. M. Rice. 2007. Cellular cofactors affecting hepatitis C virus infection and replication. Proc Natl Acad Sci U S A 104:12884-12889.
221. Reggiori, F., I. Monastyrska, M. H. Verheije, T. Cali, M. Ulasli, S. Bianchi, R. Bernasconi, C. A. de Haan, and M. Molinari. 2010. Coronaviruses Hijack the LC3-I-positive EDEMosomes, ER-derived vesicles exporting short-lived ERAD regulators, for replication. Cell Host Microbe 7:500-508.
222. Richter, B., D. A. Sliter, L. Herhaus, A. Stolz, C. Wang, P. Beli, G. Zaffagnini, P. Wild, S. Martens, S. A. Wagner, R. J. Youle, and I. Dikic. 2016. Phosphorylation of OPTN by TBK1 enhances its binding to Ub chains and promotes selective autophagy of damaged mitochondria. Proc Natl Acad Sci U S A 113:4039-4044.
223. Roberts, R., and N. T. Ktistakis. 2013. Omegasomes: PI3P platforms that manufacture autophagosomes. Essays in biochemistry 55:17-27.
224. Rodriguez-Madoz, J. R., A. Belicha-Villanueva, D. Bernal-Rubio, J. Ashour, J. Ayllon, and A. Fernandez-Sesma. 2010. Inhibition of the type I interferon response in human dendritic cells by dengue virus infection requires a catalytically active NS2B3 complex. J Virol 84:9760-9774.
225. Rodriguez-Madoz, J. R., D. Bernal-Rubio, D. Kaminski, K. Boyd, and A. Fernandez-Sesma. 2010. Dengue virus inhibits the production of type I interferon in primary human dendritic cells. J Virol 84:4845-4850.
226. Rosenwasser, S., C. Ziv, S. G. Creveld, and A. Vardi. 2016. Virocell Metabolism: Metabolic Innovations During Host-Virus Interactions in the Ocean. Trends in microbiology 24:821-832.
227. Rui, Y. N., Z. Xu, B. Patel, Z. Chen, D. Chen, A. Tito, G. David, Y. Sun, E. F. Stimming, H. J. Bellen, A. M. Cuervo, and S. Zhang. 2015. Huntingtin functions as a scaffold for selective macroautophagy. Nat Cell Biol 17:262-275.
228. Russell, R. C., Y. Tian, H. Yuan, H. W. Park, Y. Y. Chang, J. Kim, H. Kim, T. P. Neufeld, A. Dillin, and K. L. Guan. 2013. ULK1 induces autophagy by phosphorylating Beclin-1 and activating VPS34 lipid kinase. Nat Cell Biol 15:741-750.
229. Russell, R. C., H. X. Yuan, and K. L. Guan. 2014. Autophagy regulation by nutrient signaling. Cell research 24:42-57.

230. Sakurai, H. 2012. Targeting of TAK1 in inflammatory disorders and cancer. Trends in pharmacological sciences 33:522-530.
231. Samsa, M. M., J. A. Mondotte, N. G. Iglesias, I. Assuncao-Miranda, G. Barbosa-Lima, A. T. Da Poian, P. T. Bozza, and A. V. Gamarnik. 2009. Dengue virus capsid protein usurps lipid droplets for viral particle formation. PLoS Pathog 5:e1000632.
232. Samuel, M. A., H. Wang, V. Siddharthan, J. D. Morrey, and M. S. Diamond. 2007. Axonal transport mediates West Nile virus entry into the central nervous system and induces acute flaccid paralysis. Proc Natl Acad Sci U S A 104:17140-17145.
233. Samuel, M. A., K. Whitby, B. C. Keller, A. Marri, W. Barchet, B. R. Williams, R. H. Silverman, M. Gale, Jr., and M. S. Diamond. 2006. PKR and RNase L contribute to protection against lethal West Nile Virus infection by controlling early viral spread in the periphery and replication in neurons. J Virol 80:7009-7019.
234. Sandoval, H., P. Thiagarajan, S. K. Dasgupta, A. Schumacher, J. T. Prchal, M. Chen, and J. Wang. 2008. Essential role for Nix in autophagic maturation of erythroid cells. Nature 454:232-235.
235. Sargent, G., T. van Zutphen, T. Shatseva, L. Zhang, V. Di Giovanni, R. Bandsma, and P. K. Kim. 2016. PEX2 is the E3 ubiquitin ligase required for pexophagy during starvation. J Cell Biol 214:677-690.
236. Sarraf, S. A., M. Raman, V. Guarani-Pereira, M. E. Sowa, E. L. Huttlin, S. P. Gygi, and J. W. Harper. 2013. Landscape of the PARKIN-dependent ubiquitylome in response to mitochondrial depolarization. Nature 496:372-376.
237. Schirmer, P. L., C. A. Lucero-Obusan, S. R. Benoit, L. M. Santiago, D. Stanek, A. Dey, M. Martinez, G. Oda, and M. Holodniy. 2013. Dengue surveillance in Veterans Affairs healthcare facilities, 2007-2010. PLoS neglected tropical diseases 7:e2040.
238. Schroeder, B., R. J. Schulze, S. G. Weller, A. C. Sletten, C. A. Casey, and M. A. McNiven. 2015. The small GTPase Rab7 as a central regulator of hepatocellular lipophagy. Hepatology 61:1896-1907.
239. Scortegagna, M., T. Subtil, J. Qi, H. Kim, W. Zhao, W. Gu, H. Kluger, and Z. A. Ronai. 2011. USP13 enzyme regulates Siah2 ligase stability and activity via noncatalytic ubiquitin-binding domains. J Biol Chem 286:27333-27341.
240. Sengupta, S., T. R. Peterson, and D. M. Sabatini. 2010. Regulation of the mTOR complex 1 pathway by nutrients, growth factors, and stress. Mol Cell 40:310-322.
241. Seok, S., T. Fu, S. E. Choi, Y. Li, R. Zhu, S. Kumar, X. Sun, G. Yoon, Y. Kang, W. Zhong, J. Ma, B. Kemper, and J. K. Kemper. 2014. Transcriptional regulation of autophagy by an FXR-CREB axis. Nature 516:108-111.
242. Settembre, C., R. De Cegli, G. Mansueto, P. K. Saha, F. Vetrini, O. Visvikis, T. Huynh, A. Carissimo, D. Palmer, T. J. Klisch, A. C. Wollenberg, D. Di Bernardo, L. Chan, J. E. Irazoqui, and A. Ballabio. 2013. TFEB controls cellular lipid metabolism through a starvation-induced autoregulatory loop. Nat Cell Biol 15:647-658.

243. Settembre, C., C. Di Malta, V. A. Polito, M. Garcia Arencibia, F. Vetrini, S. Erdin, S. U. Erdin, T. Huynh, D. Medina, P. Colella, M. Sardiello, D. C. Rubinsztein, and A. Ballabio. 2011. TFEB links autophagy to lysosomal biogenesis. Science 332:1429-1433.
244. Sharma, M., S. Bhattacharyya, M. Nain, M. Kaur, V. Sood, V. Gupta, R. Khasa, M. Z. Abdin, S. Vrati, and M. Kalia. 2014. Japanese encephalitis virus replication is negatively regulated by autophagy and occurs on LC3-I- and EDEM1-containing membranes. Autophagy 10:1637-1651.
245. Shaw, R. J., M. Kosmatka, N. Bardeesy, R. L. Hurley, L. A. Witters, R. A. DePinho, and L. C. Cantley. 2004. The tumor suppressor LKB1 kinase directly activates AMP-activated kinase and regulates apoptosis in response to energy stress. Proceedings of the National Academy of Sciences of the United States of America 101:3329-3335.
246. Shelly, S., N. Lukinova, S. Bambina, A. Berman, and S. Cherry. 2009. Autophagy is an essential component of Drosophila immunity against vesicular stomatitis virus. Immunity 30:588-598.
247. Shi, J., G. Fung, H. Deng, J. Zhang, F. C. Fiesel, W. Springer, X. Li, and H. Luo. 2015. NBR1 is dispensable for PARK2-mediated mitophagy regardless of the presence or absence of SQSTM1. Cell death & disease 6:e1943.
248. Shiba-Fukushima, K., Y. Imai, S. Yoshida, Y. Ishihama, T. Kanao, S. Sato, and N. Hattori. 2012. PINK1-mediated phosphorylation of the Parkin ubiquitin-like domain primes mitochondrial translocation of Parkin and regulates mitophagy. Scientific reports 2:1002.
249. Shintani, T., N. Mizushima, Y. Ogawa, A. Matsuura, T. Noda, and Y. Ohsumi. 1999. Apg10p, a novel protein-conjugating enzyme essential for autophagy in yeast. EMBO J 18:5234-5241.
250. Shoji-Kawata, S., R. Sumpter, M. Leveno, G. R. Campbell, Z. Zou, L. Kinch, A. D. Wilkins, Q. Sun, K. Pallauf, D. MacDuff, C. Huerta, H. W. Virgin, J. B. Helms, R. Eerland, S. A. Tooze, R. Xavier, D. J. Lenschow, A. Yamamoto, D. King, O. Lichtarge, N. V. Grishin, S. A. Spector, D. V. Kaloyanova, and B. Levine. 2013. Identification of a candidate therapeutic autophagy-inducing peptide. Nature 494:201-206.
251. Shrivastava, S., A. Raychoudhuri, R. Steele, R. Ray, and R. B. Ray. 2011. Knockdown of autophagy enhances the innate immune response in hepatitis C virus-infected hepatocytes. Hepatology 53:406-414.
252. Sim, A. T., and D. G. Hardie. 1988. The low activity of acetyl-CoA carboxylase in basal and glucagon-stimulated hepatocytes is due to phosphorylation by the AMP-activated protein kinase and not cyclic AMP-dependent protein kinase. FEBS letters 233:294-298.
253. Singh, R., S. Kaushik, Y. Wang, Y. Xiang, I. Novak, M. Komatsu, K. Tanaka, A. M. Cuervo, and M. J. Czaja. 2009. Autophagy regulates lipid metabolism. Nature 458:1131-1135.
254. Sorrentino, A., N. Thakur, S. Grimsby, A. Marcusson, V. von Bulow, N. Schuster, S. Zhang, C. H. Heldin, and M. Landstrom. 2008. The type I TGF-beta receptor engages TRAF6 to activate TAK1 in a receptor kinase-independent manner. Nat Cell Biol 10:1199-1207.

255. Spandl, J., D. Lohmann, L. Kuerschner, C. Moessinger, and C. Thiele. 2011. Ancient ubiquitous protein 1 (AUP1) localizes to lipid droplets and binds the E2 ubiquitin conjugase G2 (Ube2g2) via its G2 binding region. J Biol Chem 286:5599-5606.
256. Spencer, C. M., X. L. Schafer, N. J. Moorman, and J. Munger. 2011. Human cytomegalovirus induces the activity and expression of acetyl-coenzyme A carboxylase, a fatty acid biosynthetic enzyme whose inhibition attenuates viral replication. J Virol 85:5814-5824.
257. Stadler, K., S. L. Allison, J. Schalich, and F. X. Heinz. 1997. Proteolytic activation of tick-borne encephalitis virus by furin. Journal of virology 71:8475-8481.
258. Stevanovic, A., and C. Thiele. 2013. Monotopic topology is required for lipid droplet targeting of ancient ubiquitous protein 1. Journal of lipid research 54:503-513.
259. Su, H. L., C. L. Liao, and Y. L. Lin. 2002. Japanese encephalitis virus infection initiates endoplasmic reticulum stress and an unfolded protein response. J Virol 76:4162-4171.
260. Sun, Q., W. Fan, K. Chen, X. Ding, S. Chen, and Q. Zhong. 2008. Identification of Barkor as a mammalian autophagy-specific factor for Beclin 1 and class III phosphatidylinositol 3-kinase. Proc Natl Acad Sci U S A 105:19211-19216.
261. Suzuki, M., T. Otsuka, Y. Ohsaki, J. Cheng, T. Taniguchi, H. Hashimoto, H. Taniguchi, and T. Fujimoto. 2012. Derlin-1 and UBXD8 are engaged in dislocation and degradation of lipidated ApoB-100 at lipid droplets. Molecular biology of the cell 23:800-810.
262. Tal, M. C., M. Sasai, H. K. Lee, B. Yordy, G. S. Shadel, and A. Iwasaki. 2009. Absence of autophagy results in reactive oxygen species-dependent amplification of RLR signaling. Proc Natl Acad Sci U S A 106:2770-2775.
263. Talloczy, Z., W. Jiang, H. W. t. Virgin, D. A. Leib, D. Scheuner, R. J. Kaufman, E. L. Eskelinen, and B. Levine. 2002. Regulation of starvation- and virus-induced autophagy by the eIF2alpha kinase signaling pathway. Proc Natl Acad Sci U S A 99:190-195.
264. Talloczy, Z., H. W. t. Virgin, and B. Levine. 2006. PKR-dependent autophagic degradation of herpes simplex virus type 1. Autophagy 2:24-29.
265. Tang, W. C., R. J. Lin, C. L. Liao, and Y. L. Lin. 2014. Rab18 facilitates dengue virus infection by targeting fatty acid synthase to sites of viral replication. J Virol 88:6793-6804.
266. Tanida, I., N. Mizushima, M. Kiyooka, M. Ohsumi, T. Ueno, Y. Ohsumi, and E. Kominami. 1999. Apg7p/Cvt2p: A novel protein-activating enzyme essential for autophagy. Molecular biology of the cell 10:1367-1379.
267. Teramoto, T., H. S. Chiang, R. Takhampunya, M. Manzano, R. Padmanabhan, and M. Maric. 2013. Gamma interferon-inducible lysosomal thioreductase (GILT) ablation renders mouse fibroblasts sensitive to dengue virus replication. Virology 441:146-151.
268. Thurston, T. L., M. P. Wandel, N. von Muhlinen, A. Foeglein, and F. Randow. 2012. Galectin 8 targets damaged vesicles for autophagy to defend cells against bacterial invasion. Nature 482:414-418.

269. Tu, Y. C., C. Y. Yu, J. J. Liang, E. Lin, C. L. Liao, and Y. L. Lin. 2012. Blocking double-stranded RNA-activated protein kinase PKR by Japanese encephalitis virus nonstructural protein 2A. J Virol 86:10347-10358.
270. Tylki-Szymanska, A., M. M. Wamelink, T. J. Stradomska, G. S. Salomons, J. Taybert, N. Dabrowska-Leonik, and M. Rurarz. 2014. Clinical and molecular characteristics of two transaldolase-deficient patients. European journal of pediatrics 173:1679-1682.
271. van den Hurk, A. F., S. A. Ritchie, and J. S. Mackenzie. 2009. Ecology and geographical expansion of Japanese encephalitis virus. Annual review of entomology 54:17-35.
272. van der Schaar, H. M., M. J. Rust, C. Chen, H. van der Ende-Metselaar, J. Wilschut, X. Zhuang, and J. M. Smit. 2008. Dissecting the cell entry pathway of dengue virus by single-particle tracking in living cells. PLoS Pathog 4:e1000244.
273. Verma, S., M. Kumar, U. Gurjav, S. Lum, and V. R. Nerurkar. 2010. Reversal of West Nile virus-induced blood-brain barrier disruption and tight junction proteins degradation by matrix metalloproteinases inhibitor. Virology 397:130-138.
274. Verma, S., Y. Lo, M. Chapagain, S. Lum, M. Kumar, U. Gurjav, H. Luo, A. Nakatsuka, and V. R. Nerurkar. 2009. West Nile virus infection modulates human brain microvascular endothelial cells tight junction proteins and cell adhesion molecules: Transmigration across the in vitro blood-brain barrier. Virology 385:425-433.
275. Wang, C., K. Guo, D. Gao, X. Kang, K. Jiang, Y. Li, L. Sun, S. Zhang, C. Sun, X. Liu, W. Wu, P. Yang, and Y. Liu. 2011. Identification of transaldolase as a novel serum biomarker for hepatocellular carcinoma metastasis using xenografted mouse model and clinic samples. Cancer letters 313:154-166.
276. Wang, P., J. Dai, F. Bai, K. F. Kong, S. J. Wong, R. R. Montgomery, J. A. Madri, and E. Fikrig. 2008. Matrix metalloproteinase 9 facilitates West Nile virus entry into the brain. J Virol 82:8978-8985.
277. Wang, T., T. Town, L. Alexopoulou, J. F. Anderson, E. Fikrig, and R. A. Flavell. 2004. Toll-like receptor 3 mediates West Nile virus entry into the brain causing lethal encephalitis. Nature medicine 10:1366-1373.
278. Wang, X., L. Hou, J. Du, L. Zhou, X. Ge, X. Guo, and H. Yang. 2015. Capsid, membrane and NS3 are the major viral proteins involved in autophagy induced by Japanese encephalitis virus. Veterinary microbiology 178:217-229.
279. Ward, A. M., K. Bidet, A. Yinglin, S. G. Ler, K. Hogue, W. Blackstock, J. Gunaratne, and M. A. Garcia-Blanco. 2011. Quantitative mass spectrometry of DENV-2 RNA-interacting proteins reveals that the DEAD-box RNA helicase DDX6 binds the DB1 and DB2 3' UTR structures. RNA biology 8:1173-1186.
280. Weekes, J., S. A. Hawley, J. Corton, D. Shugar, and D. G. Hardie. 1994. Activation of rat liver AMP-activated protein kinase by kinase kinase in a purified, reconstituted system. Effects of AMP and AMP analogues. European journal of biochemistry / FEBS 219:751-757.

281. Weidberg, H., T. Shpilka, E. Shvets, A. Abada, F. Shimron, and Z. Elazar. 2011. LC3 and GATE-16 N termini mediate membrane fusion processes required for autophagosome biogenesis. Developmental cell 20:444-454.
282. Weidberg, H., E. Shvets, and Z. Elazar. 2011. Biogenesis and cargo selectivity of autophagosomes. Annu Rev Biochem 80:125-156.
283. Weidberg, H., E. Shvets, T. Shpilka, F. Shimron, V. Shinder, and Z. Elazar. 2010. LC3 and GATE-16/GABARAP subfamilies are both essential yet act differently in autophagosome biogenesis. The EMBO journal 29:1792-1802.
284. Welsch, S., S. Miller, I. Romero-Brey, A. Merz, C. K. Bleck, P. Walther, S. D. Fuller, C. Antony, J. Krijnse-Locker, and R. Bartenschlager. 2009. Composition and three-dimensional architecture of the dengue virus replication and assembly sites. Cell Host Microbe 5:365-375.
285. Wirth, M., J. Joachim, and S. A. Tooze. 2013. Autophagosome formation-The role of ULK1 and Beclin1-PI3KC3 complexes in setting the stage. Seminars in cancer biology 23:301-309.
286. Woods, A., K. Dickerson, R. Heath, S. P. Hong, M. Momcilovic, S. R. Johnstone, M. Carlson, and D. Carling. 2005. Ca2+/calmodulin-dependent protein kinase kinase-beta acts upstream of AMP-activated protein kinase in mammalian cells. Cell metabolism 2:21-33.
287. Wrana, J. L., L. Attisano, R. Wieser, F. Ventura, and J. Massague. 1994. Mechanism of activation of the TGF-beta receptor. Nature 370:341-347.
288. Wu, L., H. Nakano, and Z. Wu. 2006. The C-terminal activating region 2 of the Epstein-Barr virus-encoded latent membrane protein 1 activates NF-kappaB through TRAF6 and TAK1. J Biol Chem 281:2162-2169.
289. Wu, W., W. Tian, Z. Hu, G. Chen, L. Huang, W. Li, X. Zhang, P. Xue, C. Zhou, L. Liu, Y. Zhu, X. Zhang, L. Li, L. Zhang, S. Sui, B. Zhao, and D. Feng. 2014. ULK1 translocates to mitochondria and phosphorylates FUNDC1 to regulate mitophagy. EMBO reports 15:566-575.
290. Wu, X., and S. C. Sun. 2007. Retroviral oncoprotein Tax deregulates NF-kappaB by activating Tak1 and mediating the physical association of Tak1-IKK. EMBO reports 8:510-515.
291. Xiao, B., R. Heath, P. Saiu, F. C. Leiper, P. Leone, C. Jing, P. A. Walker, L. Haire, J. F. Eccleston, C. T. Davis, S. R. Martin, D. Carling, and S. J. Gamblin. 2007. Structural basis for AMP binding to mammalian AMP-activated protein kinase. Nature 449:496-500.
292. Xiao, B., M. J. Sanders, E. Underwood, R. Heath, F. V. Mayer, D. Carmena, C. Jing, P. A. Walker, J. F. Eccleston, L. F. Haire, P. Saiu, S. A. Howell, R. Aasland, S. R. Martin, D. Carling, and S. J. Gamblin. 2011. Structure of mammalian AMPK and its regulation by ADP. Nature 472:230-233.
293. Xie, M., D. Zhang, J. R. Dyck, Y. Li, H. Zhang, M. Morishima, D. L. Mann, G. E. Taffet, A. Baldini, D. S. Khoury, and M. D. Schneider. 2006. A pivotal role for endogenous TGF-beta-activated kinase-1 in the LKB1/AMP-activated protein kinase energy-sensor pathway. Proc Natl Acad Sci U S A 103:17378-17383.
294. Xie, Z., U. Nair, and D. J. Klionsky. 2008. Atg8 controls phagophore expansion during autophagosome formation. Molecular biology of the cell 19:3290-3298.

295. Yeh, H. M., C. Y. Yu, H. C. Yang, S. H. Ko, C. L. Liao, and Y. L. Lin. 2013. Ubiquitin-Specific Protease 13 Regulates IFN Signaling by Stabilizing STAT1. J Immunol.
296. Yordy, B., N. Iijima, A. Huttner, D. Leib, and A. Iwasaki. 2012. A neuron-specific role for autophagy in antiviral defense against herpes simplex virus. Cell Host Microbe 12:334-345.
297. Yorimitsu, T., U. Nair, Z. Yang, and D. J. Klionsky. 2006. Endoplasmic reticulum stress triggers autophagy. J Biol Chem 281:30299-30304.
298. Yu, C. Y., Y. W. Hsu, C. L. Liao, and Y. L. Lin. 2006. Flavivirus infection activates the XBP1 pathway of the unfolded protein response to cope with endoplasmic reticulum stress. J Virol 80:11868-11880.
299. Yuan, J., K. Luo, L. Zhang, J. C. Cheville, and Z. Lou. 2010. USP10 regulates p53 localization and stability by deubiquitinating p53. Cell 140:384-396.
300. Zaffagnini, G., and S. Martens. 2016. Mechanisms of Selective Autophagy. Journal of molecular biology 428:1714-1724.
301. Zhang, H. S., and M. R. Wu. 2009. SIRT1 regulates Tat-induced HIV-1 transactivation through activating AMP-activated protein kinase. Virus research 146:51-57.
302. Zhao, X., B. Fiske, A. Kawakami, J. Li, and D. E. Fisher. 2011. Regulation of MITF stability by the USP13 deubiquitinase. Nature communications 2:414.
303. Zhong, Y., Q. J. Wang, X. Li, Y. Yan, J. M. Backer, B. T. Chait, N. Heintz, and Z. Yue. 2009. Distinct regulation of autophagic activity by Atg14L and Rubicon associated with Beclin 1-phosphatidylinositol-3-kinase complex. Nat Cell Biol 11:468-476.